Removal of Methylene Blue Dye from Aqueous Solutions by Sodium Carbonate Activated Bentonite

Sena Megersa Jida

Thesis Submitted to Department of Applied Chemistry

School of Applied Natural Science

Presented in Partial Fulfillment of the Requirements for the Master of Science Degree in Applied Chemistry (Specialization in Inorganic Chemistry)

Office of Graduate Studies

Adama Science and Technology University

August, 2021

Adama, Ethiopia

Removal of Methylene Blue Dye from Aqueous Solutions by Sodium Carbonate Activated Bentonite

Sena Megersa Jida

Advisor: Eneyew Amare (Ph.D.)

Co-Advisor: Rajalakshmanan Eswaramoorthy (Ph.D.)

Thesis Submitted to Department of Applied Chemistry

School of Applied Natural Science

Presented in Partial Fulfillment of the Requirements for the Master of Science Degree in Applied Chemistry (Specialization in Inorganic Chemistry)

Adama Science and Technology University

August, 2021

Adama, Ethiopia

DECLARATION

I hereby declare that this Master thesis entitled "**Removal of Methylene Blue Dye from Aqueous Solutions by Sodium Carbonate Activated Bentonite**" is my original work. I also declare that it has not been submitted for the award of any academic degree, diploma, or certificate in any other university. All sources of materials that are used for this thesis have been duly acknowledged through citation.

_____	_____	_____
Name of student	Signature	Date

RECOMMENDATION

We, the advisors of this thesis, hereby certify that we have read the revised version of the thesis entitled "**Removal of Methylene Blue Dye from Aqueous Solutions by Sodium Carbonate Activated Bentonite**" prepared under our guidance by **Sena Megersa Jida** submitted in partial fulfillment of the requirements for the degree of Mater's of Science in Applied Chemistry (Specialization in Inorganic Chemistry). Therefore, we recommend the submission of the revised version of the thesis to the Department following the applicable procedures.

_____	_____	_____
Advisor	Signature	Date
_____	_____	_____
Co-advisor	Signature	Date

APPROVAL SHEET

We, the advisors of the thesis entitled "**Removal of Methylene Blue Dye from Aqueous Solutions by Sodium Carbonate Activated Bentonite**" and developed by **Sena Megersa Jida**; hereby certify that the recommendation and suggestions made by the board of examiners are appropriately incorporated into the final version of the thesis.

_____	_____	_____
Advisor	Signature	Date
_____	_____	_____
Co-advisor	Signature	Date

We, the undersigned, members of the Board of Examiners of the thesis by **Sena Megersa Jida** have read and evaluated the thesis entitled "**Removal of Methylene Blue Dye from Aqueous Solutions by Sodium Carbonate Activated Bentonite**" and examined the candidate during the open defense. This is, therefore, to certify that the thesis is accepted for partial fulfillment of the requirement of the degree of Master of Science in Applied Chemistry (Specialization in Inorganic Chemistry).

_____	_____	_____
Chairperson	Signature	Date
_____	_____	_____
Internal Examiner	Signature	Date
_____	_____	_____
External Examiner	Signature	Date

Finally, approval and acceptance of the thesis are contingent upon submission of its final copy to the Office of Postgraduate Studies (OPGS) through the Department of Graduate Council (DGC) and School of Graduate Committee (SGC).

_____	_____	_____
Department Head	Signature	Date
_____	_____	_____
School Dean	Signature	Date
_____	_____	_____
Office of Postgraduate Studies, Dean	Signature	Date

ACKNOWLEDGEMENTS

First and foremost, I would like to thank the Almighty God and his mother St. Marry for giving me the health, strength, wisdom, and patience to complete this thesis.

Second, I would like to express my deepest gratitude and thanks to my advisor Eneyew Amare (Ph.D.) for his cooperation, suggestions, supervision and remarks, appreciable encouragement, fatherly consultation, and taking his time to read and correct my document, starting from the proposal writing to the completion of this thesis.

I would also like to thank my Co-Advisor Rajalakshmanan Eswaramoorthy (Ph.D.) for his continuous technical, practical, and moral support from the starting to the end of my works.

I would like to appreciate my colleagues, Analytical Chemistry Laboratory Technicians, Applied Chemistry Department, Chemical Engineering Department, Applied Biology Department, Material Engineering Department, and all individuals who supported me by sharing ideas or offering materials support which is an input for this work.

I would like to transfer also my special thanks to Addis Ababa University, Chemistry Department, and the Ethiopian Geological survey for FT-IR and complete silicate analysis.

I would like to acknowledge Adama Science and Technology University for providing me the financial support and sponsorship opportunity to continue my post-graduate study.

Finally, I would like to thank all my beloved family and my entire friends who stood beside me through the difficult times.

TABLE OF CONTENTS

LIST OF TABLES

LISTS OF FIGURES

LIST OF ACRONYMS AND ABBREVIATIONS

AAS ……. Atomic Absorption Spectroscopy

AB2.5……..... 2.5g Na_2CO_3/100 g bentonite

AB5……..... 5g Na_2CO_3/100 g bentonite

AB7.5……..... 7.5g Na_2CO3/100 g bentonite

AB15…….. 15g Na_2CO_3/100 g bentonite

AB-MB……... Activated Bentonite-Methylene Blue

AC …….. Activated Carbon

AOPs……..…… Advanced Oxidation Processes

ASTM……..…..... American Society Test and Material

BET……..…….…..... Brunauer Emmett Teller

BOD……..…..……. Biochemical Oxygen Demand

CB ……..……... Conduction band

COD……..…..…….…..... Chemical Oxygen Demand

CZBC ……..……..... Calcined Zinc oxide/bentonite nanocomposites

CZBC12 ……..……... Calcined Zinc oxide/bentonite nanocomposites

CZBC11 ……..……..... Calcined Zinc oxide/bentonite nanocomposites

CZBC32 ……..……..... Calcined Zinc oxide/bentonite nanocomposites

CEC……..……..….....…..... Cation Exchange Capacity

FT-IR……..……..……..…..…..... Fourier Transform Infrared Spectrometry

IUPAC …….....……..…. International Union of Pure and Applied Chemistry

JCPDS ……..……..….. Joint Committee on Powder Diffraction Standards

LIO …….....…… Loss in Ignition

MB ……..……..…….. Methylene Blue

MINPs…….…..... Magnetic Iron oxide Nanoparticles

MICNCs ……..…..... Magnetic Iron oxide/clay nanocomposites

MM …….……...…….. Molecular Mass

MMT…….…….…....….... Montmorillonite

NB…… Natural bentonite

μm …….……..…...….. Micrometer

nm …….……..….....…..……. Nanometer

PB……. Purified bentonite

pH…….……..... Potential of Hydrogen

pHpzc …….…..……...…...…….. pH at Point of Zero Charge

rpm……...…..……...……... Revolution per minute

SEM …….…..…….……..... Scanning Electron Microscope

TOT……..……..……..……... Tetrahedral-Octahedral-Tetrahedral

VB ……...…….…..... Valance band

UV-Vis……..……...…….. Ultra Violet -Visible Spectroscopy

UZBC ……...…….....….... Uncalcined Zinc oxide/ bentonite nanocomposites

UZBC12 ……...…….....….... Uncalcined Zinc oxide/ bentonite nanocomposites

UZBC11 ……...……..….... Uncalcined Zinc oxide/ bentonite nanocomposites

UZBC32 ……...……..... Uncalcined Zinc oxide/ bentonite nanocomposites

XRD ……..……..…...…….….. X-ray powder Diffraction

ZNPs ……..…….……..... Zinc oxide nanoparticles

ZBNC……...…..……...…… Zinc Oxide/bentonite nanocomposites

ABSTRACT

The leather and textile industries are the leading dyestuff consumers and the main sources of pollutants in the water environment. There is a continuously increasing worldwide concern for the development of organic dye wastewater treatment technologies. The present study focused on the removal of methylene blue (MB) dye from an aqueous solution using sodium carbonate-activated bentonite adsorbent and its ZnO/bentonite nanocomposites for photodegradation. To achieve the objective of the study, the bentonite sample was collected from Gewane, Afar regional state, purified, and activated by Na_2CO_3. Proximate analyses and characterizations of adsorbents and ZnO/bentonite nanocomposites were carried out by using XRD, FT-IR, SEM, and AAS. The XRD showed the bentonite adsorbent contains Montmorillonite, Quartz, Muscovite, Cristobalite, Hematite, and Feldspar as a major phase and ZnO/bentonite nanocomposites contain the ZnO with hexagonal Wurtzite structure and bentonite characteristics. The SEM study revealed the availability of porous morphology on the surface of the bentonite adsorbent before adsorption and coverage of the surface porous by methylene blue after adsorption. The AAS study showed that the local Gewane bentonite is Ca-bentonite but after activation by 5% sodium carbonate, it was changed to Na-bentonite. Optimization of adsorbent was carried out to identify the best adsorbent for the removal of MB dye from an aqueous solution. The result indicated 5% Na_2CO_3 activated bentonite (AB5) has (100%) removal efficiency of the targeted dye. Then, the adsorption experiment was conducted using activated bentonite (AB5) to establish the effect of different parameters such as adsorbent dosage, pH of the solution, initial concentration of MB, contact time, and temperature on the adsorption efficiency of MB dye. The adsorption isotherm was performed using Langiumer, Freundlich, and Temkin isotherm models. The result indicated Langiumer adsorption isotherm best fit the adsorption study for the present experimental data with $R^2=1$. The kinetic adsorption of MB dye by activated bentonite (AB5) was conducted using pseudo-first-order and pseudo-second-order models. The result specified that the pseudo-second-order fit experimental data well and the process was chemisorption. The endothermic and spontaneous nature of the adsorption process of MB dye by activated bentonite (AB5) was carried by studying the thermodynamic parameters of the system. The result indicated the positive value of the ΔS° and negative values ΔG° shows the adsorption capacity of MB dye molecules is on the adsorbent surface. Desorption of MB dye from the spent adsorbent and recyclability of adsorbent were studied by thermo-chemical methods by heating the spent adsorbent at 200°C for 45 min and dipped in ethanol, acetone, and distilled water heated at 25, 35, and 45 °C for 2hrs. The result showed the desorption capacity of MB dye in this study was low. But, the ZnO/bentonite nanocomposites have high degradation efficiency. The adsorbent in this study was recycled at least three times and its adsorption capacity decreases with adsorbent recycling times.

Keywords: *Adsorbent, Adsorption, Activated-bentonite, Desorption, Methylene blue dye*

CHAPTER ONE

INTRODUCTION

1.1. Background of the study

Water is basic for life. Clean water is the key to a healthy society. But in the present universal scenario, the existence of freshwater is very serious because of the rapid development of urbanization and industrialization [1]. Chemical contamination of drinking water sources is a concern for millions of people and long-term exposure to chemical pollutants can have serious health implications. According to recent reports, many industries discharge about 70% of their waste products into water bodies directly without any refinements [2].

The textile industry discharges a large number of dye effluents into the water bodies during the printing and dyeing process. The process of printing and dyeing materials, in chemical industries, makes human beings in a colorful world. Dyes are colorful substances that are used widely as part of the coloring processes in textile, paper, plastics, leather tanning, food, polymer, cosmetics, printing, and dye manufacturing industries, to give color to the supplies such as papers, fabrics, or any other type of colorable materials [3]. Humans have widely used these materials for thousands of years for several applications [4]. Dye producers and users have an interest in the stability and fastness of dyes and consequently, producing dyestuffs are harder to degrade. These dyes are released without additional care into the environment and natural water bodies after performing their purpose. However, an illegal and massive discharge of wastewaters contains dyes from textile industries into lakes and rivers has posed a serious risk to ecosystems because of their high carcinogenic and mutagenic potential [5].

Based on their nuclear structures, dyes are divided into anionic, cationic, and non-ionic dyes [6]. Anionic dyes give a net negative charge when dissolved in an aqueous solution, such as those of sulfonate ($-SO_3^-$) and carboxyl (-COOH) groups. Methyl orange is an example of anionic dyes, it is toxic, mutagenic, and carcinogenic [7], a hard-braking molecular structure [8], and it is difficult for adsorption by adsorbents. On the other hand, cationic dyes are organic dyes that give a net positive charge when dissolved in an aqueous solution, due to their functional groups such as amine or sulfur. Methylene blue (MB) dye is an example of cationic dyes which is used as a reference to show the cation exchange capacity (CEC) of clay. MB dye has a high solubility in

water and is one of the thiazine colorants. It may cause harmful effects on human health because of its carcinogenicity and toxicity in nature it leads to severe headaches, chest pain, breathing difficulty, eye irritation, vomiting, increased heart rate, diarrhea, and cyanosis [9]. Also, the presence of MB dye in water bodies significantly endangers the aquatic systems by producing unpleasant colors to the water and blocking the direct sunlight for photosynthesis organisms in the aquatic system [10]. Also, the occurrence of MB dye in water sources restricts these waters from regular events like; drinking, cooking, washing bathing, and living places for animals. For instance removal of this dye has received special attention to get good quality water by an environmentally friendly method.

Removal of MB dye from the wastewater needs various treatment methods including; coagulation, chemical oxidation, membrane separation, electrochemical process, photocatalysis, and adsorption methods. From the above-mentioned techniques, adsorption was recognized to be promising and cost-effective, simple and flexible, easy to operate, easily regenerating of adsorbent, and control to remove dyes from wastewater [11]. The choice and type of adsorbent may depend upon parameters like cost, availability, toxicity and regeneration, and re-usability. There are different adsorbents were reported for the removal of methylene blue from wastewater such as activated carbon, chitin, cellulose, agriculture wastes, zeolites, and clays minerals [12]. From the mentioned above adsorbents in recent years, the activated carbon (AC) adsorbents used successfully for the removal of methylene blue from wastewater but, it has some drawbacks such as the effectiveness of cost and difficulty to regenerate limits its use [13]. Because of these drawbacks, the low-cost and easily regenerated adsorbents were preferable for the removal of MB dyes from wastewater. Clay minerals are very attractive adsorbents due to it shows strong attraction between their surface and dyes, high surface area, morphology and ion-exchange potentials [14]. As a low-cost clay adsorbent, bentonite clay is increasingly one of the most and readily available adsorbents that give attention to the researcher in the removal of organic pollutants from wastewater. It is preferable for the removal of organic dye especially cationic dye because it has very important properties that are suitable for the removal of MB dyes like; high specific surface area (SSA), cation exchange capacity (CEC), plasticity, and swelling capacity that swell many times in comparison to its original size [15].

The other method used for the removal of MB dyes from wastewater in the last few years was using the photocatalytic process [16]. Among different kinds of photocatalyst, ZnO is the most

widely used for wastewater treatment due to its high oxidizing properties, super hydrophilicity, and chemical stability [17]. However, this process requires UV-light radiation to promote the electron from the valance band (VB) to the conduction band (CB) and leave the hole (h^+) in the VB. When the hole meets the H_2O molecule in the presence of oxygen, it will produce hydroxyl radical ($OH^\bullet$), and this $OH^\bullet$ will break down the MB dye molecule into a simple compound [16]. But the ZnO has some disadvantages such as instability in acidic media, photo-corrosive nature, spontaneous growth, and aggregation restricts their application in wastewater treatment. To avoid this problem, a suitable material is support to incorporate ZnO particles into porous materials like clay materials [18].

Hence, the present study was focused on the removal of methylene blue dye from an aqueous solution using adsorption and photocatalytic degradation on activated bentonite and ZnO/bentonite nanocomposites. For the present study, the Ethiopia bentonite clay collected from Gewane, Afar Regional State was used as an adsorbent and ZnO/bentonite nanocomposites synthesized by the green method from the precursor zinc nitrate hexahydrate and bentonite using *H. Abyssinica* (Local name Koso) as capping agent is used as photocatalytic degradation of MB dye. The adsorption capacity of the activated bentonite for the removal of methylene blue dye from an aqueous solution was obtained by optimizing experimental parameters. Desorption of MB dye from the exhausted bentonite after adsorption and recyclability of bentonite adsorbent after usage was done by the thermo-chemicals method.

1.2. Statement of the problem

Water is one of the most important resources for sustainable development and core for socio-economic developments, healthy ecosystems, survival of humans, and living organisms. But, the fast growth of industrial activities especially textile industries ends in the generation of organic pollutants that contain organic dyes like methylene blue dye, phenols, and other persistent organic pollutants. Discharging of these organic pollutants can cause serious problems, to the environment and human health due to their carcinogenicity [19]. The removals of these pollutants efficiently from the industrial wastewater make the environment safe for living organisms.

Removal of organic dyes from wastewater is one of the environmental challenges and a public health matter. Azo dyes like MB dye are the most important sources of textile dyes utilized in

industrial applications. Removal of MB dye by conventional treatment methods is difficult due to their stability and non-biodegradable nature hence, different physicochemical methods were developed for removing dyes from wastewater but it's not sufficient for elimination of those dyes [20]. As a result, the only and straightforward method, adsorption as a high-quality treatment process by using adsorbent is the most preferable and desirable method for removal of MB dye.

The well-known adsorbent activated carbon is used for the removal of MB dye from industrial pollutants. This adsorbent is efficient for the removal of MB dye but, it is expensive, and high operating costs limit its usage. However, the low cost and high adsorption efficiency adsorbent like bentonite clay was preferable for the removal of MB dyes. Hence, the present study focused on the investigation of the removal of MB dye from an aqueous solution using activated bentonite clay and its recyclability for water and environmental remediation.

1.3. Objectives of the study

1.3.1. General objective

The overall objective of this study is to investigate the removal efficiency of methylene blue dye from an aqueous solution using sodium carbonate activated bentonite and photocatalytic degradation with ZnO/bentonite nanocomposites.

1.3.2. Specific objectives

The specific objectives of the study are:

i. To activate natural bentonite by sodium carbonate.

ii. To characterize the natural, purified, activated, and used bentonite adsorbents, and ZnO/bentonite nanocomposites by FT-IR, XRD, SEM, and AAS.

iii. To evaluate the adsorption efficiency of bentonite towards methylene blue dye from an aqueous solution by adsorption process.

iv. To investigate the effect of adsorbent dosage, pH of the solution, initial concentration, contact time, and temperature on removal efficiency of methylene blue dye from an aqueous solution using activated bentonite by sodium carbonate.

v. To evaluate the amount of methylene blue dye desorbed from the exhausted adsorbent by thermochemical methods.

vi. To synthesis, ZnO/bentonite nanocomposites using the green method.

vii. To evaluate the photodegradation efficiency of methylene blue dye using ZnO/bentonite nanocomposites.

1.4. Significance of the study

This study will help to develop green adsorbents from locally available clay materials for the removal and recycling of industrials discharge organic dyes for water and environmental remediation.

1.5. Scope of the study

This project work focuses on the activation of bentonite by sodium carbonate for the removal of methylene blue dye from an aqueous solution through adsorption. Desorption study of the adsorbate by thermochemical methods. Characterizations of the natural, purified, activated and used bentonite, ZnO/bentonite nanocomposites (UZBNC11, CZBC11, and CZBC12) by FT-IR, XRD, SEM, and AAS. It also includes the synthesis of ZnO/bentonite nanocomposites for the photo-degradation of methylene blue dye. Also, it is limited to synthetic dye polluted water.

1.6. Outline of the thesis

In a general, this thesis paper consists of five chapters. Each chapter was discussed different issues associated with this study. Chapter one describes a summary of the thesis background, statement of the problem, objectives of the thesis, the significance of the study, and scope of the study. Chapter two focuses on the review from previous studies that were helpful to realize knowledge and to know the study well. Chapter three describes the methods and experimental procedures that were useful for the study. Chapter four presents the result and discussion. The last chapter five provides conclusions and recommendations of the thesis.

CHAPTER TWO

LITERATURE REVIEW

2.1. Wastewater pollutions

Wastewater pollution is a very serious environmental hazard all around the world due to increasing urbanization and rapid industrialization. This pollution is produced by introducing biological and chemical materials either naturally or manufactured to the natural water forms [21]. Different organic, inorganic, and biological impurities are added to water through anthropogenic and natural activities [22]. From these pollutants' wastewater from textile industries becomes a serious impact on pollution due to the increasing demand for textile products is because of the utilization of synthetic dyes [23].

2.1.1. Organic dyes from the textile industry

Naturally, occurring organic dyes were mainly utilized in textile coloring until 1856 using dyes extracted from plants and animal resources. Organic dyes contain aromatic rings in their chemical structures that contain delocalized electrons and also different functional groups. The color of the dye is due to the chromogens-chromophore i.e., acceptor of electrons, within the molecule of dye, and the dyeing capacity of the dye is due to it contains auxochrome groups i.e., donor of electrons. The chromogens are an aromatic structure that normally contains benzene, naphthalene, or anthracene rings carrying binding chromophores that contain double conjugated links with delocalized electrons forming conjugated systems. The groups which mainly act as chromophores are the azo group (-N=N-), methine group (-CH=), ethylene group (=C=C=), carbonyl group (=C=O), carbon-sulfur (=C=S; ≡CS-S-C≡), nitro (-NO_2; -NO-OH), nitroso (-N=O; =N-OH), carbon-nitrogen (=C=NH; -CH=N-), or chinoid groups. The auxochrome groups are ionizable groups, which are responsible for the binding capacity of the dye's molecules onto the textile material. The presence of auxochromes may raise the intensity of dye color. The common auxochrome groups are: -COOH (carboxyl), -NH_2 (amino), - SO_3H (sulphonate) and -OH (hydroxyl) [24].

2.1.2. Classification of textile dyes

The textile dyes classified depend on:

1) Its characteristics application like- acid, basic, mordant, reactive, direct, disperse, sulfur dye, pigment, vat, azo insoluble.
2) Its chemical structure like- nitro, azo, carotenoid, acridine, quinoline, indamine, diphenylmethane, xanthene sulfur, anthraquinone, indigoid, amino- and hydroxy ketone, phthalocyanine, inorganic pigment, etc.
3) Its solubility- such as anionic, nonionic, and cationic dyes supported the overall structure. The main anionic dyes are the direct, acid, and reactive dyes [25]. The most problematic ones are the brightly colored, water-soluble reactive and acid dyes because they cannot be eliminated from textile industry effluents by conventional treatment systems.

2.1.3. Methylene blue dye (MB)

Methylene blue dye is known as methyl thioninium chloride. It is a basic cationic dye with the molecular formula $C_{16}H_{18}N_3SCl$ with a molecular mass of 319.87g/mol. This dye gives a net positive charge when introducing with an aqueous solution because of the presence of chemical groups like amine or sulfur. At room temperature, methylene blue is solid, odorless, dark green powder and gives a blue solution if dissolved in water [26]. This dye is used in several applications like the coating and coloring of paper, hair, cotton, and wool; it is also used as an indicator of oxidation-reduction and as a disinfectant, besides its many other medical usages in medicine, in pharmaceutical formulations, in pesticide production, varnish, and lacquer manufacturing, among others [27]. The IUPAC name of MB dye is 3, 7-bis (Dimethylamino) -phenazathionium chloride, or Tetra methylene blue, the chemical structure is present in Figure 1.

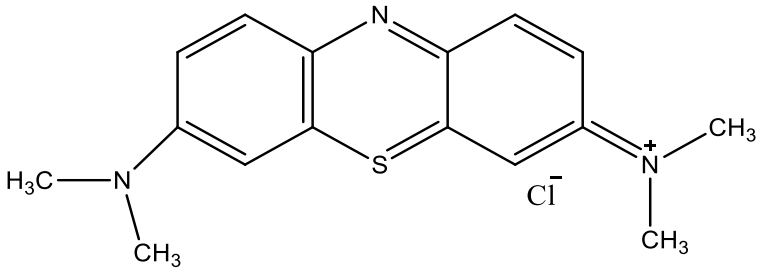

Figure 1: Structure of methylene blue dye

2.1.3.1. Effect of methylene blue dye on living organisms

Methylene blue dye is one of the foremost commonly used dyes within the dyeing of cotton, silk, and wood [28]. MB dye is causing harmful effects on human health; it affects humans eye burns to cause permanent damage to the eyes of animals. Also, inhalation of these dyes results in breathing difficulty by ingestion through the mouth which produces a burning sensation, nausea, and vomiting, abundant and physiological state. To reduce the strength of the possible damages to humans, and the environment arising from the water containing dyes. For the removal of these dyes from the textile industries, there are various types of treatments technologies like adsorption, chemical flocculation, photodegradation.

2.2. Source of wastewater containing an organic dye

The textile industry gets the main contributor to the world economy. This textile industry releases wastewater contains dyes to the environment and water bodies after its usage. As a result, the pollution level of wastewater contains dye from this industry is greater and maintainable issues should be considered at each point of the source level. The textile industry manufacturing a large amount of wastewater contains dyes that have a high contaminating footprint, and it is estimated that up to 200 thousand tons of dyes are discharged into water bodies because of insufficient wastewater treatment processes [29]. The water that contains dyes within the environment is taken into account as a harmful source of pollution for organisms. The discharging of organic dyes from the textile industry are polluting agents to the environment and water bodies due to their complex and non-biodegradable chemical structures which have harmful effects on both aquatic life and human beings [30]. Discharging such wastewaters in streams and aquifers may also hamper reoxygenation and stop aquatic life photosynthesis [31]. Figure 2 shows the wastewater contains dyes from the textile industries.

Figure 2: Dye-containing wastewater from textile industries

2.2.1. Harmful consequences of wastewater containing dyes

The releasing of wastewater contains dyes to the rivers and streams severe problems to the food cycle, aquatic life, and affects aesthetic nature. Also, dyes can absorb sunlight and reflect light while entering the water, so can hinder bacterial growth and resist photosynthesis in aquatic plants. Moreover, they resist aerobic biodegradation, causing the challenge to environmental researchers [32]. Hence, dye-bearing wastewater poses a significant hazard to aquatic life and human health and causes skin irritation, allergic dermatitis, mutation, cancer, shortness of breath, produce a burning sensation. Wastewater from different textile industries contains organic dyes,

biochemical oxygen demand (BOD), chemical oxygen demand (COD) in high concentration, an enormous number of suspended solids, and other contaminants [33]. Dye molecules are stable to the UV light and can't biologically degrade easily. These molecules are immune to aerobic digestion and are difficult to get rid of from industrial wastewater [34]. To keep the essentiality of color removal, industries require some efficient and precise methods to treat wastewater that contains organic dye before discharging into environments and water bodies. Figure 3 shows the effect of wastewater contains dyes.

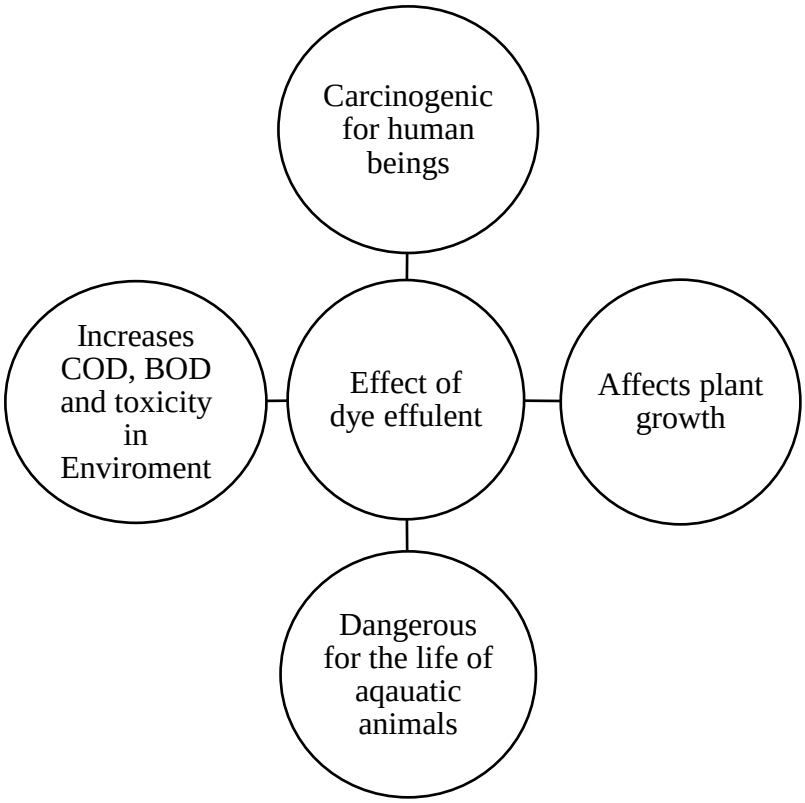

Figure 3: Effects of textile dye effluents on our surroundings and living organisms [19]

2.3. Removal of organic dye from wastewater by different methods

Dyes are used in large amounts in various applications including textiles industries, healthcare, paint, printing, leather, and food processing, to color their products. But, a small amount (10–20%) of a dye is used in the process, and the rest of the dye ends up in wastewater produced by dye-using industries [35]. To avoid these dyes contaminant from water resources and the environment, the event of some eco-friendly and efficient methods for removal of it from

industrial wastewater is very desirable before they're released into freshwater reserves [36]. Different methods include: membrane process, adsorption, photocatalytic degradation, osmosis; coagulation/flocculation, natural process, and flotation are used usually for the removal of organic dyes from wastewater and natural water bodies. The choice of the treatment process for contaminated water depends on the character of pollutants. Some methods have some disadvantages like high operating expense, incomplete removal of waste, and high energy requirements [37].

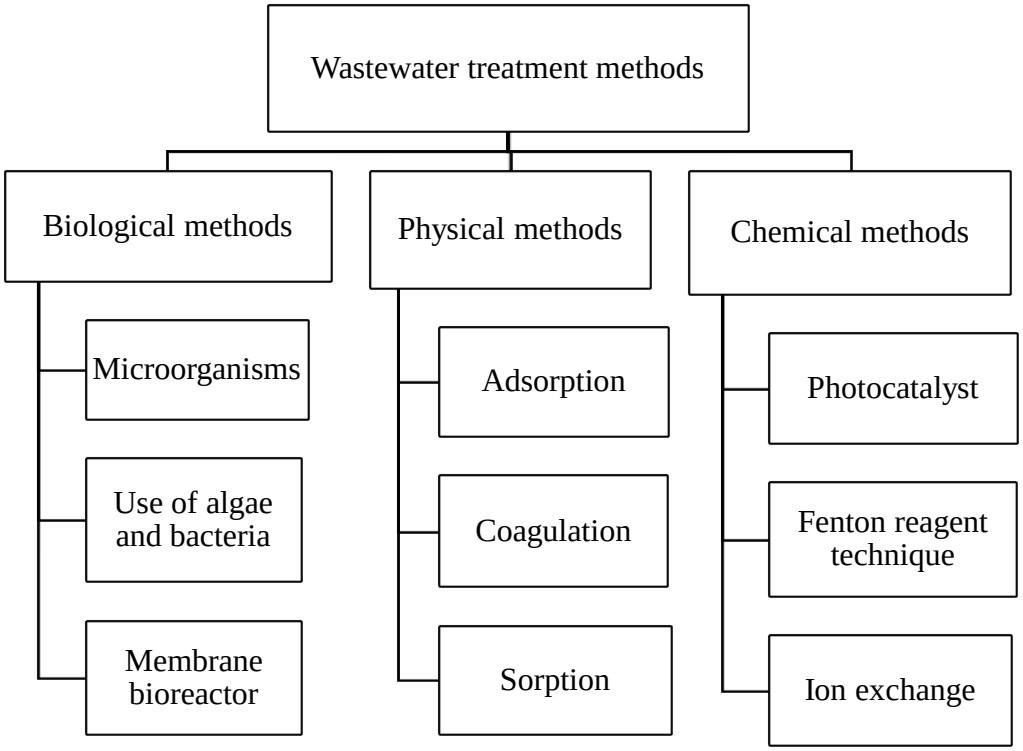

Figure 4: Methods of wastewater treatment [35]

2.3.1. Biological methods

These treatment methods are often the most economical alternative when compared with other physical and chemical processes. Methods like using fungal, microbial, adsorption by (living or dead) microbial biomass and bioremediation systems are commonly applied to remove organic dyes of industrial effluents because many microorganisms such as bacteria, yeast, algae, and fungi can accumulate and degrade different dyes [38]. This method is acceptable to eliminate dissolved organic materials from textile effluents. The removal efficiency of those materials

depends on organic load ratio versus dye load and a load of micro-organism, range of temperature, and concentration of oxygen [39].

2.3.2. Chemical methods

Chemical methods include advanced oxidation methods using Fenton's reagent, hydrogen peroxide, ozonation, solvent-extraction method, photocatalyst, ion exchange, and oxidation. These methods include an advanced oxidation process, which is based on the mechanism of hydroxyl radical's generation. These radicals are used as oxidizing agents. Organic peroxide radicals are generated by attacking chromogenic groups. Similarly, H_2O, CO_2, and inorganic salts formation also happen as a result of these chemical reactions. Using hydrogen peroxide attained a prominent position among oxidizing agents due to its commercial availability and its oxidative nature. It's used for the oxidation process directly or together with catalysts or with UV radiation. However, some drawbacks are found with its use because it fails to oxidize some organic pollutants [40].

2.3.3. Coagulation-flocculation methods

This technique is widely utilized in the solid-liquid separation procedure for completely remove dissolved and suspended solids, organic matter, and colloids present within the industrial wastewater. Coagulation-flocculation is an efficient and straightforward technique that's extensively utilized in the treatment of several wastewater effluents like vegetable oil mill effluent, pulp mill, and textile wastewater. Dispersed or finely divided particles are gathered to make the massive particles (flocs) when coagulants or flocculants are added they calm down and clarify the system [41].

2.3.4. Physical methods

Physical methods include the method of adsorption of adsorbate on adsorbents materials includes: clay, activated carbon, agricultural waste, and industrial adsorbents, surfactant, sorption, electro-kinetic coagulation, and coagulation-flocculation [14].

2.3.5. Electrocoagulation methods

The electrocoagulation process is a simple, reliable physicochemical technique and an efficient tool for the removal of organic dyes from an aqueous solution. It contains 3 stages, in 1^{st} stage, oxidation of sacrificial anodic electrodes then generation of coagulants occurs. 2^{nd} stage involves

the destabilization of pollutants and their emulsions escape. Within the 3rd stage formations of flocs occur. This method contains coagulants formation within the reactor site without using the assistance of an external agency by the oxidation of sacrificial anodic electrodes like aluminum, chrome steel, iron, and lots of others. The method is found to be quite effective in the removal of contaminants, colloidal particles, metal ions, and dyes [42]. But this treatment produces foul odor and by-products and is the type of expensive method. Among all treatment techniques for the removal of pollutants from wastewater, adsorption is found one of the most attractive techniques to treat contaminated water which has a prevalence in developing countries [43]. The benefits and drawbacks of various methods for the removal of organic dyes from wastewater are mentioned in Table 1 below.

Table 1: Wastewater treatment methods, their advantages, and disadvantages during the treatment [44]

Treatment methods	Advantages	Disadvantages
i. Chemical methods		
Ozonation	No sludge generation	Operational cost is very high, the half-life is short (20 min)
Photocatalyst	Operational cost is low and economically feasible	Some photocatalyst degrades into toxic by-products
Fenton reagent	Low-priced reagent and efficient procedure	Disposal issues and sludge production
ii. Biological methods		
Anaerobic degradation	By-products can be used as energy resources	Under anaerobic conditions require more treatment and yield of methane and hydrogen sulfide
Aerobic degradation	Operational cost is low and effective in the removal of azo dyes	Provide a suitable environment for the growth of microorganisms and very slow process
iii. Physicochemical methods		
Adsorption/sorption	High adsorption capacity for all dyes	Low surface area for some adsorbents, high cost of adsorbents
Ion exchange	No loss of sorbents	For disperse dyes not effectively
Electro-Coagulation	Economically feasible	Need further treatments by flocculation and filtration and production of sludge

2.4. Treatment of wastewater containing organic dyes by adsorption process

2.4.1. Adsorption process

Adsorption is the process at which atoms, ions, and molecules are attached to the surface of the adsorbent. The layer of adsorbate (atoms, ions, & molecules) to be adsorbed is made on the adsorbent (material which adsorbs). Adsorption takes place on the surface of the adsorbent and covers the whole surface of the adsorbent. The process takes place due to physical forces (physisorption) and chemical forces (chemisorption) due to chemical bonds, between adsorbate and adsorbent [45].

Among many treatment techniques, adsorption is gaining importance as a process of treating aqueous effluent. It's the simplest technology for the decontamination of water and the removal of just about all kinds of contaminants. This physicochemical technique has the benefits of getting the supply of known process equipment, low-cost, recovery of adsorbent, and sludge-free operation [46]. This method is the top-quality treatment process for the removal of dissolved organic contaminants like dyes from wastewater. During this process, the concentration of adsorbed substance takes place on the surface of solid bodies or adsorbent materials deals with the operation of surface forces. When adsorbable solute, also referred to as adsorbate, in solution, attaches a solid (adsorbent) with a highly porous surface, then liquid-solid intermolecular forces of attraction cause the adsorbable molecules to be concentrated at the surface of adsorbents. Adsorption has gained interest for dye removal due to its flexibility in design, low price, and this method does not generate any harmful substances after removal of the target compounds make the method are preferable. Removal of waste is often suffering from a specific surface area, adsorption capacity, grain size, pore-volume, and pore size distribution. In the present years, various commercially available and cost-effective adsorbents are used for the removal of dyes from textile wastewater [47].

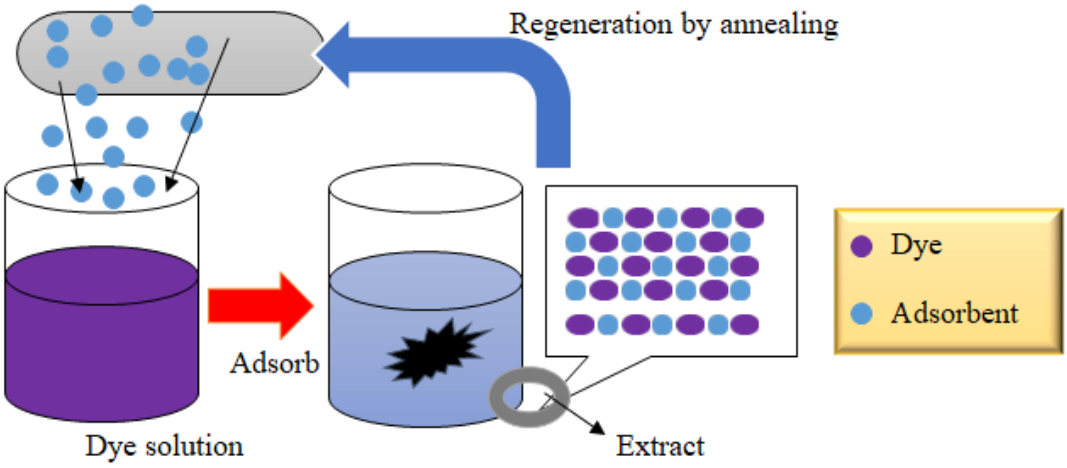

Figure 5: Process of adsorption of organic dye from wastewater [46]

2.4.2. Adsorption mechanism

The adsorption takes place by physical and chemical binding like; Van der Waals forces, electrostatic interactions, hydrogen bonding, and hydrophobic interactions. According to [48], the adsorption process can be followed by three steps:

a) The adsorbate (dye) transfer from the bulk solution to the adsorbent surface. This means molecules (adsorbate) diffuse into the thin layer of fluid (called fluid film) which is attached to the adsorbent.

b) Adsorption on the dyed surface: - Consistent with the development of diffusion, the surface diffusion process attached the vapor or gas along with the pores. It is called mixed diffusion because there contains two diffusions of pore diffusion and surface diffusion. The bulk adsorption occurs within the pores of the adsorbent where the major available surface area is out there. Hence, the adsorbate is migrating from the external area into the pores within each adsorbent particle.

c) Transport the adsorbate within the adsorbent particle**.**

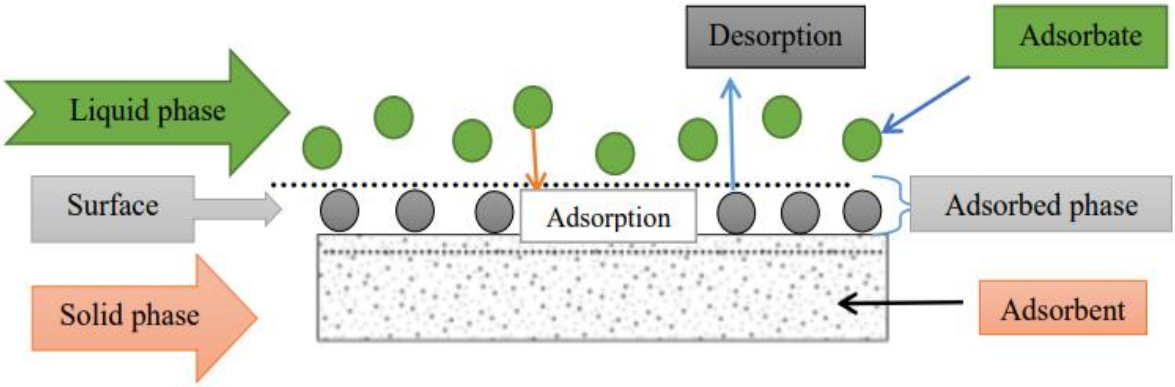

Figure 6: Adsorption mechanisms and desorption process [48]

2.4.3. Parameters affecting the adsorption process

2.4.3.1. Effect of initial dye concentration

Adsorption capacity with the adsorbent increases with the rise of dye concentration till saturation is reached. Initial dye concentration generates a big driving gradient force to overwhelmed mass transfer resistance to the dyes between solid and aqueous phases [49].

2.4.3.2. Effect of pH

The adsorption capacity of dyes depends on the pH of the solution. The initial pH of the dye solution is known to affect the adsorption process of dye removal. The initial pH is known to be affected by various factors such as surface charge of the adsorbent, degree of ionization of the adsorbed molecule, and the extent of dissociation of functional groups on the active sites of the adsorbent. As the previously reported study indicated the removal efficiency of MB dye is low at a low pH range but is known to increase at a high pH range. The minimum removal efficiency of MB dye was observed between pH 1.5 and pH 3. However, no significant change in the removal efficiency of MB dye was observed at higher pH values. The lower removal efficiency of MB dye at low pH may be due to the availability of excessive H^+ ions that may compete with the cationic dye for adsorption sites as reported by [50], on Moroccan clay.

2.4.3.3. Effect of contact time

Adsorption of dye was found to extend with a rise of your time over bentonite adsorbent. The quantity of dye adsorbed on clay was found to be fast at the initial period of contact time then become slow and stagnant with the rise in contact time; the mechanism of adsorbate removal is

often described within the migration of the dye molecule from the solution to the adsorbent particle and diffusion through the surface [51].

2.4.3.4. Effect of adsorbent dosage

The amount of bentonite dosage significantly affects the adsorption capacity of dyes from the aqueous solution. With increasing the dosage, the removal efficiency was found to increase due to the increased availability of adsorbent surface sites during increased adsorbent particles. The effect of the adsorbent dosage estimates the adsorption capacity of the adsorbate [52].

2.4.4.5. Effect of temperature

With the rise in temperature, the removal efficiency of cationic dyes increases [53]. By increasing temperature, the adsorption of dyes over adsorbent increased due to the increased kinetic energy of molecules. When the temperature of the solvent increased, the number of adsorbent pores also increased with temperature, and therefore the adsorption procedure is positively affected [54].

2.4.5. Adsorbents

2.4.5.1. Definitions of adsorbents and it's characteristics

The adsorbent is a solid substance that sometimes adsorbs gas, liquid, or dissolved substance on its surface. They're utilized in the shape of spherical pellets, rods, moldings, or monoliths. Adsorbents must have high abrasion resistance, high thermal stability, and little pore diameters, which ends up in a higher exposed area and hence the high capacity for adsorption of substance on its surface. In recent years, the utilization of clay materials to exchange commercially available adsorbents has attracted much attention due to their low cost, availability in every place, high specific surface area, lack of toxicity, and potential for the natural process [55]. Their particular properties like high specific surface area, and surface chemistry, a spread of surface, and structural properties, chemical, and mechanical stabilities give these materials have many applications [56]. Characteristics of good adsorbents [57] include:-

- It's locally available.
- Its cost must be economic.
- It does not give other side effects after the operation.
- It must be a simple operation.

- It should readily acceptable by the users.

2.4.5.2. Adsorbents for removal of organic dyes from wastewater

The adsorbent is an insoluble sponge-like porous material with the capacity to trap adsorbate elements onto its surface. Natural materials and sometimes waste materials are used as adsorbents for the removal of dye from textile wastewater [58]. Some high adsorption efficiency and low-cost materials are often used as adsorbents for dye removal from wastewater as listed in Table 2.

Table 2: Advantages and disadvantages of different adsorbents for adsorption of organic dyes from textile wastewater

Adsorbent	Advantages	Disadvantages	References
Activated carbon	High specific surface area	High cost	[59]
Bio-sorbents	High adsorption capacity	High market cost	[60]
Agricultural and industrial by-products	Available in abundance	Sorption properties depend on the origin	[61]
Bentonite	High specific surface area, high cation exchange capacity, and low-cost	Needs modification for adsorption of anionic dye	[62]
Zeolite	High ion exchange capacity and specific surface area	Complex sorption mechanism	[63]

2.5. Bentonite clay and its structure

Bentonite clay, mainly composed of montmorillonite (MMT), with a 2:1 structural sheet i.e., two tetrahedral silica sheets sandwiching a central octahedral alumina sheet (TOT). The clay surface layers have a negative crystal charge due to an isomorphic substitution within the layers (e.g., Al^{3+} for Si^{4+} in the tetrahedral sheet and Fe^{2+}or Mg^{2+} for Al^{3+} within the octahedral sheet) which is balanced by exchangeable cations such as Na^{+}, K^{+}, Ca^{2+} within the interlayer alongside water

molecules bonded by ion-dipole forces [64]. This ensures the great performance of clay during adsorbing cationic pollutants via cationic exchange. These inorganic cations are often substituted for a cationic surfactant or hydroxy metal, producing materials like organo-bentonite and pillared bentonite.

Bentonite features a great affinity towards the cationic dye due to the attraction of negative charges on the surface of the bentonite adsorbent and positive charges on the adsorbate. Different properties are obtainable in bentonites like the high specific surface area, swelling capacity, and cation exchange capacity [65]. Bentonite is mainly composed of SiO_2, Al_2O_3, CaO, Na_2O, K_2O, MgO, Fe_2O_3, FeO, MnO, and TiO_2. The cation contents between the interlayer divide the bentonite into; either Na or Ca bentonite. sodium bentonite (has swelling properties), has a single water layer containing Na^+ as exchangeable ions, and calcium bentonite (a non-swelling mineral) with a double water layer containing Ca^{2+} exchangeable ions [66]. Ca-bentonite is an efficient adsorbent of ions not only in solution but too in fats and oils. Na-bentonite, when added to water; adsorbs several times as its dry mass find in water and become larger when it is wetted, it's vital due to its extremely good colloidal properties. It's utilized for environmental and geotechnical study via drilling fluid for gas wells and oil [67]. On the other hand, Na-bentonites have different applications due to their layered structure, high CEC, ability to swell, and their high platelet ratio. Inorganic cations are present on the basal plane of montmorillonite layers, which makes them hydrophilic. However, cation-exchange reactions are traditionally employed as a way to exchange these inorganic cations with organic surfactant cations, which intercalate into the clay layers resulting in a rise within the basal space diameter. This not only changes the surface properties to hydrophobic but also facilitates penetration of the polymer between the clay layers [68].

Bentonite has the chemical composition and formula of the extreme montmorillonite unit cell of the series $(Al_{3.33}Mg_{0.67})\ Si_8O_{20}\ (OH)_4\ M^+_{0.67}$, where M^+ may be a monovalent cation. This formula indicates that the unit cell has a negative electric charge due to the isomorphic substitution of Al^{3+} by Mg^{2+}. The M^+ cation that balances the negative charge is called an exchangeable cation, since it is often reversibly exchanged for other cations (depending on the cation) [69]. The structure of bentonite is indicated in Figure 7.

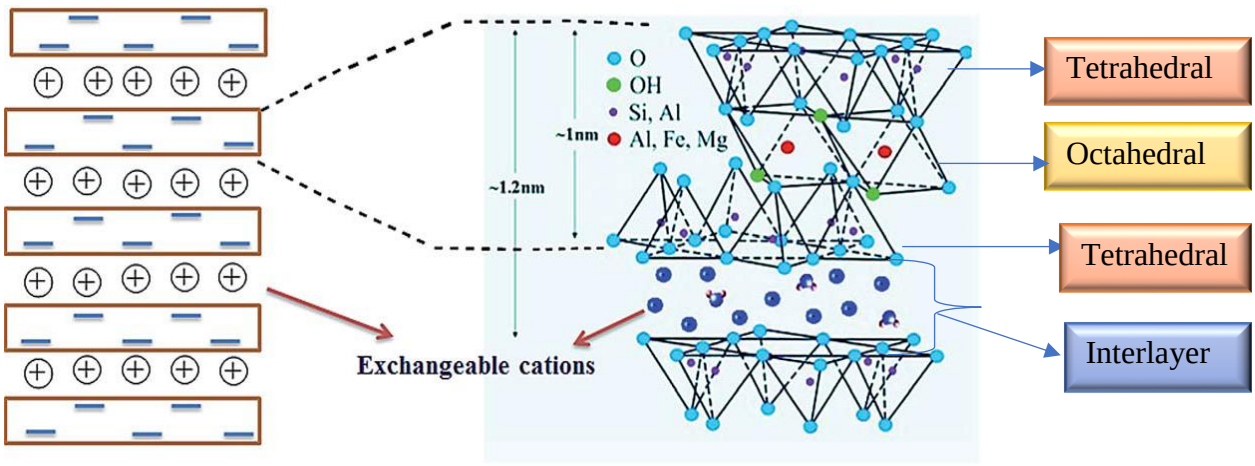

Figure 7: Structure of bentonite clay [70]

2.5.1. Bentonite clay in Ethiopia

Bentonite clay resources are found within the Afar, and Southern, Nations, Nationalities, and People's Regional States. The Afar Regional State bentonite occurrences are easily accessible, as they are located near the main road. Most occurrences in Afar are located at Warssiso, Hadar, Gewane, and Ledi. The Warssiso bentonite deposit is located at 500 Km from Addis Ababa to Semera main roads and 0.7 Km-3.0 Km towards the north, between Badona River and Warseiso. Gewane is located 376 Km northeast of Addis Ababa to Semera main road, Gewane bentonite deposit on 15 Km Gewane town [71].

Table 3: Location of bentonite deposits (source: *www.mome.gov.et* (Ministry of Mines of Ethiopia))

Area (province)	Location of deposits	Easting	Northing	Resource (million tons)
Afar	Gewane Bentonite	40° 38' 05"E	10° 17' 50"N	126
Sidamo	Gidicho Bentonite	37° 56' 00"E	06° 24' 00"N	5
Afar	Warsissa Bentonite	40° 39' 00"E	11° 22' 20"N	10.5

2.5.2. Properties of bentonite clay

Bentonites are lamellar aluminosilicate possessing a good range of physicochemical properties like swelling, adsorption, ion exchange, and surface acidity [72]. It's a heterogeneous rock formed highly from the colloidal and plastic smectite group, composed mainly of

Montmorillonite (MMT) [73]. Minerals of the smectite group have exchangeable cations, which are easily substituted with other cations which create adsorption capability on sheet surfaces these cations can be replaced reversibly. Montmorillonite, the most component of bentonite, feature a high cation exchange capacity, which is small suffering from particle size [74].

2.5.2.1. pH of bentonite clay

The pH of soils and clays is commonly determined by electrometric measurement of the pH value of a clay suspension or clear supernatant after centrifugation or filtration. The pH of a clay suspension strongly influences its technical applications and some essential properties including, adsorption and rheological properties [75].

The pH value of clay can be used to predict the dominant cations on soil-cation exchangers pH 2-3 indicates the free mineral acids, pH 4-5 indicate the exchangeable Al^{3+} and Fe^{3+}, pH > 5.5 indicates the Al hydroxide ions/polymers, pH 7.6-8.3 indicates the presence of $CaCO_3$, and pH > 9 indicates the presence of Na_2CO_3 in clay minerals. This classification refers mainly to Al speciation and the presence of carbonates does not take into account, possible effects of Na^+ ions compared to Ca^{2+} ions at the surfaces of swelling clay minerals. The pH of bentonite suspension is decided by a minimum of two parameters. The effect of carbonate dissolution on the pH of a solution is well familiar and calculated easily. In addition, Ca^{2+} is known to be more acidic than Na^+, due to hydrolysis [76].

The hydrolysis of montmorillonite, caused by an exchange of Na^+ for H^+ from water molecules, leaves OH^- in solution and thus increases the pH. Also, the type of interlayer cation of swelling clay minerals (particularly Na^+) is more important concerning pH than the carbonate content [77]. The typical pH of Ca-bentonite suspensions ranges from seven to eight (7-8) in contrast to Na-bentonites with pH values starting from nine to ten (9 to 10). This trend is not mattered regardless of the carbonate concentration. Generally, the effect of the type of clay mineral, or to be more precise, the exchangeable cations, on pH at high solid-liquid ratios (e.g. 2% w/w suspension) dominates over the effect of carbonate content.

2.5.2.2. Cation exchange capacity (CEC) of bentonite clay

Cation exchange capacity is a measure of the clay's ability to hold positively charged ions. During the process, cations bound to clay particles are dissolved in clay water. Then cations in

clay water are attracted and bound to clay particles, due to the surface of clay were negatively charged and attract positive cation. This process is called the cation exchange process. The clay minerals and a few organic materials found in clay materials can carry adsorbed cations and anions which are exchangeable for other ions by simple treatment, usually an aqueous solution. This sorption from solution is generally considered an easy exchange process [78].

The physical properties of clay materials depend to some extent on the character of the adsorbed or exchangeable ions carried by the clay mineral components. Hence, sodium bentonite is probably possessing different plastic properties than calcium bentonite. This difference is going to be great or small counting on the CEC of the clay. Also, the relative abundance of the adsorbed ions present is vital in determining their properties. The very fact that adsorbed ions can significantly alter the properties of clay provides a possible way of altering those properties to suit a specific function [79]. The stacking of the structural layers of clay is governed by relatively weak polar and Van der Waals forces and, between these layers, there are gaps called galleries or intermediary layers during which the exchangeable cations, like Na^{+}, Ca^{2+}, and Li^{+}, are fixed electrostatically. The main ions associated with CEC in clays are the exchangeable cations like calcium (Ca^{2+}), magnesium (Mg^{2+}), sodium (Na^{+}), and potassium (K^{+}), and are generally referred to as the base cations.

There are different methods for the determination of the CEC of clays. Most of the methods involve natural cation exchange with the clay minerals include cationic species like ammonium, K^{+}, Na^{+}, methylene blue, Co (III) hexamine complex, Ba, Mg, Ag thiourea complex, Cu (II) complex of ethylene diamine, followed by the removal of their excess species [80]. There are four most known methods to determine and evaluate the CEC of clays: (a) conventional NH_4-Na exchange, (b) methylene blue capacity with MB acid, (c) CEC of tetrasodium pyrophosphate (TSPP), and (d) MB-water filter paper spot test titration methods [81].

The values of CEC depend upon the used method. However, the determination of CEC values is usually tough and time-consuming within the process to realize an ideal cation exchange. But, the utilization of a much simpler and time-saving method methylene blue test is used to characterize the CEC, swelling potential, specific surface area, and smectite content of clay deposits [82]. MB is a large polar organic molecule with a positive charge that's adsorbed onto the negatively charged surfaces of the adsorbent. Its high selectivity for adsorption by smectite

and is additionally adsorbed by the smectite component of mixed-layer clays but is essentially unaffected by other clay minerals [79]. The exchangeable cation contents in clay are expressed in milliequivalents (meq) of the cation per 100 g of clay. It is determining by Equation (2.1);

$$\mathrm{CEC} = 100 * \frac{\mathrm{VMB}}{\mathrm{ms}} * \mathrm{NMB} \qquad (2.1)$$

Where CEC is the cation exchange capacity of the soil (meq/g), m_s is the mass of the clays adsorbent used (g), V_{MB} is the volume of methylene blue (L), and N_{MB} is the normality of the methylene blue (meq/100g).

The previous work done by [83] indicates the montmorillonite sandwich clay with the 2:1 layer linkage, has a high cation exchange capacity (CEC) ranging from 70 to 130 meq/100 g, most of which is due to the isomorphous substitution of its main cations, Si^{4+} and Al^{3+} within the structure with cations of lower valence, but a lesser amount is due to the charges at the edge of the sheets. These substitutions mainly take place in the octahedral sheets and may induce an enormous change in the physicochemical properties of clay minerals. The CEC for bentonite clays was done by different researchers and methods as shown in Table 4.

Table 4: Cation exchange capacity of bentonite clay with different methods

Adsorbent	CEC in (meq/g)	Methods	Reference
Raw bentonite	61.44	Ethylene di-amine copper complex ($Cu(EDA)_2Cl_2$)	[84]
Raw bentonite	41.67	Methylene blue titration spot test	[85]
Raw bentonite	95	-	[86]
Raw bentonite	67.32	Methylene blue titration spot test	[87]
Raw bentonite	108	NH_4OAc	[88]
Clay	145	Methylene blue titration spot test	[89]
Activated bentonite by Na_2CO_3 (AB5)	137.5	Methylene blue titration spot test	This study

2.5.3. Activation of bentonite

Bentonite adsorbent extremely has a rough surface, formed from volcanic ash. It has different applications in different areas such as in wastewater treatment. There are two types of bentonite

either Na-bentonite or Ca-bentonite. Abundantly presented bentonite is calcium bentonite, which has hydraulic conductivity above sodium bentonite. The properties of calcium bentonite are often modified to some extent by processing like removing impurities or 'activating' by additives. Additives include dispersants, flocculants, or gelling agents [90]. The abundantly available calcium bentonite is treating with different sodium compounds like NaOH, NaCl, Na_2CO_3, and Na_2SiO_3 to obtain Na-bentonite. The obtained Na-bentonite has preferable properties for the adsorption of pollutants from wastewater. The exchangeable Na^+-bentonite imparts many beneficial properties, including water absorption, dispersion, and sealing, all these properties make sodium bentonite particularly fitted to use in different applications. Na-bentonite is employed as a component of prefabricated liners due to its high swelling and low permeability. The very low permeability of Na-bentonite is obtained due to its small particle size, shape, and subsequent micropores, and enormous negative surface charge [90].

On the other hand, polycationic bentonite clays are often changed to Na-bentonite by a reversible double-exchange reaction using Na_2CO_3, since the interlamellar distance within the bentonites is higher when the lamellae have their charge compensated by the sodium ion, of lower valence, allowing the penetration of a greater amount of water within the space between the lamellae. This explains why the expansion capacity of sodium bentonite is far above that of calcium bentonite [69]. The bentonite activation process by Na_2CO_3 is often simply expressed by an Equation (2.2):

$$Ca^{2+} - MMT + 2\ Na^+ \leftrightarrow 2\ Na^+ - MMT + Ca^{2+} \qquad (2.2)$$

From the point of view of the economy, the widely available sodium carbonate (Na_2CO_3) is used for activation of Ca-bentonite to get Na-bentonite. Multivalent (Ca^{2+}, Mg^{2+}) less hydrated cations operate coagulating while on the contrary, the monovalent hydrated cations (Na^+) operate dispersingly, i.e., they prevent the agglomeration of particles (increasing swelling). Among the main reasons why the Na_2CO_3-activation are important includes:

a) High swelling – more swelling bentonite features a higher strength within the water condensation zone (wet tensile strength) what allows to scale back the bentonite content.
b) The susceptibility of bentonite mixtures to over moistening decreases (higher resistance to a dry).

c) The reduction of warmth stress of the mold from braked thermal expansion of the bottom sand (SiO_2). During dehydration, the montmorillonite clays begin to shrink under lower temperatures (the reduction of stress and therefore the increase of the resistance to defects caused by stress).
d) The growth of the binder thermostability (temperature of the clay dihydroxylation [91].

2.6. Application of bentonite clays and their composites

Bentonite is widely utilized in various industrial products and processes like pharmaceuticals, cosmetics, and drilling fluids to switch the rheology and control the steadiness of systems [92]. Bentonite is used as a plasticizer in ceramics, as an emulsifying agent in asphaltic substances, as thickener and extender for paints, as adhesive in concrete mixtures, horticultural sprays, and insecticides, also used as the adsorbent for removal dyes and heavy metals from wastewater, and bleaching clay in refining oils and fats [93].

2.6.1. Bentonite clay as adsorbent of waste pollutants from wastewater

Bentonite is the most extensively used adsorbent [94]. It exhibits different exclusive properties like high cation exchange capacity, adsorption capability, porosity, high specific surface area, and structural properties. It's impermeable, plastic, and highly viscous when suspended within the water. Bentonite clay is usually utilized in applications of water decontamination. It's available in most regions of the planet [62]. Natural bentonite clay is employed for the removal of various contaminants from wastewater due to its low cost, easy availability, and eco-friendly nature [95]. Several cationic dyes were adsorbed through bentonite clay, due to its negative surface charge [96]. So far, bentonite clay could probably be utilized for the dye's removal because of its capacity, abundance, obtainability, and economic benefits.

2.6.2. Bentonite clay nanocomposites for wastewater treatment

Composites are materials made up of two or more materials with significantly different physical and chemical properties which remain separate and distinct at the microscopic or macroscopic scale within the material. Composites are synthesized to mix the specified properties of the materials within the composite. In nanocomposite, nanoparticles like clay, metal, nanotube, etc. act as fillers during a matrix. Nanoparticles are particles that have 1-100 nm in diameter that exhibit new or enhanced size-dependent properties compared with larger particles of equivalent

material. Clay nanocomposites are materials during which a serious component of the material is clay together with other materials like metals, polymer. Minimal additions of nano-clay enhance mechanical properties, thermal properties, dimensional, and barrier performance significantly because of the massive contact area between polymer and clay on a nanoscale [97]. Bentonite-nanocomposites are used as adsorbents for the removal of waste pollutants from wastewater by different researchers as shown in Table 5.

2.6.2.1. Fe_3O_4/clay nanocomposites in wastewater treatments

Magnetite (Fe_3O_4), the foremost commonly studied material due to the outstanding properties they exhibit on a nanometric scale, including high specific surface area, super-para magnetism [98]. Materials that have 1-100nm dimensions are often developed to enhance the standard and functionalize the surfaces to be used in applications for environmental and biomedical. Also, magnetic nanocomposites are developed for sensor, adsorption, catalytic, and photocatalytic applications.

Magnetic iron oxide nanoparticles (MNPs) could also be good candidates to be used within the development of high-capacity adsorbents and photocatalyst. With their saturation magnetization, magnetic iron oxide-based nanocomposites provide a low-price approach for adsorption and photocatalysis through their reusability and simple regeneration. A material's selectivity or affinities for a specified contaminant are often enhanced by modifying its surface and mixing it with features of solid supports. MNPs conducted in biomedical and biological applications due to the material's property are often tailored by setting synthesis parameters [99]. Some solid supporters like zeolite, biochar, clay, carbon nanotube, and mesoporous silica are reported as supporters of magnetic nanoparticles. The clay and clay minerals have potential supports and materials which were combined with magnetic properties and MNPs. The clay features a high adsorption capacity and it attracts and holds cations, like heavy metals and cationic molecules [100].

Properties of magnetic iron oxide/clay nanocomposites (MICNCs) depend upon their source, minerals contents, and the parameters governing their synthesis [101]. The silicate layer of clay structure, CEC, and pore size distribution of nanocomposites affect critical features for specified purposes in water treatment. In wastewater treatment, MICNCs are widely used for the removal of pollutants from aqueous solutions, either by adsorption, photo-oxidation, or chemical

oxidation processes. The reduction and removal of contaminants, including chemical constituents, like dye, heavy metals, and other organic pollutants from water, are reported [102].

2.6.2.2. Treatment of wastewater by using magnetic iron oxide/clay nanocomposites via adsorption

The use of MICNCs for the treatment of wastewater via adsorption is more dominant than photocatalysis and advanced oxidation processes (AOPs). The component of the adsorptive properties of clay minerals with the magnetic properties of MNPs to supply novel MICNCs adsorbents is a promising technique for the removal of pollutants from water [102]. The surface of materials needs modifications to reinforce the adsorption capability of MICNCs, mainly through surface functionalization. The appliance of surfactants, polymers, and other compounds containing functional groups onto nanocomposites is effective for attracting the adsorbate. The adsorption behavior, studies have adopted adsorption isotherm models, including the Langmuir, Freundlich, and Temkin models. The following are the main mechanisms for the adsorption of organic dyes [102].

1. π-π interactions: are available for surface-modified MICNCs, especially by the surfactant. Additionally, chemical bond formation between MICNCs and double bonds of the organic dyes is typically both present together.
2. Hydrogen bonding: is corresponding to the interaction between the hydrogen of the hydroxyl (-C (O)-OH) in dyes and the oxygen atoms within the tetrahedral layer of the montmorillonite surface. Hydrogen bonding dominates when there's an adsorbed material electrophilic element within the functional group, like the nitrogen, for instance, -N $(C_2H_5)_2$ or the oxygen atom.
3. Lewis's interaction: is occurs when the nitrogen atom within the dye, which acts as the Lewis bases and combines with the Al^{3+} and Fe^{3+} ions which acts as the Lewis acid on the MICNC surface. This molecular dynamic of this interaction is simulated by Ouachtak for the adsorption of rhodamine B and has also been found within the adsorption of picloram herbicide by pillared montmorillonite.

2.6.3. Bentonite clay and its nanocomposites for removal of methylene blue dye from wastewater

Pollutants are removed from wastewater using different types of adsorbents in the past decades and nowadays. Bentonite's clay can extensively use for the removal of cationic dyes due to its strong adsorption and complexation capability. Bentonite is the most recognized and best from clay utilized in water purification. Table 5 shows some previous studies on adsorption by bentonite clay adsorbent to get rid of methylene blue from the wastewater.

Table 5: Removal of methylene blue dye from aqueous solution by bentonite clay adsorbent and its nanocomposites by a different researcher

Adsorbent	Pollutants Removed	Adsorption capacity (mg/g)	pH	Con. (mg/L)	Cont. time (min)	Temp (ºC)	Ref.
Fe_3O_4/ bentonite nano composites	MB	1666.7	5	-	150	25	[103]
Na-bentonite	MB	198.71	10	-	-	25	[104]
TiO_2-WO_3-bentonite composite	MB	70.9	11	-	-	35	[105]
hybrid activated bentonite/ alginate composites	MB	780	7	100	-	25	[106]
lignocellulose-g-poly(acrylic acid) / montmorillonite (LN Cg-PAA/MMT) hydrogel nanocomposites	MB	1994.38	5	2,500	120	30	[107]
Cationic surfactant (HDTMACl) organoclay	MB	399.74 μmol/g	9	-	-	-	[108]
Acid activation Clay	MB	500	-				[109]
5% Na_2CO_3 activated / 100g bentonite	MB	114.90	7	230	30	25	This study
ZnO/bentonite nanocomposites	MB	39.93	7	80	30	25	This study

2.6.4. ZnO/bentonite nanocomposites in wastewater treatment

There are different developments in nanoscience or nanotechnology in which nanoscale materials are synthesized with the capacity to change harmful pollutants into less/non-harmful

shown pollutants. Heterogeneous photocatalysis being free from toxic, highly efficient, and effective technology is regarded as showing great potential technology to address environmental challenges in past years [17].

2.6.4.1. ZnO/ nanocomposites as photocatalyst

Photocatalysis is one of the advanced oxidative processes whose principle involves the activation of a catalyst through sunlight or artificial light. The process consists of the absorption of photons with energy higher than the bandgap energy of the semiconductor that generates electron/hole (e^{-}/h^{+}) pairs in the conduction (CB) and valance bands (VB) of the semiconductor. The photogenerated e^{-}/h^{+} pairs will take part in the redox reactions to produce the final products [110].

Different semiconductor metal oxides like ZnO have a higher bandgap for the excitation of electrons from the valence band (VB) to the conduction band (CB) and require high-energy Ultraviolet radiation. ZnO is interesting as a photocatalyst for the degradation of organic pollutants from aqueous solution under Ultraviolet radiation, due to its non-toxic nature, comparatively high photocatalytic ability, chemical, and thermal stability, and have simple preparation process [111]. But the instability in acidic media, photo-corrosive nature, spontaneous growth, and aggregation restrict their application in wastewater treatment. Due to the above drawback, the ZnO has been incorporated into various porous materials like clay, activated carbon, Zeolite, and silica. Natural clays are widely used as adsorbents and catalyst supporters because of their capability in adsorption and catalytic activities. Clay-based catalysts, i.e., metal oxide supported clays, are frequently utilized in heterogeneous photocatalytic applications. The good dispersion of photocatalytic nanoparticles over porous media enables to construction more active surface. The porous materials make the concentrate pollutants incorporated into the catalyst surface. When the contact between pollutants and catalyst sites increased, the photodegradation performance was high. ZBC (Zinc oxide/clay nanocomposites) catalysts are employed within the photocatalytic degradation of organic pollutants like organic dyes, phenol, and some phenolic derivates, and other persistent compounds [112].

The previous researcher investigated that the porous structure and high specific surface area of bentonite were beneficial to photoactivity via enhancing adsorption, which is that the determining step within the heterogeneous photocatalytic reaction. Therefore, a combination of

adsorption and heterogeneous photocatalysis makes photo-oxidation easier for the removal of dye compounds from wastewater [113].

2.6.4.2. Green synthesis of ZNPs and ZnO/bentonite (ZBC) nanocomposites

ZNPs prepared from the starting materials such as zinc acetate dihydrate, zinc nitrate hexahydrate, zinc chloride, zinc sulfate and zinc acetylacetonate using physical or chemical methods are either in pure form or anchored on a suitable matrix. The limitations of ZNPs include low surface area, rapid agglomeration, and small particle size, which make recovery from the aqueous phase very difficult. Additionally, the discharge of ZNPs into the environment could pose potential health and environmental risks. Therefore, the incorporation of ZNPs on a suitable matrix could help to blocks these problems [114].

The synthesis of ZBC is carried out by incorporating ZNPs into aluminosilicate layers of clay to get a hybrid with discrete and uniformly distributed photo-active sites on a matrix with a wider surface area as shown in Figure 9. The ZnO was synthesized from zinc acetate precursor since acetates (Ac) are good complexing ligands for Zn (II) [115]. ZnO was attached to bentonite clay, using zinc acetate as a starting material to produce ZnO/bentonite nanocomposites. Due to bentonite has a low price, available everywhere, having good adsorption properties, free from sludge after usage, it's been successfully applied for the immobilization of some photocatalysts [116].

$$\mathrm{Zn-OAc + HOH}/OH^- \leftrightarrow \mathrm{Zn-OH\ +\ HOAc}/AcO^- \quad (2.3)$$

$$\mathrm{Zn-OH\ +\ Zn-OAc\ \leftrightarrow\ Zn-O-Zn\ +\ HOAc} \quad (2.4)$$

$$\mathrm{Zn-OH\ +\ Zn-OAc\ \leftrightarrow\ Zn-O-Zn\ +HOAc} \quad (2.5)$$

$$Zn-OH + Zn-OAc \xrightarrow{\Delta} ZnO \quad (2.6)$$

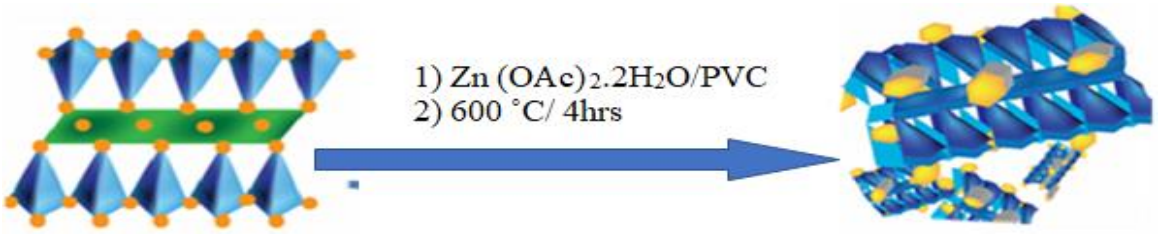

Na^+ exchanged bentonite ZnO incorporated into bentonite (Phot-Zn-Bent)

Figure 8: Synthesis of ZnO/bentonite nanocomposites from precursor [116]

2.6.4.2. Wastewater treatment by ZnO/bentonite nanocomposites via photodegradation

Natural clay is used for the elimination of different organic pollutants from wastewater by adsorption process due to its easy availability and low cost. The incorporation of clay with semiconductor photocatalyst forms photocatalyst/bentonite nanocomposites which are effectively used for the degradation of organic pollutants from wastewater due to they have enhanced photocatalytic activity. Also when the clay is introduced with semiconductors causes an increase in basal space and cation exchange capacity and these are responsible for the increase in photocatalytic activity [117].

Semiconductors like ZnO have unique electrical and optical properties. It has good photocatalytic properties and is found to be the promising substrate for the degradation of organic pollutants under ultraviolet light due to ZnO has a large bandgap between CB and VB [118]. The process of degradation of organic pollutants by ZnO/bentonite nanocomposites occurred by adsorbing organic pollutants on the surface near the ZnO particles, with the presence of UV light, and the photocatalytic degradation process happen. The degradation process is initiated by the excitation of an electron from the VB of the ZnO catalyst to the CB, as a result of generating a hole (h^+) in the VB and make hydroxyl radical when attacks with H_2O. After that, the hydroxyl radical attacks the organic pollutant molecule and the degradation process happens. After the degradation of organic pollutant molecule was finished, some of the degradation product was released to water, and some possibly remain attached to the surface of the adsorbent. This process continues up to the product of degradation covers the surface of ZnO particles and becomes deactivated. However, if organic pollutant molecules are adsorbed on the surface far from the location of the ZnO particle, the photocatalytic degradation process did not occur [26].

2.7. Adsorbents regeneration

The adsorbent is employed for the removal of various pollutants from the wastewater. However, spent adsorbent loaded with pollutants is a challenge for the environmental problem due to the toxicity of methylene blue or adsorbate leaching [119]. Regeneration of adsorbents is vital by employing a proper technique that assists to improve the removal efficiency of pollutants from the adsorbent; the cost of the treatment process reduces the generated waste from the environment and blocks the harmful matter. The common and widely used regeneration

techniques for clay-based adsorbents are chemical, thermal, supercritical extraction, photocatalytic, and biological methods [120].

2.7.1. Thermo-chemicals method

The regeneration of pollutant-loaded adsorbents improves the general cost of treatment, alleviates the disposal problem of adsorbents, and reduces the prospect of sludge formation. The foremost widely used predominant regeneration methods for different adsorbents are chemical and thermal regeneration. In chemical regeneration, different solvents like acid, base, or salt mixed with spent adsorbents are used to extract adsorbate. The regeneration efficiency of exhausted adsorbents in chemically modified regeneration technique depends on the solubility of adsorbate in solvents and it's going to alter the structure of the adsorbent whereas, in thermal regeneration, the regeneration efficiency depends upon the heating temperature of the solvent [121]. During regeneration of adsorbent, the combination of two regeneration methods are used, thermal regeneration followed by chemical regeneration (named as thermo–chem).

The boiling point of MB is 110 ˚C at this point there is no peak appeared. The interaction between MB and clay adsorbent is an electrostatic [122], which thereby fails to desorb MB dye at 110 ˚C (the boiling point of MB is 110 ˚C). According to the report by [122] pointed out in Table 6 desorption results of MB from bentonite adsorbent were affected by the change in temperature.

Table 6: Desorption efficiency of MB dye at different heating temperatures [122]

Heating Temperature (˚C)	Desorption Efficiency (%)
150	8.03 ± 1.07
160	8.14 ± 0.5
170	8.39 ± 0.67
190	8.99 ± 1.12

Other studies [123], [124], and [125] also indicate the desorption efficiencies of MB performed with a 3:1, 1:1, and 1:3 ratios of HCl to C_2H_5OH heated at 60 ˚C for both chemical regenerations, and the combination of thermal and chemical regeneration. The desorption capacity of the dye using different ratios of HCl and C_2H_5OH mix was found to be shown in Figure 10 [124].

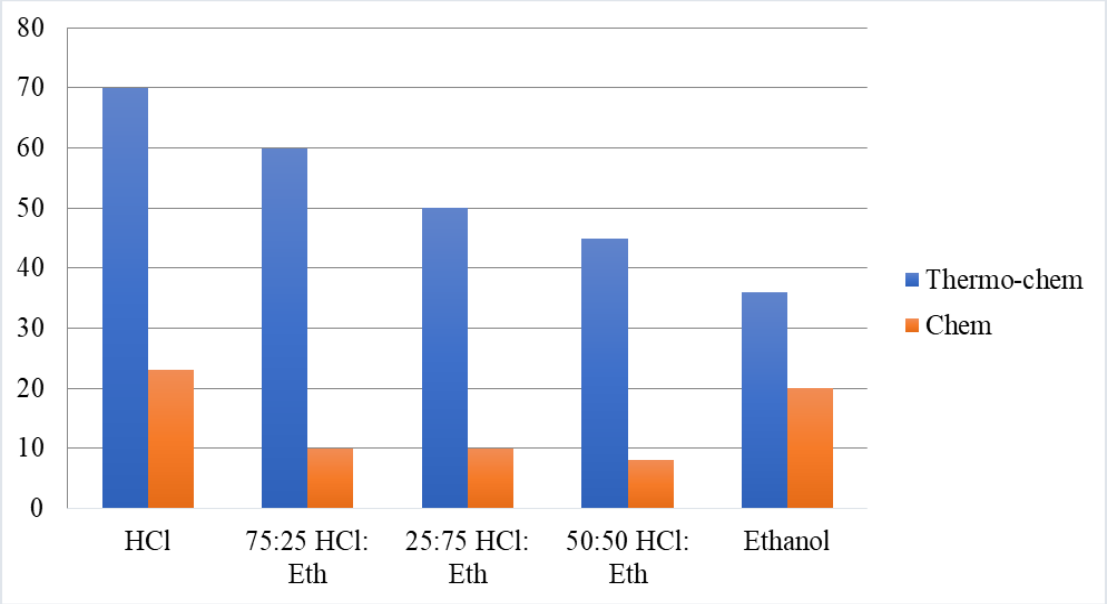

Figure 9: Effect of solvents for desorption of methylene blue dye from the adsorbent coated [125]

2.7.2. Mechanism of desorption of methylene blue dye from the spent adsorbent

The desorption mechanism of MB dye from spent adsorbent was indicated in Figure 11 is a combined effect of the concentration, temperature, and contact time. The temperature destabilizes adsorptive forces followed by reorientation of the molecules then kinetic energy. The solvating power of the solvent and concentration gradient helps within the diffusion or migration of MB dye molecules from the solid to the liquid phase or solvents. In other words, the extension of desorption is proportional to the temperature and concentration followed by the exposure time of the adsorbed molecules to the equilibrating solutions. In this way, all three factors affect the desorption of the adsorbed molecules. Another factor could be the area of the adsorbent, i.e., the higher the surface areas the faster desorption. In other words, desorption was inversely proportional to the particle size of the adsorbent, because the surface area decreased with a rise in particle size [125].

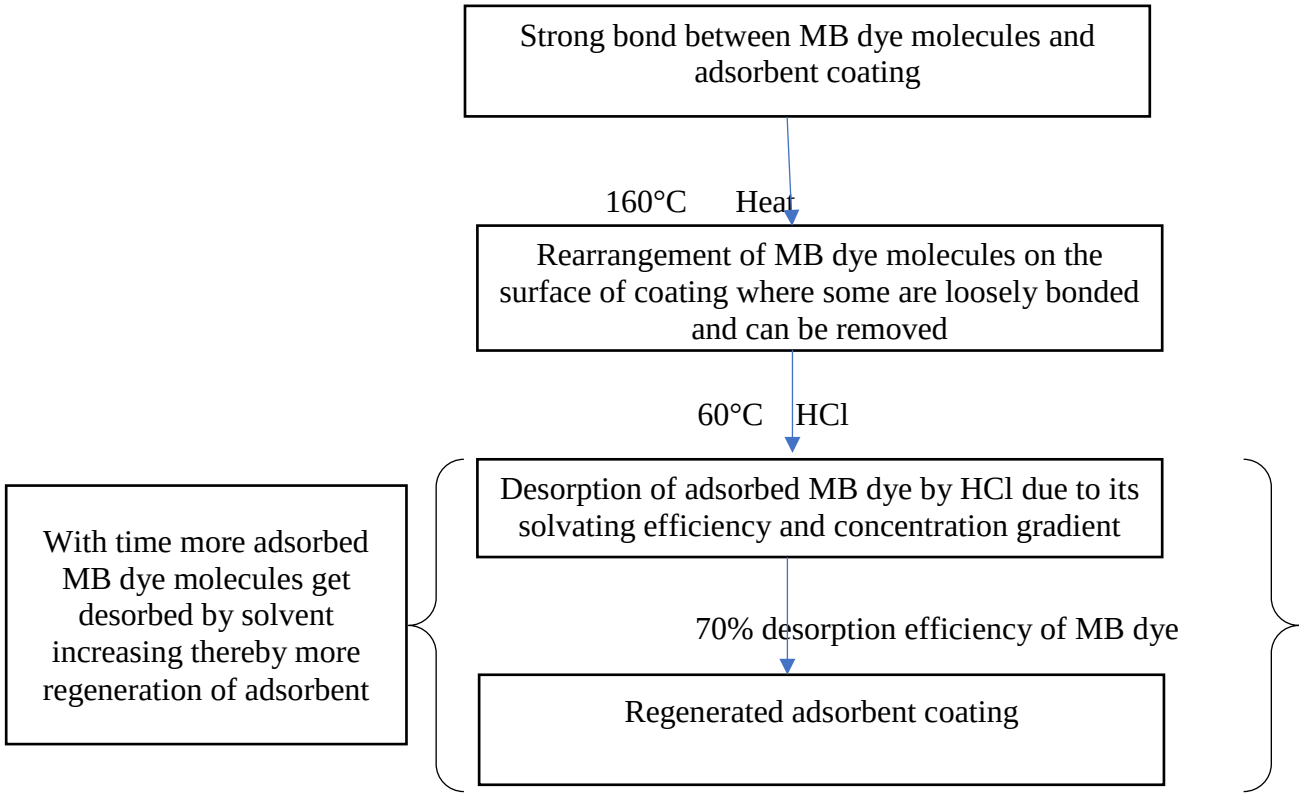

Figure 10: Schematic mechanism for desorption of the adsorbed MB dye from spent adsorbent [125]

CHAPTER THREE

MATERIALS AND METHODS

3.1. Apparatus and instruments

The materials used during this research study included: conical flask, measuring cylinder, volumetric flask (100, 250, 500, and 1000 ml), crucibles, funnel, beaker, burette, sieve (125 μm, 75μm), mortar and pestle, dropper, ball milling, Whatman no 1 filter paper, pH meter, analytical balance, universal drying oven, muffle furnace, and magnetic stirrer with the hot plate.

3.2. Chemicals and reagents

The chemicals and reagents used in this study were: hydrochloric acid (HCl), distilled water, acetone, ethanol, sodium hydroxide (NaOH), sodium carbonate (Na_2CO_3), Zinc (II) nitrate hexahydrate (Zn $(NO_3)_2.6H_2$), Methylene blue dye ($C_{16}H_{18}N_3ClS$). All chemicals and reagents used for the study were analytical grades and purchased from the Fine Chemical industry and trading (Addis Ababa). All aqueous solutions were prepared using distilled water.

3.3. Sampling and Sample collection area

Bentonite was taken from the Gewane area, Afar Region, Ethiopia, and kept in ASTU, at the physical chemistry laboratory. The *H. Abyssinica* (local name Koso) was taken from Karsa, East Arsi zone, Oromia Regional, Ethiopia and dried in ASTU, at physical chemistry laboratory.

3.4. Experimental procedures

3.4.1. Purification of natural bentonite

The purification process was carried out by taking a 300 g of natural bentonite and crushed, milled, and screened by 125 μm sieve, and washed with distilled water several times to remove impurities likes: quartz, carbonates, calcites, and compounds of iron, then dried at 105 °C in the oven for 12 hr to remove moisture contents and volatile organic compounds. The dried sample of purified bentonite was milled again using mortar and pestle and sieved by (200 meshes) which has a particle size (75 μm) was retained, weighed, and preserved in an air-tight plastic bag for the next step [126].

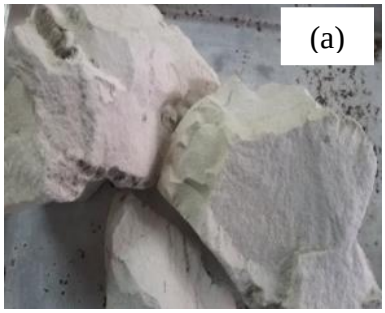

Natural bentonite

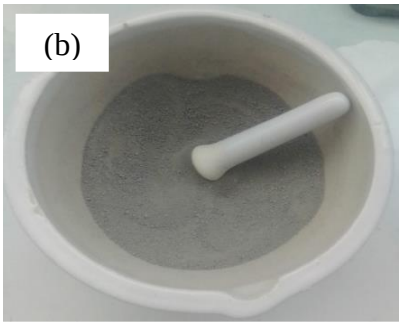

Powdered bentonite

Sieved powder bentonite with (75μm)

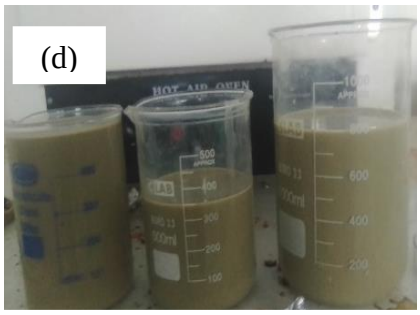

Bentonite suspension

Figure 11: Physical treatment of natural bentonite

3.4.2. Activation of purified bentonite by sodium carbonate (Na_2CO_3)

Activation of bentonite was carried out to reducing the residual sludge volume and the oil loss in the sludge by [127] with little modification. The first 100 g of purified bentonite was dispersed into 1 L boiled for 1 hr distilled water. Then, different amounts of Na_2CO_3 (2.5, 5, 7.5, and 15g) were added to each suspension of bentonite in 1 L boiled distilled water in the beaker. The suspension was stirred vigorously with a magnetic stirrer and boiled for 1hr. After, 1hr the suspension was cooled down to room temperature and diluted with distilled water in three beakers (1 L) in each beaker added bentonite suspension equally. After that added distilled water up to 1 L mark and waited for 24 hrs. Repeatedly, the dilution continuous up to clear supernatant appeared above the settlement. After clear supernatant appeared decant the supernatant and dry the solid in the beaker in the oven at 105 °C for 12 hrs.

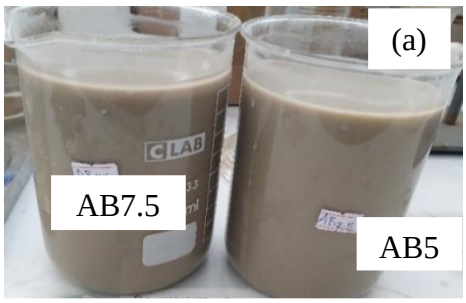

Activation of bentonite by Na_2CO_3

Dried activated bentonite (AB5)

Figure 12: Bentonite activation process by Na_2CO_3

3.4.3. Preparation of extract

The extraction of the leaf of *H. Abyssinica* (local name Koso) was carried out using 25 g of dried leaf and added into 500 mL distilled water and heated for 1hrs at 60 °C. Then cool down the solution and separated the solid from the solution using a centrifuge, then filter using filter paper, and kept the filtrate for further use [128].

3.4.4. Synthesis of ZnO/bentonite nanocomposites by green method

The synthesis of ZnO/bentonite nanocomposites with different ratios of ZnO to bentonite (ZBC12, ZBC11, and ZBC32) was carried out as followed procedure. 33, 67, and 100 mL 0.2 M of Zn $(NO_3)_2.6H_2O$ and 4 g of activated bentonite (AB5) were vigorously stirred for 30 min at room temperature. Then 200 mL aqueous extract of the Koso leaf which is used as a capping and reducing agent for the *synthesis* of *ZnO NPs* was added drop by drop to stirring solutions at room temperature for 30 min. During the time of addition, the color of the solution changed from white to light brown. After 30 min, the light brown precipitations were centrifuged at 3000 rpm, washed with distilled water, and dried at room temperature. Then, the dried sample was calcined in the furnace at 450 °C for 1 hr [129].

3.5. Preparation of stock solutions

3.5.1. Preparation of stock solution of 1g/L MB dye

The preparation of 1 g/L stock solution of MB dye was performed by dissolving 1 g of commercial-grade MB dye in a 1 L volumetric flask by filling distilled water up to mark at room temperature. Then, the prepared solution of MB dye was protected from light by aluminum foil due to it is light sensitive. Then the solution was analyzed using the UV-Vis spectrum [130].

3.5.2. Preparation of stock solution of 1M NaOH

The preparation of 1M stock solution of NaOH was performed by dissolving 40 g of commercial-grade NaOH in a 1 L volumetric flask by filling distilled water up to mark at room temperature. Then, the prepared solution of NaOH was diluted to the appropriate concentration.

3.5.3. Preparation of stock solution of 1M of HCl

The preparation of 1M stock solution of HCl was performed by taking 22.6 mL HCl (35%) of commercial-grade in a 1L volumetric flask by filling distilled water up to mark at room temperature. Then, the prepared solution of HCl was diluted to the appropriate concentration.

3.5.4. Preparation of stock solution of 0.2M of Zn $(NO_3)_2.6H_2O$

The preparation of 0.2 M of $Zn(NO_3)_2.6H_2O$ was performed by dissolving 59.5 g of Zn $(NO_3)_2.6H_2O$ in a 1 L volumetric flask by filling distilled water up to mark at room temperature.

3.6. Proximate analysis of bentonite adsorbent

3.6.1. Determination of moisture content

The moisture content of natural and activated bentonite (AB5) was determined by drying 2g of bentonite clay in an oven at 105°C until the mass became constant for 12 hrs and cooled down to room temperature [131]. Then after cooling, the moisture content was determined using Equation (3.1).

$$\%W = \frac{W_1 - W_2}{W_1} * 100 \qquad (3.1)$$

Where: - %W is the percentage of moisture in the sample, W_1 is the weight of the wet sample (g) and W_2 is the weight of the dry sample (g).

3.6.2. Determination of bulk density by (ASTM D 1895-96)

The bulk density was determined [127], with little modification. First, the mass of the empty measuring cylinder (5 mL) was measured and recorded. Then a known amount of natural and activated bentonite (AB5) was transferred to the empty cylinder. The cylinder was tamped using a rubber pad while the sample was being added until there was no further settling produced. After all, the sample was transferred; the final mass of the cylinder was weighed (mass of sample plus cylinder) and recorded. Finally, the bulk density of bentonite was calculated by Equation (3.2):

$$\rho B = \frac{Msc - Mec}{Vc} \qquad (3.2)$$

Where ρB is bulk density of bentonite in g/mL, Msc is mass of sample and cylinder in g, Mec is mass of empty cylinder in g, and Vc is the volume of the cylinder in ml.

3.6.3. Determination of pH

The pH of natural and activated bentonite (AB5) was determined by soaking 2.5 g of bentonite in 25 mL of distilled water for twelve hours. Then the mixture was stirred vigorously, the pH of the bentonite suspension was measured using a pH meter to know the bentonite was either basic or acidic behaviors [132].

3.6.4. Determination of pH at point of zero charges (pHpzc)

The pH at the point of zero charges (pHpzc) for natural and activated bentonite (AB5) was determined using 0.1 M NaCl solution. Then, 0.1 g of natural and activated bentonite (AB5) was added to the conical flask that contains 20 mL of 0.1M NaCl with different initial pH. The initial pH (pHi) of the NaCl solution was adjusted between 2-11 pH by using 0.1M HCl and NaOH on a digital pH meter. The final pH (pHf) of the solution was measured after 24 hrs. The graph was drawn by plotting the final pH values against ΔpH. From the plotted graph, the pHpzc of the adsorbent was determined [133].

3.6.5. Determination of swelling index by (ASTM D 5890-95)

The free swelling index was determined for natural and activated bentonite (AB5) after drying to constant weight in the oven at 105°C and grounded using mortar and pestle to pass through a 75 μm sieve by using the following procedure. 2g of powdered sample was weighed and added into

a clean 100 mL graduated cylinder that contains 90 mL of distilled water. Then, not more than 0.1g increment of the sample was removed with a volumetric spoon from weighing paper and carefully dusted over the entire surface of the water in the graduated cylinder for approximately 30 sec. Then the inserted natural bentonite and AB5 were allowed to wet, hydrate, and settle to the bottom of the graduated cylinder for a minimum period of 10 min. The procedures were continued until the entire 2g sample was completed. After the final increment, distilled water was added until it reached the 100 mL mark. After 24 hrs hydration period from the last increment addition, the volume level was recorded the swell volume of the bentonite defined by the interface between the sediment and the supernatant was measured and recorded in mL/2g [134].

3.6.6. Determination of cation exchange capacity (CEC) and specific surface area (SSA)

The CEC and SSA of natural and 5% Na_2CO_3 activated bentonite (AB5) were determined by the methylene blue test [79], [135]. 1g of dried sample of natural bentonite and AB5 was transferred into a beaker separately which contains 50 mL distilled water and stirred for titration with standard 0.0125M (4g/L) MB solution separately in each beaker. Then small quantities of the methylene blue solution were gradually added from a burette to the stirred bentonite suspension in the beaker and stirred for 1min on the magnetic stirrer. Take out drops of the suspension with a glass rod on a filter paper, then the colorless waterfront distributes in a circle on the filter paper, whereas the blue-colored clay in the center stuck to the paper. At the endpoint, a light blue halo appeared around the center. The clay suspension was then stirred for two more minutes and the dotting test was carried out to show whether a blue halo was shaped again or not. When a blue halo appeared again, this marked the endpoint of the test. Otherwise, further titration was carried out carefully until the halo did not disappear any longer after 2 min. Finally, the CEC and SSA of bentonite were calculated by Equations (3.3) and (3.4).

$$\mathrm{CEC} = \frac{\mathrm{E} * \mathrm{V}}{\mathrm{m}} * 100 \qquad (3.3)$$

Where CEC is the cation exchange capacity in (meq/100 g clay), E is milliequivalents of methylene blue per milliliter, V is milliliters of methylene blue solution required for the titration, and m is the mass of dry material in grams.

$$\mathrm{SSA} = \frac{\mathrm{mMB}}{\mathrm{MMB}} * \mathrm{AN} * \mathrm{AMB} * \frac{1}{\mathrm{ms}} \qquad (3.4)$$

Where, SSA is Specific Surface Area, m_s - is the mass of the bentonite adsorbent used, M_{MB} - is the molecular weight of methylene blue dye which is 319.87g/mol, Av - is Avogadro's number ($6.02 * 10^{23}$/mol) and A_{MB} - is an area covered by one methylene blue molecule which is 130Å^2 ($1A° = 0.1$nm).

3.7. Characterization of adsorbent

3.7.1. XRD analysis

The mineralogical composition of purified bentonite (PB), activated bentonite (AB5), and calcined ZnO/bentonite nanocomposites (CZBC11 and CZBC12) was conducted by taking a small number of powder samples packed with a standard sample holder and analyzed using X-ray Diffraction (XRD-700 Shimadzu Co., Japan, λCuK1 = 0.15406 nm, tube voltage 40 kV, current 30 ma). X-ray diffractograms of PB, AB5, CZBC11 and CZBC12 powders were obtained for the 2θ angles ranging from 0˚ to 80˚ with scans step 0.02˚. All the experiments were performed at room temperature, with a scans speed of 3˚/min, an angular step of 0.02˚, and a counting time of 0.40 sec [136]. This XRD analysis was performed in ASTU, at the Department of Material Engineering.

3.7.2. FT-IR analysis

Structural analyses of purified bentonite, activated bentonite (AB5) after adsorption, after desorption, and ZnO/bentonite (CZBC11 and UZBC11) were performed by FT-IR transmission spectra using the KBr pellets disc technique. The analysis was carried out on (PerkinElmer, Spectrum 65 FT-IR) in the wavenumber range of 400–4000 cm^{-1} at a resolution of 4 cm^{-1}, with number of scans 4. This FT-IR analysis was performed at Addis Ababa University, at the Department of Chemistry.

3.7.3. Scanning Electron Microscope (SEM) analysis

Morphological analyses of the activated bentonite before (AB5) and after adsorption (AB-MB) were analyzed using SEM (SEM, JCM-6000). Before scanning, the AB5, AB-MB was coated with gold using a sputter coater, and subsequently, the SEM images were taken. This SEM analysis was performed in ASTU, at the Department of Applied Biology.

3.7.4. Complete silicate analysis of bentonite

0.1 gram of natural bentonite and activated bentonite was added to 1.5 grams of $LiBO_2$ and the mixture was heated in a furnace for 45 min at 950 °C. After it cooled overnight the mixture was stirred with a magnetic stirrer, washed, and transferred to a round bottom flask by adding lanthanum chloride. The prepared solutions were used for AAS to determine metals like Ca, Al, K, Mg, Fe, Na, etc. The amount of silica was determined by taking 0.1 g of bentonite, 3 mL of hydrochloric acid (HCl), and 2 mL of boric acid (H_3BO_3) directly read by AAS, and the amount of TiO_2 and P_2O_5 was determined by UV-Vis spectroscopic method at the Ethiopian geological survey.

3.8. Adsorption experiment

Adsorption experiments were carried out using the procedures reported [137] with, little modification. 0.1 g of bentonite sample was mixed with 50 ml of methylene blue dye aqueous solution having an initial concentration of 80 mg/L in a 250 ml beaker at constant parameters like pH = 7, at a temperature of 25˚C, and mixing speed at 300 rpm for 30 min. After 30 minutes, the aqueous phase was separated from the solid by filtration using Whatman no 1 filter paper and the filtrate was analyzed using UV-Vis spectroscopy (Double Beam Spectrophotometer, SM-1600, India) at a maximum wavelength of 663nm, for the determination of the residual concentration of MB dye in the filtrate. Then the adsorption efficiency (%) and adsorption capacity of MB dye q_e (mg/g) was calculated using Equation (3.5) and (3.6). The adsorbent loaded with MB dye after adsorption carried out was dried in an oven at 70°C for 4 h and used for the desorption study:

$$\%\ \text{removal} = \frac{C_o - C_r}{C_o} * 100 \qquad (3.5)$$

$$qe = \frac{C_o - C_r}{m} * V \qquad (3.6)$$

Where C_o is the initial concentration of MB dye (mg/L), C_r is the residual concentration of MB dye (mg/L), m is mass of adsorbents (g), V is the volume of MB dye solution taken during adsorption (L) and q_e is adsorption capacity (mg/g).

3.8.1. Optimization of activated bentonite for removal of MB dye from aqueous solution

Optimization of activated bentonite by different amounts of Na_2CO_3 for removal of MB dye from aqueous solution was carried out by the following procedure. 0.1 g of activated bentonite (AB2.5, AB5, AB7, and AB15) was added into the beaker which contains 50 mL of MB dye solution with an initial concentration of 80 mg/L at constant parameters like pH=7, at a temperature of 25˚C and mixing speed at 300 rpm for 30 min. After 30 min filter, the suspension using Whatman No 1 filter paper and the filtrate were analyzed using UV-Visible spectroscopy at wavelength 663 nm. Then, the adsorption capacity and residual concentration in the filtrate of MB were calculated.

3.8.2. Optimization of adsorbent for removal of MB dye from aqueous solution

Optimization of adsorbent for removal of MB dye from aqueous solution was conducted on natural bentonite, purified bentonite, activated bentonite, and ZnO/bentonite nanocomposites with different ratios of ZnO: bentonite to identify the best adsorbent that has the best removal efficiency. The experimental work was carried out by taking 0.1 g of each adsorbent in each 250 ml beaker that contains 50ml of MB dye with an initial concentration of 80 mg/L at constant parameters like pH = 7, at a temperature of 25 ˚C, and mixing speed at 300 rpm for 30 min. After 30 min the suspension was filtered using Whatman No 1 filter paper and the filtrate was analyzed using UV-Visible spectroscopy at wavelength 663nm. Then, the adsorption capacity and residual concentration in the filtrate of MB were calculated.

3.9. Effect of different factors affecting the removal efficiency of MB dye

Optimization of different parameters was carried out based on previous work [137] with, little modification to identify the optimized parameter at which the best removal efficiency of MB dye was observed. The effects of major parameters like adsorbent dosage, initial dye concentration, temperature, contact time, and pH were evaluated.

3.9.1. Effect of pH

The effect of pH on the removal of MB dye from aqueous solution was determined by performing the adsorption experiments at different initial pH (4, 7, 9, and 11) of the solution by adjusting the pH of the mixture using 0.1M HCl and 0.1M NaOH. Then 0.1 g of AB5 was added into 50 mL of MB dye solution with an initial concentration of 80 mg/L, at a temperature of 25

°C and mixing speed at 300 rpm for 30 min. The solid particles were removed from the solution by filtration using Whatman No 1 filter paper and the remaining concentration of dye in the filtrate was measured using UV-Visible spectroscopy at wavelength 663nm. Then, the adsorption capacity and residual concentration in the filtrate of MB dye were calculated.

3.9.2. Effect of adsorbent dosage

The experimental work was carried out to know the effect of AB5 dosage on the removal efficiency of MB dye. It was studied by using 0.1, 0.5, 1, and 1.5g of activated bentonite (AB5) added into 50 mL of MB dye solution with an initial concentration of 80 mg/L at pH = 7, at temperature of 25°C, and mixing speed at 300 rpm for 30 min. The solid particles were removed from the solution by filtration using Whatman No 1 filter paper and the remaining concentration of colorant in the filtrate was measured using UV-Visible spectroscopy at a maximum wavelength of 663nm. Then, the adsorption capacity and residual concentration in the filtrate of MB dye were calculated.

3.9.3. Effect of initial concentration

0.1 g of AB5 was added to 50 ml of the prepared initial concentrations of MB dye (80, 130, 180, and 230) mg/L. The effect of initial concentration on adsorption of MB dye was conducted in an aqueous solution by keeping the pH = 7, at temperature of 25 °C, and stirring suspension at 300 rpm for 30 min. Then the solid was separated from the solution by filtration using Whatman No 1 filter paper and the filtrate was analyzed. The ability of the AB5 to adsorb methylene blue dye was analyzed using UV-Visible spectroscopy at a maximum wavelength of 663 nm. Then, the adsorption capacity and residual concentration in the filtrate of MB dye were calculated.

3.9.4. Effect of temperature

The effect of temperature on removal of MB dye from aqueous solution using AB5 was determined at 25 °C, 30 °C, 40 °C, and 50 °C. Then 0.1 g of AB5 was added into 50 mL MB dye solution with an initial concentration of 80 mg /L at pH = 7 and mixing speed at 300 rpm for 30 min. The solid particles were removed from the solution by filtration using Whatman No 1 filter paper and the remaining concentration of dye in the filtrate was measured using UV-Visible spectroscopy at wavelength 663nm. Then, the adsorption capacity and residual concentration in the filtrate of MB dye were calculated.

3.9.5. Effect of time

The influence of contact time on the removal of MB dye from aqueous solution using AB5 was carried out at 30, 45, 60, and 90 min. Then 0.1g of AB5 was added into 50 ml of MB dye solution with an initial concentration of 80 mg/L at 25°C, pH = 7, and mixing speed at 300 rpm. Then the adsorbent was separated from the solution by filtration using Whatman No 1 filter paper and the filtrate was analyzed by UV-Visible spectroscopy at wavelength 663 nm. Finally, contact time versus removal efficiency was plotted to describe the adsorption behavior of the adsorbent at each contact time.

3.10. Adsorption isotherms models

Adsorption isotherm is a fundamental property in adsorption studies; numerous studies have been conducted to determine the number of species adsorbed under a given set of conditions. To optimize the design of an adsorption system for MB dye removal from aqueous solutions, it is important to find the most appropriate correlation for the equilibrium curve [138]. In the present study, three adsorption isotherm models were done to the experimental equilibrium data to verify which model presented the best adjustment were tested for their ability to describe the experimental results, namely the Langmuir, Freundlich, and Temkin isotherm models.

3.10.1. Langmuir adsorption isotherm model

Langmuir's model of adsorption indicates the existence of monolayer coverage of the adsorbate at the outer surface of the adsorbent. The isotherm equation further assumes that adsorption takes place at specific homogeneous sites within the adsorbent, which indicates that all adsorption sites are identical and energetically equivalent. Theoretically, the adsorbent features a finite capacity for the adsorbate. Therefore, a saturation value is reached beyond which no further adsorption can occur [139]. The saturated or monolayer capacity is often represented as the known Langmuir equation:

$$\frac{\mathrm{Ce}}{\mathrm{qe}} = \frac{1}{\mathrm{K_L} * q_{max}} + \left(\frac{1}{q_{max}}\right) * \mathrm{C_e} \qquad (3.7)$$

Where C_e is the equilibrium concentration, q_e is equilibrium adsorption capacity, q_{max} is maximum adsorption capacity.

The Langmuir constants q_{max} and K_L were determined from the plotted graph the slope and intercept of the plot. The essential characteristics of the Langmuir isotherm are often expressed in terms of a dimensionless constant separation factor R_L that's given by

$$RL = \frac{1}{1 + K_L + C_O} \quad (3.8)$$

Where; Co- is that the highest initial concentration of adsorbate (mg/L) and K_L (L/mg) is Langmuir constant.

3.10.2. Freundlich adsorption isotherm model

The Freundlich isotherm model of adsorption indicates the existence of multi-layer coverage of the adsorbate at the outer surface of the adsorbent. It is an empirical equation employed to explain heterogeneous systems. This model proposes an exponential decrease in the adsorption energy upon completion of the sorption centers of the sorbent [140]. The linear form for the Freundlich model is often expressed by the following Equation (3.9).

$$Lnqe = LnK_f + \left(\frac{1}{n}\right) * LnC_e \quad (3.9)$$

Where K_F (and) and n are Freundlich constants, 1/n is the adsorption capacity of the sorbent, and n indicating how favorable the adsorption process is.

The magnitude of the exponent, 1/n shows the favorability of adsorption. The Value of K_F and n are calculated from the intercept and slope of the plotted graph.

3.10.3. Temkin adsorption isotherm model

This model considers that the adsorption heat of all molecules decreases linearly with the increase in coverage of the adsorbent surface and that adsorption is characterized by a uniform distribution of binding energies, up to maximum binding energy [141].

The Temkin isotherm has been utilized in the following form:

$$qe = B * lnA + B * lnC_o \quad (3.10)$$

$$\text{Where } B = R * \frac{T}{K_T} \quad (3.11)$$

K_T is the Temkin constant related to the heat of sorption (J/mol), A is the Temkin isotherm constant (L/g), R is the gas constant (8.314 J/mol °K), and T: the absolute temperature (°K).

By plotting, qe vs ln Ce, the constants A and B can be determined.

3.11. Adsorption kinetics models

The mechanism of adsorption and potential rate determining-steps, different kinetic models are accustomed to test experimental data obtained from the variables (initial MB dye concentration). The sorption dynamics of the adsorption by AB5 were tested with the Lagergren pseudo-first-order model, proposed in 1898, and the chemisorption's pseudo-second-order model [142].

3.11.1. Pseudo-first-order model

The adsorption kinetics is often described by a pseudo-first-order equation as suggested by Lagergren.

$$\frac{dq}{dt} = K_2 * (qe - qt) \quad (3.12)$$

Where; K_1 (min^{-1}) is that the rate constant of the pseudo-first-order model and qe and qt are expressed by (mg/g) and indicate sorption capacity at equilibrium and at time t, respectively.

When integrating the above Equation (3.12):

$$\ln(qe - qt) = \ln qe - K_1 * t \quad (3.13)$$

Log (qe – qt) values were linearly correlated with t

K1 and qe are often determined from the slope and intercept of the plot

3.11.2. Pseudo-second-order model

In this model, the rate-limiting step is that the surface adsorption that involves chemisorption, where the removal from a solution is due to physicochemical interactions between the two phases. The pseudo-second-order equation can be written as:

$$\frac{dq}{dt} = K_2 * (qe - qt)^2 \quad (3.14)$$

When integrate Equation (3.14) the following equation for the boundary conditions t= 0 to t = t and q = 0 to q = qe gives:

$$\frac{1}{qe - qt} = \frac{1}{qe} K_2 * t \quad (3.15)$$

In the linear form, the above Equation (3.15) looks like the following Equation (3.16)

$$\frac{t}{qt} = \frac{1}{K_2 * qe^2} + \frac{1}{qe} * t \quad (3.16)$$

From this equation, K_2 and q_e can be obtained from the intercept and slope plotting t/qt vs t.

3.12. Thermodynamic parameters

A very important factor affecting the adsorption of MB dye on the surface of AB5 was temperature. The ΔG° (standard free energy change) is the fundamental criteria to determine the process occurs spontaneously or is nonspontaneous. For a given temperature, a phenomenon is considered to be spontaneous when ΔG° has a negative value and nonspontaneous when ΔG° has a positive value. Moreover, when ΔH° (standard enthalpy change) is positive and larger the process is endothermic and ΔH° is negative and lower, the process is exothermic. For the determination of ΔH° and ΔS°, the relationship between adsorption equilibrium constant Ka and Gibbs free energy was considered at any temperature [140]. The influence of temperature on the adsorption behavior of MB dye onto activated bentonite (AB5) was explained by determining the thermodynamic parameters such as standard enthalpy change (ΔH°), standard free energy change (ΔG°), and standard entropy change (ΔS°) [143], using Equation (3.17) & (3.18):

$$\Delta G\ ^\circ = -RT\ln Ka \quad (3.17)$$

$$\ln Ka = \frac{\Delta S^\circ}{R} - \frac{\Delta H^\circ}{RT} \quad (3.18)$$

Where: - R is the gas constant (8.31451 J/mol K), T is the temperature in kelvin, and the values of Ka are estimated from temperature by plotting ln qe/Ce vs qe and extra plotting qe to zero. The values of ΔS° and ΔH° are calculated from the intercept and slope of the straight-line plot between ln Ka and 1/T, respectively.

3.13. Desorption of methylene blue from exhausted bentonite and recyclability of it

Desorption of MB dye from the adsorbent coated by MB dye (AB-MB) was carried out by Momina et.al. [125] with, little modification. Desorption of MB dye from the dried AB-MB was performed using thermo-chemicals regeneration methods. The spent adsorbent coated by MB dye was heated at 200˚C in a muffle furnace for 1hr. Then the heated AB-MB dipped in heated solvents (ethanol, acetone, and distilled water) at 25, 35, and 40 ˚C then stirred on the magnetic stirrer for 2hrs. After two hours the concentration of MB dye desorbed in solvents was measured

using UV-Visible spectroscopy at wavelength 663 nm. Then desorption capacity and desorption efficiency of the MB dye was determined using Equation (3.19) and (3.20) respectively:

$$\text{qe, desorption}\left(\frac{\text{mg}}{\text{g}}\right) = \text{V}\left(\frac{\text{Cf}}{\text{M}}\right) \quad (3.19)$$

Where qe: is desorption capacity, m is that the weight of spent adsorbent (g), V is the volume of the solvent (L), C_f is the MB dye concentration in the solvent (mg/L).

Desorption efficiency is defined as the amount of dye desorbed per gram of spent adsorbent at equilibrium.

$$\%\ \text{Desorption} = \left(\frac{\text{qe, desorbtion}}{\text{qe, adsorption}}\right) \times 100 \quad (3.20)$$

3.14. Optimization of ZnO/bentonite nanocomposites for removal of MB dye from aqueous solution

Optimization of calcined and uncalcined ZnO/bentonite nanocomposites ($UZBC_{12}$, $UZBC_{11}$, $UZBC_{32}$, $CZBC_{12}$, $CZBC_{11}$, and $CZBC_{32}$) for removal of MB dye from aqueous solution was carried out at constant parameters like pH = 7, at a temperature of 25˚C. Then 0.1g of $UZBC_{12}$, $UZBC_{11}$, $UZBC_{32}$, $CZBC_{12}$, $CZBC_{11}$, and $CZBC_{32}$ was added into 50 ml MB dye with an initial concentration of 80mg/L. Then the suspension in the beaker was stirred at 300 rpm for 30 min. After 30 min the suspension was filtered using Whatman No 1 filter paper and the filtrate was analyzed using UV-Visible spectroscopy at wavelength 663nm. Then determine the residual concentration in the filtrate and calculate the adsorption capacity and adsorption efficiency of MB dye.

3.15. Photocatalysis experiments

The experimental study on ZnO/bentonite nanocomposites for photodegradation of MB dye was done by Haithem Bel Hadjltaief, et al. [112], with little modification. The experiment was carried out in a photocatalytic reactor, containing 400W mercury lamps. A cooling water jacket was used to maintain the inside temperature of the reactor. Then 1 g of ZnO/bentonite nanocomposites ($CZBC_{12}$, $CZBC_{11}$, and $CZBC_{32}$) was added into 50 mL MB dye solution with an initial dye concentration of 80mg/L at pH of solution = 8. Then the mixture was placed in a photocatalytic reactor, and an adequate amount of the sample was withdrawn at 60 min. After that, the taken suspension was centrifuged and filtered; the residual MB dye concentration

present in the filtrate was determined using UV-Visible spectroscopy at wavelength 663nm. Then calculate the degradation capacity and degradation efficiency of MB dye using Equation (3.21).

$$\text{Degradation } (\%) = \left(\frac{A_o - A_t}{A_o}\right) * 100 \qquad (3.21)$$

Where, A_0 is the initial absorbance of dye solution, and A_t is the dye solution absorbance at a certain reaction time.

CHAPTER FOUR

RESULT AND DISCUSSION

4.1. Proximate analysis

The proximate analyses of bentonite samples were done based on (ASTM D 5890-95) for swelling index determination, (ASTM D 1895-90) for bulk density determination. The result of the proximate analysis was presented in Table 7. The detailed calculation part is also included in the appendix.

4.1.1. Determination of moisture content of bentonite clay

Moisture content is the important properties of clay minerals that determine the adsorption properties of clay. According to Wiedermann (1981) clay contains 8% - 18% moisture content. The higher moisture content of clay was due to the large void space on the surface of the clay. The moisture in the void space on the surface of bentonite was released at high temperatures and makes the void space large. Therefore, the removal of the moisture from the bentonite clay increases the void space of bentonite. This makes the bentonite have a different application in different areas such as in the adsorption of pollutants from water. As indicated in Table 1A in the appendix part the determination of moisture content of natural bentonite, and activated bentonite was conducted three times and the moisture content of natural and activated bentonite (AB5) was 9.67% and 9.17% as showed in Table 7. Approximately similar results have been observed by other studies [127], [144].

4.1.2. Determination of bulk density of natural and activated bentonite (AB5) by (ASTM D 1895-90)

Bulk density is one of the important properties of clay which is considered in the design of adsorption towers for use either in pilot plants or large commercial applications. It affects the overall ability of the adsorption process. It is proportional to the particle size and defined as the mass of particles of the material divided by the total volume that materials occupy. From this, the higher bulk density provides greater volume activity i.e. when the bulk density is high adsorption capacity of the clay is also high. From the present study, the bulk density of natural bentonite, and activated bentonite were 1.40 g/cm^3 and 1.45 g/cm^3 respectively as shown in Table 7.

4.1.3. Determination of pH of natural and activated bentonite

The pH of bentonite was strongly affecting the application and its properties like adsorption and its rheological properties. The pH of bentonite was determined using pH meter measurement by taking the clear supernatant of bentonite after filtration. The result indicates that the pH of natural bentonite and activated bentonite (AB5) was 10.013 and 10.49 respectively. From these results, the activated bentonite was more basic than raw bentonite this shows the activated bentonite by sodium carbonates has dominants by Na^+ ions in the bentonite structure. As shown from the result the pH of clay is used to indicate the dominant cations on clay structure [76].

4.1.4. Determination of cation exchange capacity (CEC) and specific surface area (SSA) of adsorbent by methylene blue test method

In this study, the CEC of natural and activated bentonite (AB5) was carried out by the methylene blue test method. During CEC determination by this method, the suspension of bentonite sample in the beaker was titrated against MB dye from burette and stirred for 1min. After 1min take out the suspension in the beaker by dropper and put it onto the filter paper. The appearance of the unadsorbed MB dye forms a permanent blue halo around the bentonite aggregate spot onto the filter paper; this indicated that the MB has replaced cations in the double layer and coated the entire surface as indicated in Figure 2B appendix. The result showed that the MB^+ cations in the process bond to negatively charged surfaces of, bentonite clay. The bond between MB dye and bentonite clay was strong enough to displace almost all of the exchangeable cations bound on bentonite clay. The CEC of natural and activated bentonite was 113.63 and 137.5meq/g respectively. From this result, AB5 has high CEC than raw bentonite due to it contains higher Na^+ contents than raw bentonite. Based on, this reason the mass of dry clay and CEC of the clay in nature, being able to allow a greater basal spacing by the greater amount of Na^+. This makes the penetration of a greater amount of water in the space between the sandwich of bentonite and greater adsorption of methylene blue dye molecules happened. This was explaining the cause of the increase of the CEC by the additive samples concerning them in the natural state. The result of this study was similar to the previous work by [145].

Also, specific surface area (SSA) for natural and activated (AB5) was determined by methylene blue test method the result indicates the activated bentonite by sodium carbonate was shows the higher SSA than natural bentonite as indicated in Table 7.

Table 7: Proximate analysis and physicochemical characterization of natural and activated bentonite

Parameters	Units	Result	
		Natural bentonite	AB5 (activated bentonite)
Moisture content	%	9.67	9.17
Bulk density	g/cm^3	1.40	1.45
Cation exchange capacity	meq/g	113.63	137.5
Specific Surface Area	m^2/g	879	1076
pHpzc		9.47	9.0

4.1.5. Determination of pH at point of zero charges (pHpzc) of bentonite

pHpzc is the pH value at which the charge on the surface of the adsorbent is zero. From the present study, the result of pHpzc for natural bentonite, and 5% Na_2CO_3 activated bentonite (AB5) was 9.47 and 9.0 respectively. This indicates the bentonite operates well for adsorption at this value of pHpzc. Due to this result, the evaluated pH of bentonite adsorbent generally falls in the basic and slightly neutral region. The values of pHpzc < 9.47 and < 9.0 show the dominancy of acidic groups over basic groups for natural and activated bentonite (AB5) respectively. And values of pHpzc > 9.47 and > 9.0 show dominance of basic groups over-acidic groups for raw and activated bentonite (AB5) for the present study respectively. The net surface charge of the bentonite under pHpzc is positive, while it is negative above pHpzc. Therefore, knowledge of pHpzc value helps in deciding which pH value should work during adsorption studies.

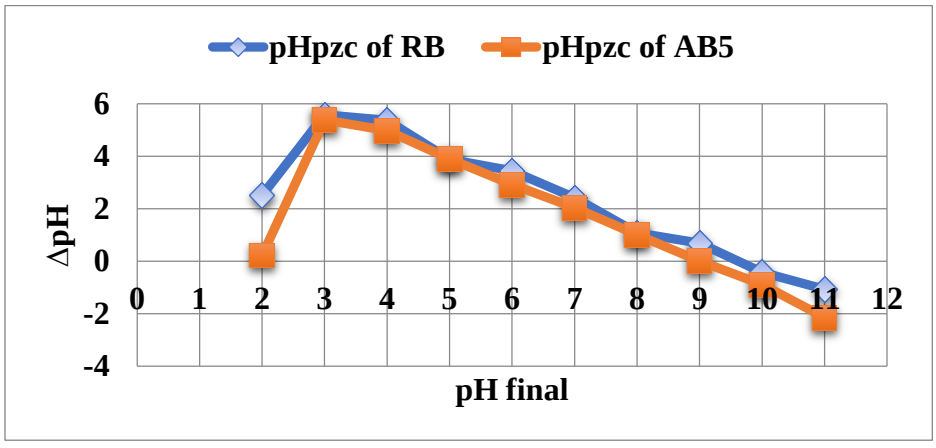

Figure 13: Plot of ΔpH vs. final pH of the adsorbent to determine the zero-point charge

4.1.6. Free swelling index of bentonite by (ASTM D 5890-95)

The free swelling index is used to identify the swelling capacity of the bentonite. The swelling capacity of bentonite within the presence of water is a sign of the standard bentonite. Na_2CO_3 was used as an activator to increase the swelling index of bentonite clay. In the present study, the swelling index of the bentonite clay was done for NB, AB2.5, AB5, and AB7.5. The result shows, as the amount of Na_2CO_3 increases for activation of bentonite the swelling volume of bentonite also increases. This indicates the progressive replacement of exchangeable Ca^{+2} by Na^{+}, facilitates the swelling capacity of bentonite. This was due to the weak electrostatic interaction between the Na^{+} ions and the negatively charged bentonite layer, which allows the entrance of excess water molecules between the layers. In this study, the maximum possible replacement of Ca^{+2} observed at AB7.5 was 17.1ml/2g as shown in Table 8, nearly similar result was reported previously by [146].

Table 8: The free swelling index of natural, 2.5%, 5%, and 7.5% activated bentonite

Type of sample	Natural bentonite	2.5%	5%	7.5%	Reference
Free swell (ml/2g	16	16.5	17.9	19.2	[146]
	14.6	15.7	16.3	17.1	Present study

Variation of the free swell of bentonite indicates smaller ions have greater hydration energies, due to this reason the interlayer of bentonite can attract more water than large ions. This shows why Na-bentonite has greater swelling properties than Ca-bentonite. The degree of attraction to the bentonite surface of Na^{+} is less, so Na^{+} is more conductive to swelling when present at the clay surface because adjacent negatively charged layers are often made to repel each other during the absorption of water into the interlayer. On the other hand, Ca^{2+} saturation results in only limited swelling because the attraction of the cation for an adjacent surface is stronger. Figure 16 shows the increasing swelling capacity of bentonite by the addition of additive agents Na_2CO_3.

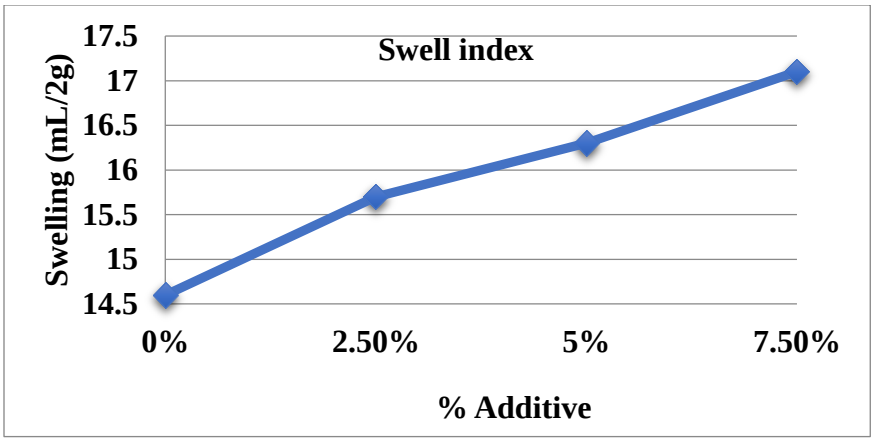

Figure 14: Variation in free swell of activated bentonite by different amounts of Na_2CO_3

4.2. Calibration plot of initial concentration of methylene blue dye

The calibration plot for MB dye at 663 nm was used to determine the residual concentration in the filtrate after adsorption of MB dye using adsorbent from an aqueous solution. The obtained data from the calibration plot were given in Table 9.

Table 9: Calibration data of MB dye

The initial concentration of MB in g/L (x)	Absorbance in (%) (y)
0.08	0.000
0.13	0.010
0.18	0.015
0.23	0.021

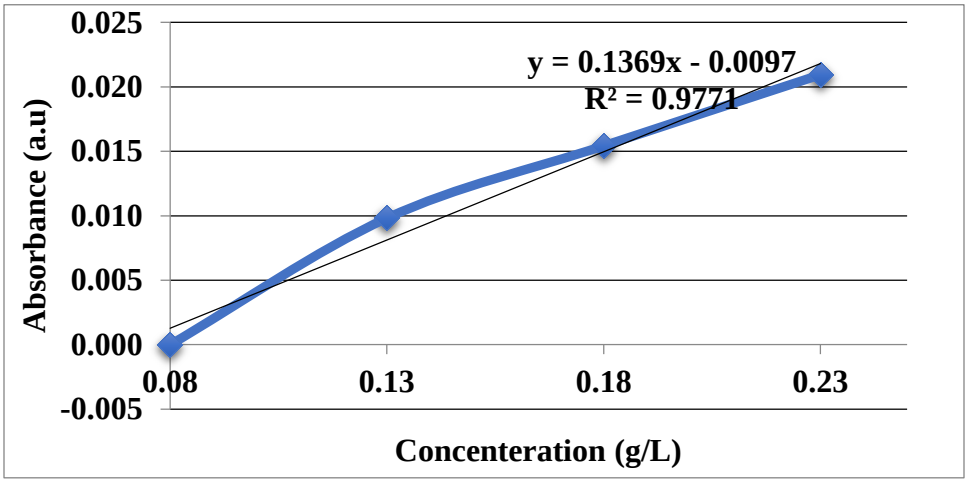

Figure 15: Calibration plot of absorbance in a.u (y) vs concentration in g/L (x)

From the graph, the slope was found to be 0.1369. Thus, equilibrium concentration at the time‘t’, was determined as the given formula Ce = (absorbance)/ (0.1369).

4.3. Characterization of adsorbent

4.3.1. XRD characterization

The mineral compositions of purified bentonite and activated bentonite (AB5) samples were identified by XRD patterns. In the present study, the XRD analysis was used to know the chemical composition of bentonites. The presence of minerals in bentonite clay was determined by 2θ or d-spacing values. As shown in Figure 18 (a) the presence of diffraction peaks corresponding to angles 2θ (19.79º, 26.63º, 35º, and 61.44º), confirming the presence of montmorillonite (MMT) in the sample of purified bentonite. The data also indicates the presence of impurities such as Muscovite (17.88º), Cristobalite (22.12º), Hematite (24.26 and 55.15º), Feldspar (28.01º), and Quartz (21.03º, 26.67º, 36.5º, 51.68º, 60º, 68.2º, and 75.8º) evaluated in purified bentonite. Similar results were reported by [147], [127] on Afar bentonite. The crystalline structure of the bentonite has a small change after activating by Na_2CO_3, which is observed in Figure 18 (b) below. Generally from, the characterization of XRD patterns the local Gewane bentonite indicates the presence of Montmorillonite (MMT), Quartz (Q), Muscovite (Mu), Cristobalite (Cr), Hematite (H), and Feldspar (F) as a major phase.

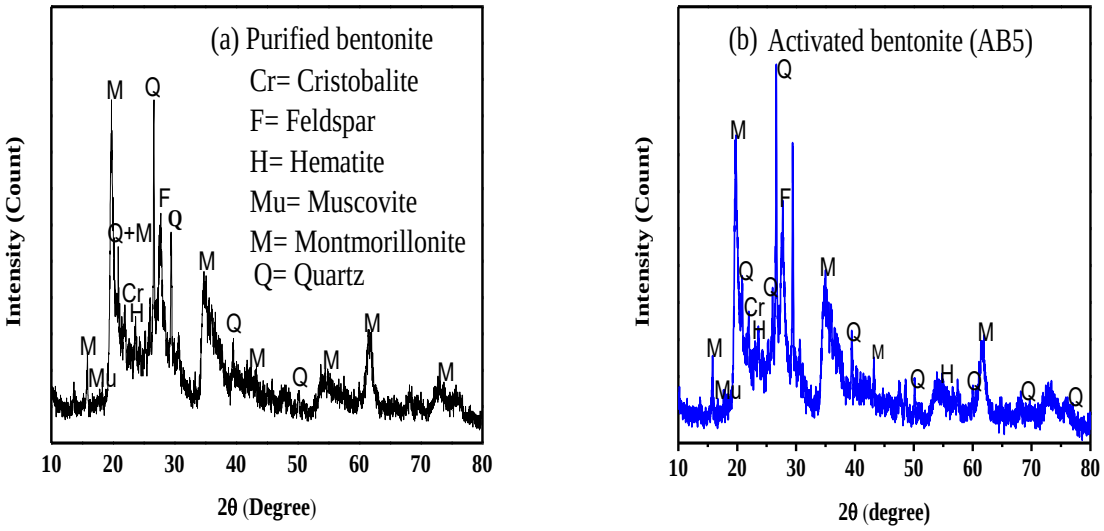

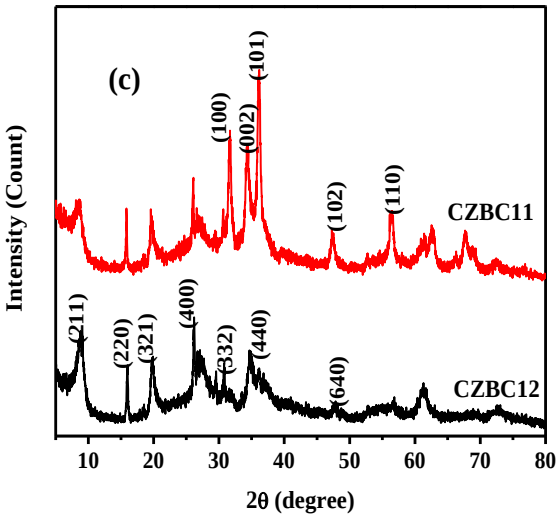

Figure 16: X-ray diffraction patterns for (a) purified bentonite, (b) activated bentonite (AB5), and (c) photocatalyst ZnO/bentonite nanocomposites (CZBC12 and CZBC11)

The crystalline structure and phase of the synthesized ZnO/bentonite nanocomposites with the ratio of ZnO to bentonite (CZBC12 and CZBC11) were analyzed using XRD. Figure 18 (c) shows the XRD patterns of the as-synthesized ZnO/bentonite nanocomposites with different ratios of ZnO and bentonite (1:1 and 1:2). The result from XRD patterns was indicated, the synthesized CZBC12 and CZBC11 samples showed a different patterns. The diffraction peaks located at (1 0 1), (1 0 0), (0 0 2), (1 0 2), (1 1 0), and (2 1 1) at 2θ values of 36.12º, 31.68º, 34.42º, 47.38º, 56.0º, and 8.87º respectively, were consistent with standard of (JCPDS Card No.75- 1533) [148]. This indicates that the peaks belong to the hexagonal wurtzite structure of ZnO. The other diffraction peaks located at (2 1 1), (2 2 0), (3 2 1), (4 0 0), (3 3 2), (4 4 0), and (6 4 0) at 2θ values of 8.87˚, 16.02º, 19.89º, 26.23º, 34.95º, 36.13º, and 47.80º respectively were indicates the bentonite characteristic peaks. A similar result was reported by [149].

Generally, from XRD analysis Scherer's equation (Equation 4.1) was applied to calculate the average crystallite size of purified bentonite, activated bentonite, and ZnO/bentonite nanocomposites [150]. $D = \frac{k\lambda}{\beta\cos\theta}$ (4.1)

where D:- crystallite size, k is Scherer's constant, which is 0.9, λ is the wavelength of the X-ray radiation which is 0.15406 nm, β is peak width at half maximum (radians), and θ is Bragg's angle. Hence, the average crystallite for all samples was calculated and reported in Table 10.

Table 10: Crystallite size for purified and activated bentonite from the XRD data

Sample code	No.	2θ	θ	d (A)	FWHS	(hkl)	D (nm)	D (Average) in nm
PB	1	19.79	9.89	4.48	0.57	1 0 0	13.73	24.63
	2	26.63	13.31	3.34	0.16	1 0 1	48.31	
	3	29.45	14.72	3.03	0.20	1 0 1	38.61	
	4	27.68	13.84	3.22	0.55	1 1 1	14.02	
	5	34.74	17.37	2.58	0.78	2 2 0	9.72	
	6	61.44	30.72	1.51	0.29	2 1 1	23.55	
AB5	1	26.61	13.31	3.35	0.16	1 0 1	48.31	30.18
	2	19.72	9.86	4.50	0.45	1 0 0	17.39	
	3	29.41	14.71	3.03	0.18	1 0 0	42.68	
	4	27.70	13.85	3.22	0.46	1 0 1	16.76	
	5	27.50	13.75	3.24	0.33	2 0 0	23.39	
	6	61.44	30.72	1.51	0.21	2 1 1	32.52	

The raw bentonite and 5% Na_2CO_3 activated bentonite (AB5) adsorbent used in this work have particle sizes 24.63 nm, and 30.18 nm respectively. From the XRD result and Table 10, the d-spacing or interlayer spacing of activated bentonite (AB5) is higher than the purified bentonite. This is due to the activated bentonite (AB5) contain more Na^+ ions than purified bentonite. The Na^+ ion is smaller in size than Ca^{+2} and it tends to have greater hydration energies, and thus within the interlayer of bentonite clay can attract more water than large ions.

Table 11: Crystallite size for ZnO/bentonite nanocomposites with different ratios of ZnO to bentonite (CZBC12 and CZBC11) from the XRD data

Sample code	No.	2θ	θ	d (A)	FWHS	(hkl)	D (nm)	D (Average) in nm
CZBC11	1	36.12	18.06	2.48	0.59	1 0 1	12.80	12.97
	2	31.68	15.84	2.82	0.52	1 0 0	14.70	
	3	34.42	17.21	2.60	0.79	0 0 2	9.61	
	4	47.38	23.69	1.92	0.41	1 0 2	17.74	
	5	56.04	28.02	1.62	0.70	1 1 0	10.02	
CZBC12	1	8.87	4.44	9.95	1.19	2 1 1	6.65	9.74
	2	26.23	13.12	3.39	0.65	4 0 0	11.90	
	3	34.96	17.48	2.56	1.28	3 3 2	5.92	
	4	16.02	8.01	5.53	0.56	2 2 0	14.05	
	5	19.89	9.95	4.46	0.77	3 2 1	10.16	

4.3.2. FT-IR characterization of the adsorbent

The functional groups of bentonites and their composites ZnO/bentonite were characterized using FT-IR spectra in the range 4000 - 400 cm^{-1}. In the present study, the FT-IR was used for analyzing the bentonite before adsorption, after adsorption, and after desorption of MB dye as indicated in Figure 19 (a). Also, calcined and uncalcined ZnO/bentonite (CZBC11 and UZBC11) was analyzed using FT-IR. This technique has been significantly used to understanding the structure, bonding, and reactivity of clay minerals.

The result for this study is shown in Figure 19 (a) which gives information on fundamental vibrational modes of the constituent units of bentonite clays. From the Figure 19 (a), there are four main absorption regions: 3600-2900 cm^{-1}, 2900-2850 cm^{-1}, 1630-1440 cm^{-1} and 1030-462 cm^{-1}. The FT-IR spectrum indicates that montmorillonite was the dominant mineral phase in bentonite clay. The KBr curve for purified bentonite was characteristic of montmorillonite with a single sharp band at 3620 cm^{-1}. This spectrum indicates the stretching vibration of -OH of water coordinated to octahedral Al^{3+} cations. And broadband at 3435 cm^{-1} indicates the stretching

vibration of -OH groups for the water molecule of hydration, which is adsorbed on the bentonite surface. The -OH deformation mode of water was indicated at 1630 cm^{-1} absorption band. The absorption band indicated at 1020 cm^{-1} was montmorillonite that has a strong band at bonding to the Si-O stretching vibration of bentonite mineral, which gives strong evidence for a silicate structure. The other band at 690 cm^{-1} corresponded to coupled Al-O and Si-O out-of-plane vibrations. Quartz was present as indicated by the bands at 522 cm^{-1} vibrations of Si-O-Al (Octahedral) and Cristobalite at band 785 cm^{-1} similar result was reported previously by [151], and the band at 462 cm^{-1} corresponds to Si-O-Si bending.

FT-IR was sensitive to the structural changes which occur in the clay upon soda activation and the IR data recorded in this study was suggested that both the octahedral and tetrahedral sheets were not influenced by soda attack. The intensity of stretching bands observed at 3620 cm^{-1} for purified bentonite (Al-OH-Al along with the Al-Mg-OH stretching vibrations) was the same as activated bentonite by sodium carbonate. Activation of bentonite by Na_2CO_3 has changed the peaks of the bands associated with the absorbed water at 3435 cm^{-1} (H-O-H stretching). Also, the activation of bentonite by Na_2CO_3 decreases the peaks of the bands associated with the absorbed water at 1630 cm^{-1} (H-O-H bending). Changes in the intensities of these bands were explained as due to loss of water molecules as pure bentonite to activated bentonite. After desorption of MB dye from the adsorbent, the intensity band at 1440 cm^{-1} disappeared. On the other hand, after soda activation, the intensity band at 1020 cm^{-1} increases due to the formation of three–dimensional networks of amorphous Si-O-Si units. But the intensity of the band at 690 cm^{-1} for (Al-OH-Si bending) almost disappeared with soda activation, signifying the partial dissolution of aluminum ions present in the octahedral sheet of bentonite. The intensity of the band at 522 cm^{-1} after desorption of MB dye from the spent adsorbent becomes bending. The result observed in this study indicates that the pattern of the spectra differs for the bentonite coated by methylene blue and purified bentonite and after desorption of MB at the region 1700 - 500 cm^{-1} were changes a certain band. In this region, interaction can occur between bentonite clay and secondary amines functional group of methylene blue in Figure 19 (a).

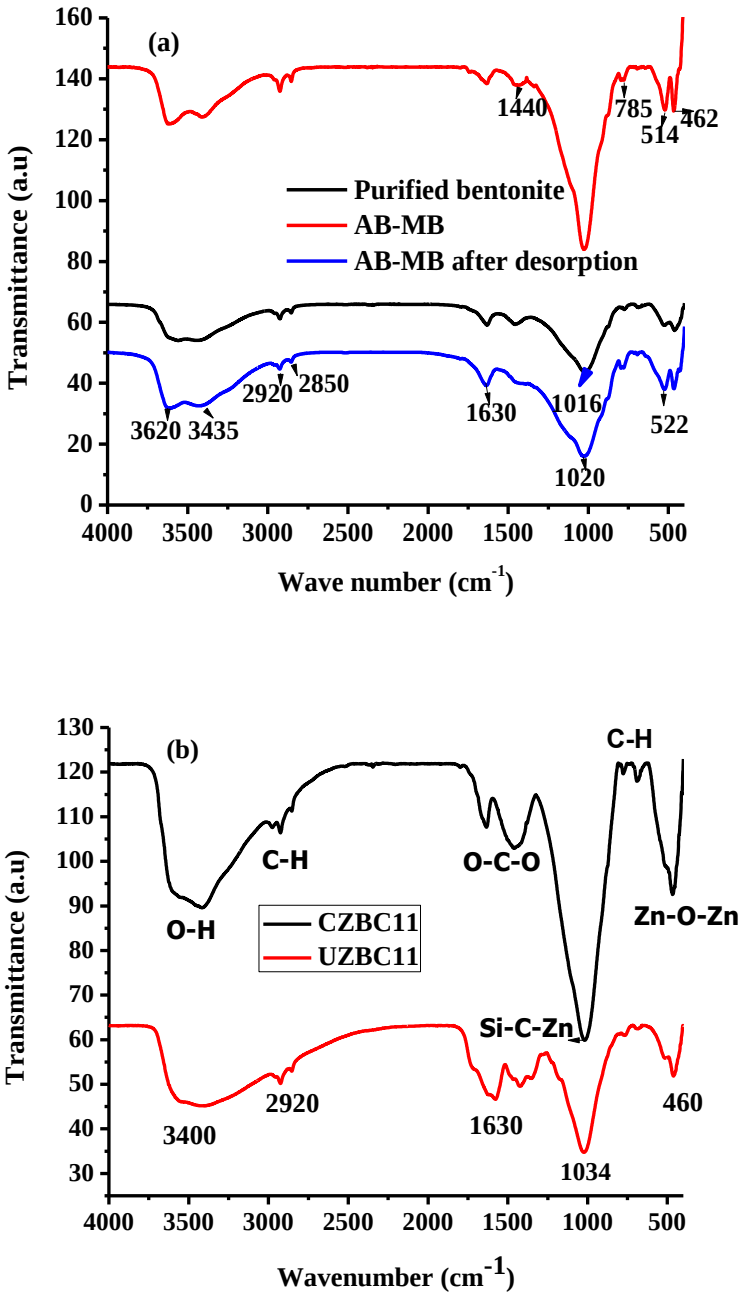

Figure 17: FT-IR spectra for (a) purified bentonite, bentonite after adsorption, and after desorption of MB, (b) uncalcined and calcined ZnO/bentonite nanocomposites

As indicated in Figure 19 (b) calcined and uncalcined ZnO/bentonite nanocomposites (CZBC11 and UZBC11) showed broadband absorption between 3400–3700 cm^{-1}, representing stretching vibration of the O-H group of Zn-OH and Si-OH interacted with water molecules to form a hydrogen bond, but small deformation of Zn-OH and Si-OH formed in calcined CZBC11. The

spectra of calcined and uncalcined ZnO/bentonite nanocomposite exhibited the intensity band at 2843 and 2920 cm^{-1}, which indicated the stretching vibration of the C-H bond in CH_2 and CH_3 groups respectively. It also appears a peak of Si-O-Zn at 1024 cm^{-1}. The absorption peaks at 460 cm^{-1} and 400 cm^{-1} in both calcined and uncalcined ZnO/bentonite nanocomposites are assigned to Zn-O bond similar to another study [152] that the vibration of Zn-O appeared in the range of 540-426 cm^{-1}.

4.3.3. Scanning electron microscope (SEM) analysis

The surface morphology of activated bentonite (AB5) before and after adsorption was analyzed using SEM (JEOL, JCM-6000Plus) at different magnification levels and results were shown in Figure 20 (a-f). The availability of pores and the internal surface is displayed in the SEM image of the AB5 before adsorption in Figure 20 (a, c & e), this shows the surface of activated bentonite (AB5) before adsorption was rough. The coverage of the surface and pores by the adsorbed methylene blue is indicated in Figure 20 (b, d & f) this, shows the surface activated bentonite (AB5) after adsorption was smooth. The porous structure that appeared in Figure 20 (a, c & e), became unclear as shown in Figure 20 (b, d & f) because of adsorption of MB dye and covers the surface.

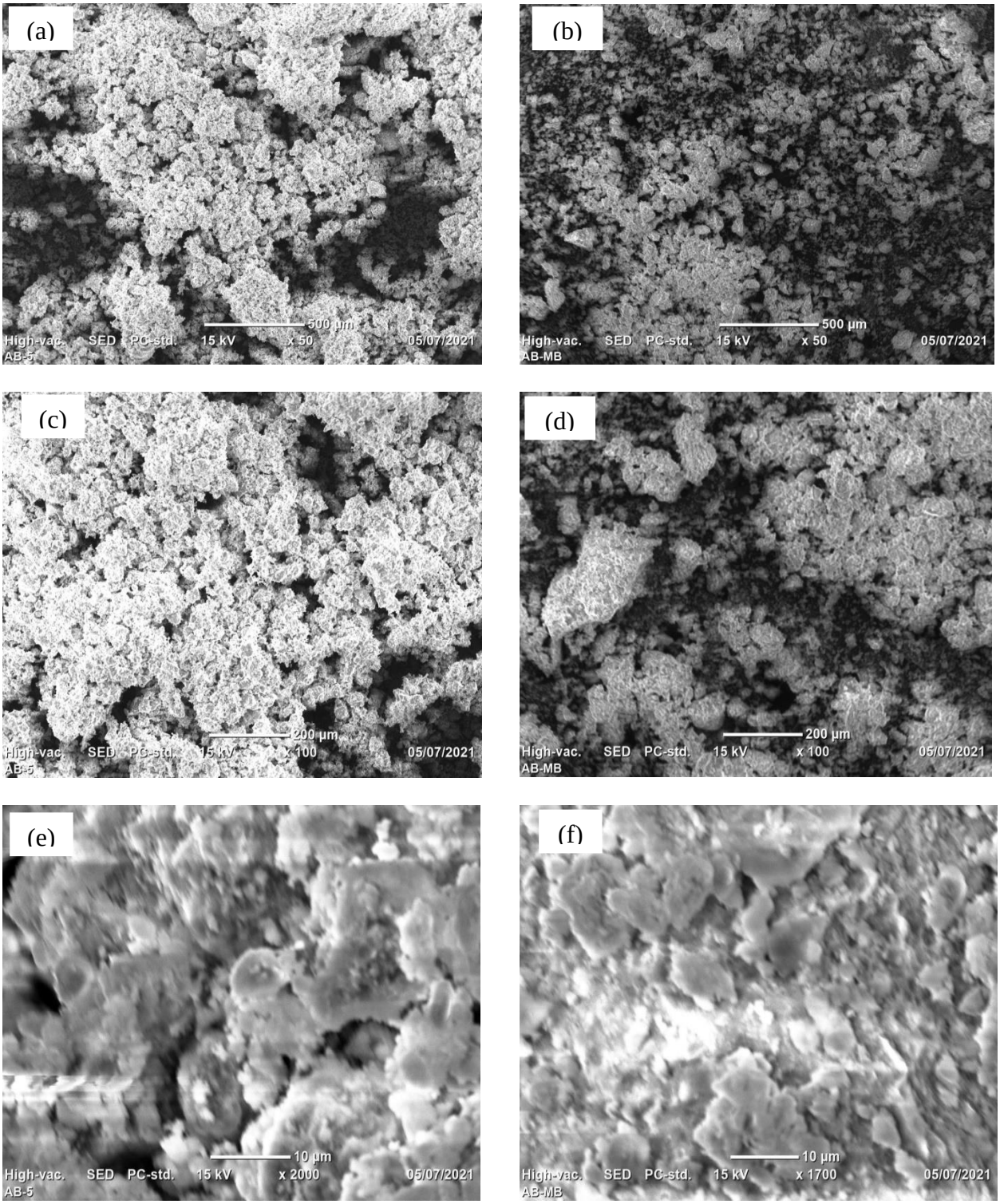

Figure 18: SEM image of (a, c, & e) activated bentonite powder and (b, d, & f) activated bentonite powder after adsorption (AB5-MB) at different magnifications

4.3.4. Complete silicate analysis of bentonite

Raw bentonite and 5% Na_2CO_3 activated bentonite (AB5) are analyzed by complete silicate analysis. For this characterization natural and activated bentonites having 75 µm sizes were analyzed by $LiBO_2$ fusion, HCl attack, gravimetric, colorimetric, and AAS analytical methods, and the results are listed in Table 12.

Table 12: Complete analysis of raw bentonite and AB5

Oxides %	Natural bentonite	Activated bentonite (AB5)
SiO_2	55.54	55.14
Al_2O_3	12.65	12.25
Fe_2O_3	7.75	6.96
CaO	3.15	<0.01
MgO	2.8	2.71
Na_2O	1.41	5.92
K_2O	0.98	0.95
P_2O_5	0.64	0.57
TiO_2	1.35	1.36
H_2O	4.38	5.32
LOI	9.75	8.82

Previously major and minor oxide composition of Gewane area bentonite was reported by (Mesfin Tessema, 2012) i.e., SiO_2 (54.2 %), Al_2O_3 (12.65 %), Fe_2O_3 (7.75 %), TiO_2 (1.35 %), CaO (4.15 %), Na_2O (1.85 %), K_2O (1.35 %), MnO (0.1%). As indicated in Table 12 the present results revealed that the Gewane area bentonite is Ca-bentonite. But for the present study when natural bentonite which is Ca-bentonite was activated by Na_2CO_3 it changes the oxide contents and becomes Na-oxides.

For instance, the sodium oxide and calcium oxide present in the natural bentonite before activation were analyzed and the results show the Na_2O of raw bentonite was lower than AB5 as presented in Table 12. The percentage of CaO decreases consistently and the percentage of Na_2O increases, with the percentage increase in a mass ratio of sodium compounds. This indicates the Ca^{2+} of the raw bentonite was replaced by Na^+ during activation. The percentage of Na_2O

increase is much higher than the percentage reduction in CaO hence the divalent ions other than Ca^{2+} like Mg^{2+} also got replaced by Na^{+}. Na_2O percentage is maximum when treated with Na_2CO_3 the result was similar to the previous study [153].

4.4. Optimization of adsorbent in the removal efficiency of MB dye from aqueous solution

4.4.1. UV-Vis spectrum of MB dye solution (80mg/L)

The λmax (663 nm) absorbance observed on UV-Vis spectrum obtained for 80 mg/L solutions indicated in Figure 14, confirmed the stock solution is MB dye [130]. As indicated in Figure 14 *Methylene blue* has two absorbance peaks at 609 and 668 nm.

- π-π* of the benzene ring and a band at low energy around 660-670 nm (moving according to the pH of the solution) and
- n-π* transitions (n is the free doublet on the nitrogen atom of C=N bond and free doublet of S atom on S=C bond) at 605nm.

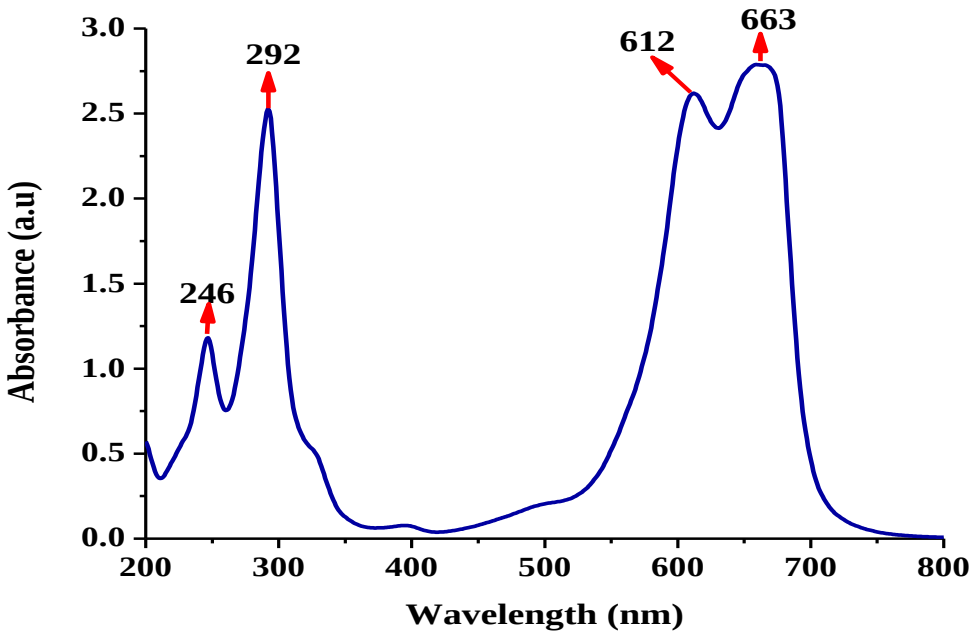

Figure 19: UV-Visible spectrum of MB dye

4.4.2. MB dye sorption from aqueous solution with activated bentonites

The activated bentonite with different amounts of Na_2CO_3 (2.5, 5, 7.5, and 15g) per 100g of bentonite clay was used to remove methylene blue dye from an aqueous solution. The experimental work was carried out by keeping the parameters constant like AB dosage = 0.1g of (AB2.5, AB5, AB7.5, and AB15), pH= 7, at a temperature of 25 ˚C, initial concentration of MB dye = 80mg/L, and mixing speed at 300 rpm for 30min. The result from this experiment shows the removal efficiency of MB dye increase from AB2.5 to AB5, and the maximum removal efficiency observed by AB5. However, the removal efficiency of MB dye from aqueous solution decrease after AB5 as indicated in Figure 21. This was due to activated bentonite by 5g Na_2CO_3/100g bentonite has very low permeability when compared with AB2.5, AB7.5, and AB15, this was AB5 has a very small particle size, shape, and subsequent micropores, and large negative surface charge. A high negative charge on the surface of activated bentonite by (AB5) makes the attraction of opposite charge MB dye highly on its surface. Also, the AB5 has higher Na_2O contents in the layer than AB2.5, AB7.5, and AB15 as reported by [90]. The higher amount of Na-in bentonite makes the removal efficiency of MB dye from aqueous solution was higher, but the lower amount of Na-in bentonite makes the removal efficiency of MB dye from aqueous solution was lower for AB2.5, AB7.5, and AB15. Due to the above reason, the high removal efficiency of MB dye occurred by AB5 when compared to AB2.5, AB7.5, and AB15.

Table 13: Effect of amount of Na_2CO_3 for activation of bentonite on removal efficiency of MB

Activated bentonite by Na_2CO_3	Remaining concentration of MB (mg/L)	Adsorption capacity qe (mg/g)	% Removal efficiency of MB
2.5%	0.055	39.972	99.93
5%	-2.37E-05	40.000	100.0
7.5%	0.056	39.971	99.92
15%	0.114	39.940	99.85

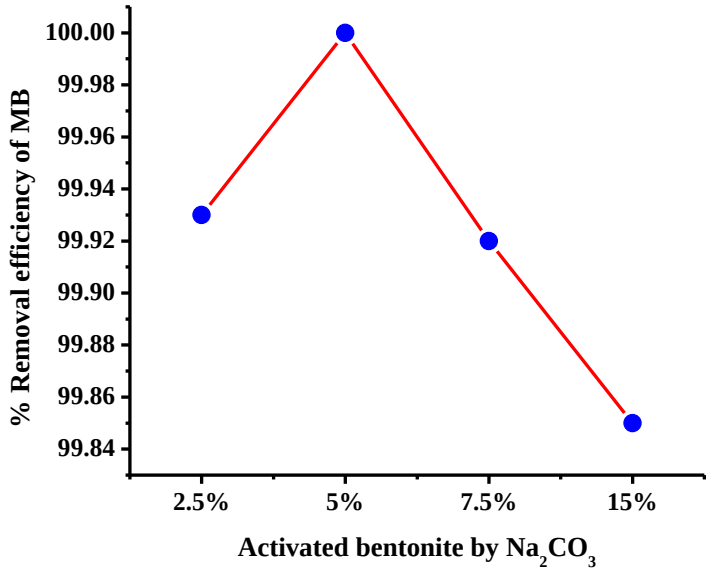

Figure 20: Effect of Na_2CO_3 for the activation of bentonite on removal efficiency of MB dye

4.4.3. MB dye sorption from aqueous solution with ZnO/bentonite nanocomposites

The experimental study for removal of MB dye from aqueous solution was carried out by taking 0.1g of calcined and uncalcined (ZBC12, ZBC12, ZBC32) ZnO/bentonite nanocomposites into each beaker contains 50ml of MB dye solution with an initial concentration = 80mg/L. Then the suspension was mixing with the speed of 300 rpm for 30 min at constant parameters like pH = 7, the temperature of 25 ˚C. The result from this study indicated the calcined ZBC with different ratios of ZnO to bentonite has higher removal efficiency of MB dye from aqueous solution than the uncalcined ZBC as showed in Table 14. This was due to the H^+ group in the ZnO structure that competed with MB^+ is absent where it was calcined at 450 ˚C, this makes the calcined ZBC shows the highest removal efficiency of MB dye from aqueous solution.

The CZBC32 has the highest removal efficiency equal to 99.94%. This might be due to zinc ions in CZBC32 were high which yields a more porous composite texture. That means, by increasing the loading of zinc ions, the distance between nanoparticles increases. When the distance between nanoparticles increases it produces more porosity. If the porosity of composites is high easily adsorbed pollutants on its surface makes the adsorption of pollutants was high. The other reason for CZBC32 has the highest removal efficiency of MB was due to its negatively charged surface. Because of this, the surface charge of ZnO/bentonite nanocomposites plays a significant

role in the adsorption of positively charged MB molecules. Or to enhance the adsorption of MB^+ by coating the pure ZnO with a substance that carries a permanent negative charge such as the negative surface bentonite clay to produce ZnO/bentonite nanocomposites. Hence, the presence of bentonite onto the surface of ZnO will act as a Lewis acid, which can interact with a Lewis base such as MB^+, which donating electron density via the nitrogen lone pair of electrons [154]. ZnO/bentonite nanocomposites dramatically enhanced the adsorption rate of the MB^+ in both acidic and basic media.

Table 14: The effect of ZnO/bentonite nanocomposites on the removal efficiency of MB dye

Sample code	Remaining conc. of MB dye (mg/L)	Adsorption capacity q_e (mg/g)	% Removal of MB dye
UZBC12	0.71	39.65	99.12
UZBC11	0.81	39.60	98.99
UZBC32	0.19	39.90	99.76
CZBC12	0.05	39.97	99.92
CZBC11	0.21	39.89	99.74
CZBC32	0.047	39.98	99.94

4.4.4. Removal of MB dye from aqueous solution with different adsorbents

The optimization tests for adsorbents were carried out to know the best adsorbent for the removal of MB dye from an aqueous solution. For this experiment, RB, PB, AB5, and CZBC32 were used for the removal of MB dye from the aqueous solution. The adsorption test was carried out at constant parameters like adsorbent dosage = 0.1g, pH of solution =7, initial concentration of MB dye 80mg/L, the temperature at 25˚C, and mixing speed 300 rpm for 30 min. From this experiment, the results showed the 5% Na_2CO_3 activated bentonite (AB5) has high removal efficiency for MB dye removal from aqueous solution than RB, PB, and CZBC32 as indicated in Table 15. This was due to the Na-activated bentonite has a more negative surface than other adsorbents. The more negative surface charge of Na-bentonite makes the best removal of cationic dye from an aqueous solution. The other reason for AB5 with high removal efficiency was due to the interactions between the negative charge of Si-O and the positive charge of methylene blue ion (MB^+), ionic exchange with the Na-bentonite.

Table 15: Removal of MB dye from aqueous solution on NB, PB, AB5, and calcined ZBC32

Sample code	Remaining conc. Of MB dye (mg/L)	Adsorption capacity qe (mg/g)	% Removal of MB dye
NB	0.055	39.97	99.93
PB	0.84	39.58	98.95
AB5	-2.37E-05	40.00	100.0
CZBC32	0.047	39.98	99.94

On the other hand, the result shows the PB has the lowest removal efficiency as indicated in Table 15; this was due to the purification of bentonite clay has effects on the mineralogical composition of the raw material and related properties; that is, organic matter is leached out and feldspar can be partly attacked (or dissolved). This process causes an increase in surface area and surface acidity and introduces permanent mesoporosity and also removes metal ions from the crystal interlayer, which partially delaminated the clay [155]. The other reason why the purified bentonite has the lowest removal efficiency of MB dye was due to after purification bentonite it was dried but the moisture content cannot be lost from the bentonite. The moisture in bentonite makes the pore sizes on the surface of bentonite was filled with water.

4.5. Investigation of the effect of different parameters on adsorbent (AB5)

4.5.1. Effect of adsorbent dosage on adsorption efficiency

The effect of adsorbent dosage (AB5) was carried out by keeping all parameters constant like pH = 7, initial dye concentration = 80mg/L, contact time = 30min, at a temperature of 25°C, mixing speed 300 rpm, and volume of MB dye = 50ml. But, varied the amount of AB5 dosage to know the effects of dosage regarding the amount of MB dye concentration. The result observed from this study after the adsorption process indicates the removal efficiency of MB dye increases as AB5 dosage increases. This might be due to the presence of more adsorption sites present on the AB5 surface as adsorbent dosage increases. As shown in Figure 22 (a) there is a slow increase of adsorption efficiency between 0.1 and 0.2g then, above 0.2g increase sharply in the adsorption efficiency but reaches almost a no change after onwards and the increase in removal efficiency was very small similar result was reported previously by [156] on organo-modified nano clay. As the adsorbent dosage increase the adsorption capacity of MB dye was decreased as shown in

Figure 22 (b). The negative sign showed for the residual concentration of MB dye after adsorption of MB dye from aqueous solution indicates the excessive adsorbent site because of high adsorbent dosage.

Table 16: Effect of AB5 dosage on removal efficiency of MB dye

Doges of AB5 (g)	Remaining concentration of MB dye (mg/L)	Adsorption capacity qe (mg/g)	% Removal efficiency of MB dye
0.1	0.00031	39.9998	99.9996
0.5	1.03E-06	8	99.9999
1	-0.002940	4.0001	100.002
1.5	-0.003058	2.6607	100.0019

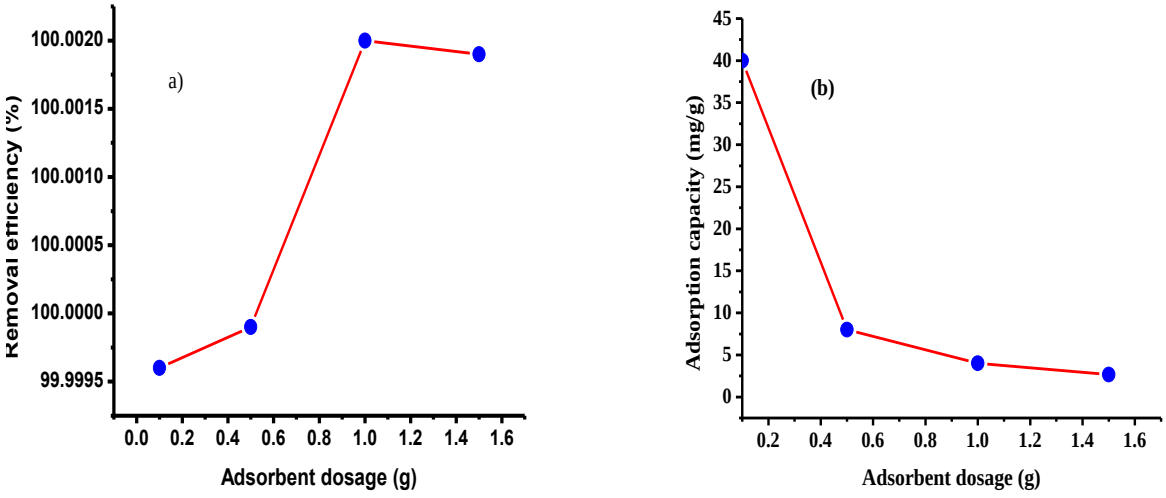

Figure 21: (a) Effect of AB5 dosage on removal efficiency of MB dye and (b) adsorption capacity of MB dye

4.5.2. Effect of initial concentration of MB dye

The experimental study of the effect of initial concentration on removal efficiency of MB dye was carried out by keeping all parameters constant AB5 dosage = 0.1g, contact time for 30min, pH = 7, at a temperature of 25˚C, mixing speed of 300 rpm, and volume of solution = 50 ml, except the initial concentration of MB dye which was varied from (80, 130, 180, and 230) mg/L.

From the present study, the result indicates, as the initial concentration of MB dye increases from 80mg/L to 230mg/L the removal efficiency of MB dye decreases as shown in Figure 23 (a). This implies the removal efficiency is inversely proportional to adsorbent surface loading. The reduction of removal efficiency of MB dye was due to the increased concentration of the methylene blue dye in the solution for the same number of AB5 sites and on the same surface of the AB5. In other words, the decrease in the removal efficiency of MB dye was attributed to the lack of sufficient surface sites to accommodate much more methylene blue dye concentrations present in the solution. At lower concentrations, all dye molecules present in the solution could interact with binding sites and thus be higher than those at higher concentrations. Thus, the removal efficiency of MB dye decreases as concentration increases, similar observations were reported by [140] for natural Saudi Red Clay.

Table 17: Effect of initial concentration of MB dye on removal efficiency of MB dye

Initial concentration of MB dye (mg/L)	Remaining concentration of MB dye (mg/L)	Adsorption capacity qe (mg/g)	% Removal of MB dye
80	- 7.01E-05	40.0	100.0
130	0.098	64.95	99.92
180	0.154	89.92	99.91
230	0.209	114.89	99.909

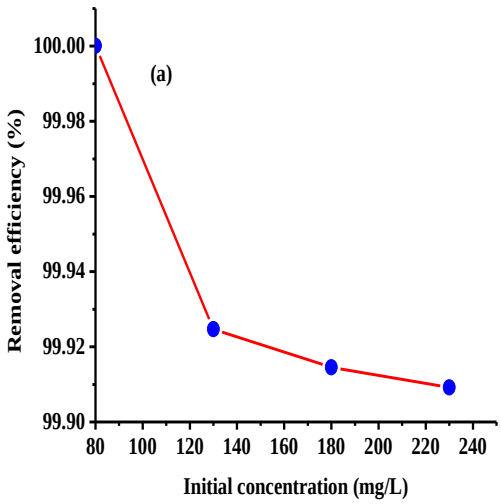

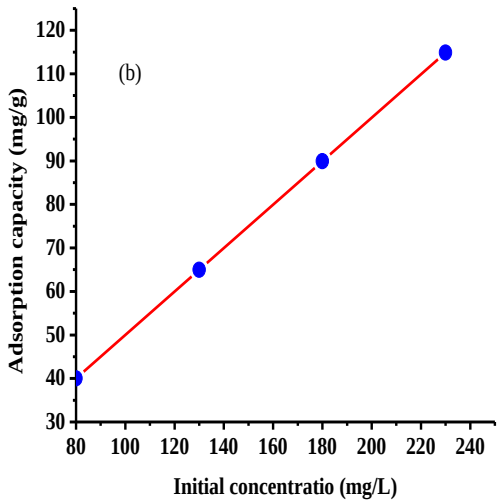

Figure 22: (a) Effect of MB dye initial concentration on removal efficiency and (b) adsorption capacity of MB dye

4.5.3. Effect of pH

During the adsorption process, the pH of the aqueous solution plays an important role [157]. The effect of pH on the removal of MB dye was carried out by keeping all parameters constant like temperature = 25˚C, AB5 dosage = 0.1g, initial concentration of MB dye = 80 mg/L, and mixing speed 300 rpm for 30 min. But the pH of the solution was varied from 4, 7, 9, and 11 to know the optimum pH of MB dye solution which had the best removal efficiency of MB dye. The result of this study indicates the removal efficiency of MB dye increase slightly with an increase in pH of solution uptake has been observed up to pH 7 thereafter, slightly a decrease in the removal of MB dye has been observed as shown in Figure 24. This was due to the surface of bentonite is negatively charged in acidic media; H^+ ions competed with MB^+ for activating bentonite sites and lead to minimal adsorption of MB dye onto AB5 at low pH of the solution. The other reason why the removal of MB dye increase as an increase in pH was due to the dissolution of MB dye into the water, the amine group in the MB dye structure enters the aqueous solution makes the dye has an overall positive charge and attracted to the negatively charged AB5 adsorbent. With the increase in pH, the number of H^+ ions decreased and the adsorbent surface carried a more negative charge resulting in greater attraction between the adsorbent and the cationic form of the adsorbate [50]. A similar result was reported for pH 7 by the previous researcher [158] on Kaolin.

Table 18: Effect of pH on removal efficiency of MB dye

pH of solution	Remaining concentration of MB dye (mg/L)	Adsorption capacity qe (mg/g)	% Removal efficiency of MB dye
4	0.30	39.85	99.60
7	-7.01E-05	40.0	100.0
9	0.299	39.85	99.63
11	0.92	39.54	98.85

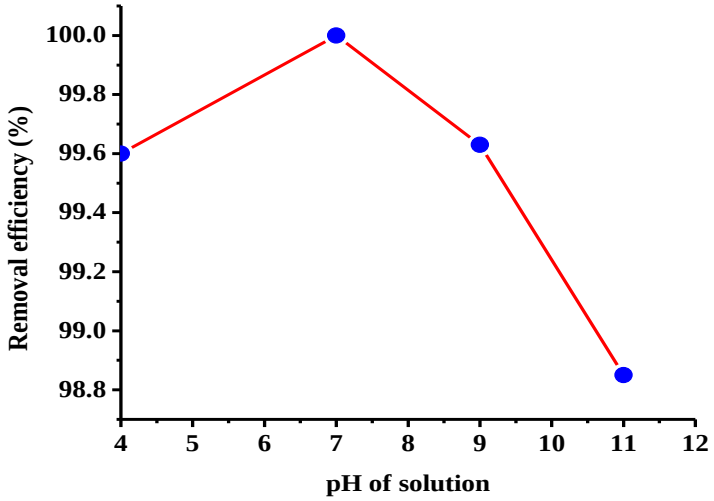

Figure 23: Effect of solution pH on removal efficiency of MB dye

4.5.4. Effect of temperature

The experimental study on the effect of temperature for the removal of MB dye was carried out by keeping all parameters constant such as pH = 7, initial concentration of MB dye = 80mg/L, contact time = 30 minutes, AB5 dosage = 0.1g, and mixing speed 300 rpm at a different temperature range of 25°C-50°C. The result indicates the removal efficiency of MB dye using AB5 was observed to increase with increasing temperature as shown in Figure 25. This was due to the increase in the kinetic energy and entropy of the system resulting in more collisions and activities at the boundary between the activated bentonite and MB dye, similar result was reported previously by [140] on natural Saudi Red clay.

Table 19: Effect of temperature on removal efficiency of MB dye

Temperature (°C)	Final concentration of MB dye (mg/L)	Adsorption capacity qe (mg/g)	% Removal efficiency of MB dye
25	0.0084	39.995	99.980
30	0.0046	39.997	99.994
40	0.0032	39.998	99.996
50	0.0013	39.999	99.998

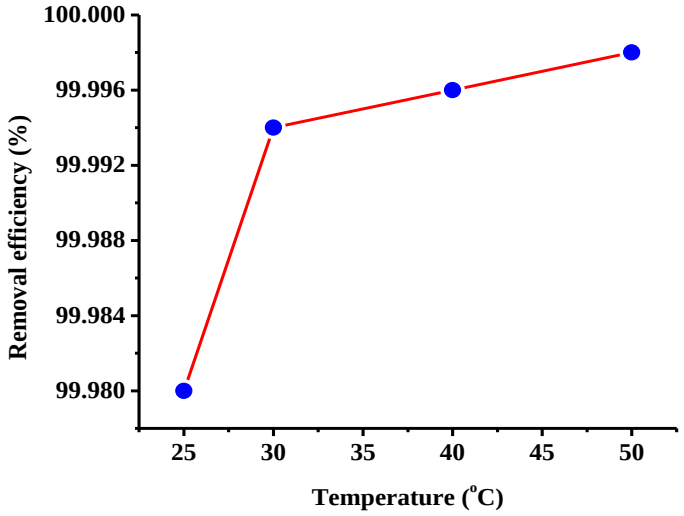

Figure 24: Effect of temperature on removal efficiency of MB dye

4.5.5. Effect of contact time

The effect of contact time on removal efficiency of MB dye from aqueous solution was carried out at constant parameters like pH = 7, initial concentration of MB dye = 80mg/L, AB5 dosage = 0.1g, mixing speed at 300 rpm, and at a temperature of 25˚C, for different contact time from 30 min to 90 min. The result of this study indicates the effect of contact time on the removal of MB dye from an aqueous solution was increase as the contact time increase. As shown in Figure 26 the removal efficiency of MB dye increase with contact time and the maximum adsorption of MB dye takes place in the first 30 minutes, this refers to the adsorption was spontaneous. After the first 30 minutes, a small increase in adsorption of MB dye and reached nearly equilibrium. But, during the first 30 minutes, the adsorption of dye was very fast. This may indicate the availability of the negatively charged surface sites of activated bentonite (AB5) which caused fast electrostatic attraction of methylene blue dye from the aqueous solution. A similar result was reported by [159] on modified bentonite.

Table 20: Effect of time on removal efficiency of MB

Time (min.)	Residual concentration of MB (mg/L)	Adsorption capacity qt (mg/g)	% Removal efficiency of MB
0	0	0	0
30	-7E-05	40.00	100.0
45	0.0096	39.99521	99.98802
60	0.0098	39.99512	99.98781
90	0.0099	39.99504	99.98760

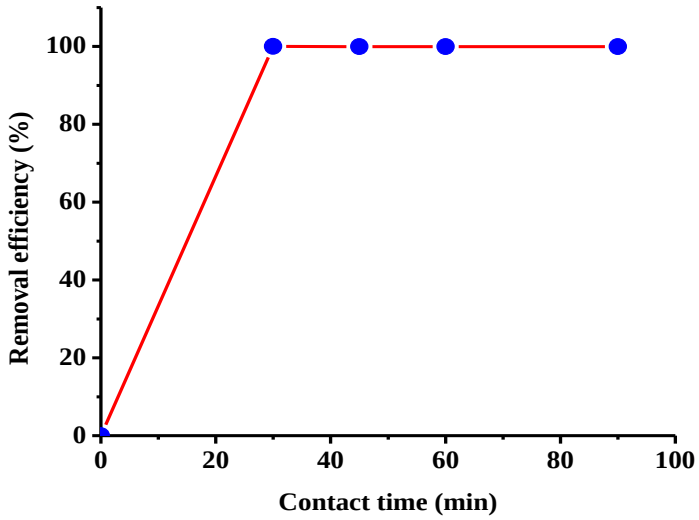

Figure 25: Effect of contact time on removal efficiency of MB

4.6. Adsorption isotherms

Adsorption isotherm describes the qualitative information on the nature of the adsorbent surface interaction as well as the specific relationship between the concentration of adsorbate and its degree of accumulation onto the adsorbent surface at a constant temperature. Adsorption isotherms are critical in optimizing the utilization of adsorbents, and therefore the analysis of the isotherm data by fitting them to different isotherm models is a crucial step to find the suitable model that can be used for design purposes [160]. Hence, three well-known isotherms were selected for the present study, namely Langmuir, Freundlich, and Temkin isotherms.

4.6.1. Langmuir adsorption isotherm model

The Langmuir isotherm model works based on the assumption of a monolayer and uniform energies of adsorption. In this Langmuir constant (K_L) and the maximum adsorption capacity (qmax) were respectively obtained from the slope and the intercept of a linearized Langmuir equation [161].

The values of qmax (mg/g) and K_L (L/mg) was determined from the plot of Ce Vs Ce/qe. The adsorption capacity is often correlated with the variation of the area and porosity of the adsorbent. Higher surface area and pore volume resulted in higher adsorption capacity [162]. The essential characteristics of the Langmuir isotherm are often expressed by a dimensionless constant called the equilibrium parameter, RL.

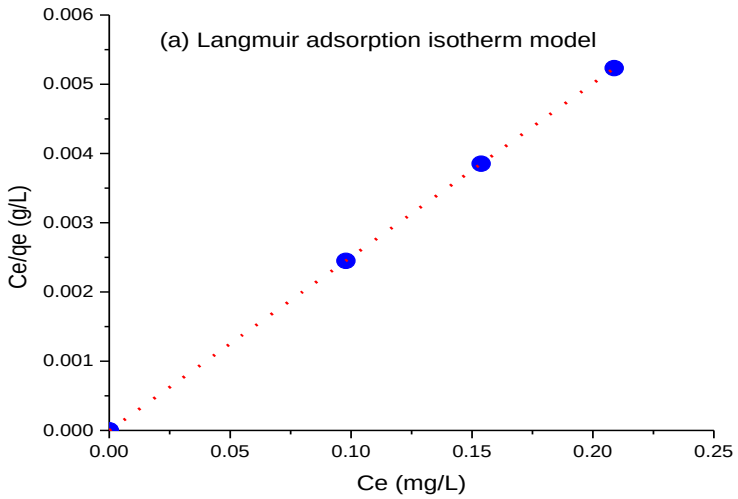

Figure 26: Langmuir adsorption isotherm curve

The Langmuir adsorption was indicated by maximum adsorption capacity (qmax) which represents the saturated monolayer adsorption at equilibrium. The result shown in Table 13 indicates the Langmuir adsorption isotherm parameters qmax (76.5 mg/g) and R^2 was 1 which is a strong correlation coefficient. The correlation coefficient was obtained from a graph of Ce/qe versus Ce plotted and linearity was determined from the correlation coefficient (R^2) as indicated in Figure 27. From the correlation coefficient R^2 of Langmuir, the adsorption isotherm indicates the adsorption study of MB dye on activated bentonite was best fits the Langmuir isotherm model than that of Freundlich and Temkin isotherm models. The Langmuir isotherm study

indicates the value of RL decided the shape of the isotherm was favorable due to the value of RL for this study was found in between 0 & 1 that means (0<RL< 1) [142].

4.6.2. Freundlich adsorption isotherm model

The Freundlich equation is an empirical equation employed to describe adsorbate on the surface of the heterogeneous adsorbent that is characterized by the heterogeneity factor 1/n, describes reversible adsorption, and is not restricted to the formation of the monolayer. The affinity between the adsorbate and adsorbent might be indicated by the heterogeneous factor, 1/n. The isotherm parameters result is presented in Table 21. The saturated adsorption capacities at 298 ˚K for AB5 were 39.90 mg/g. The Freundlich parameter, of 1/n, was between 0 & 1 which indicates the favorability of MB dye adsorption on activated bentonite. This means the value of n is greater than 1 which indicates the bond between the MB dye and bentonite adsorbent was strong. The correlation coefficient R^2 of Freundlich was 0.712 this lower than the Langmuir isotherm, this indicating it does not fit the experimental data.

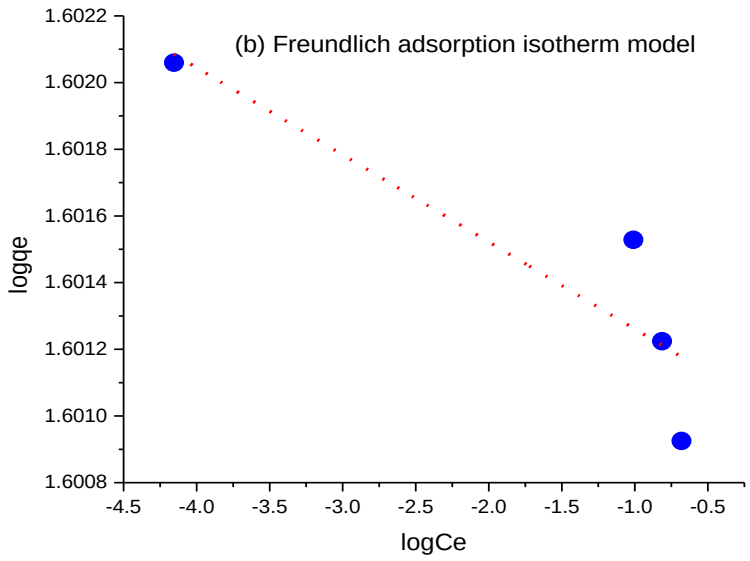

Figure 27: Freundlich adsorption isotherm curve

In Figure 28 the line does not touch all the dots. So, this model was not fit for this experimental data. The binding of MB molecule to one site on bentonite might facilitate the adsorption of subsequent molecules towards the active sites.

4.6.3. Temkin adsorption isotherm model

The Temkin adsorption isotherm model shows the adsorption heat of all molecules in the layer is assumed to decrease linearly with coverage of the adsorbent surface due to a decrease in the interactions between the adsorbent and adsorbate.

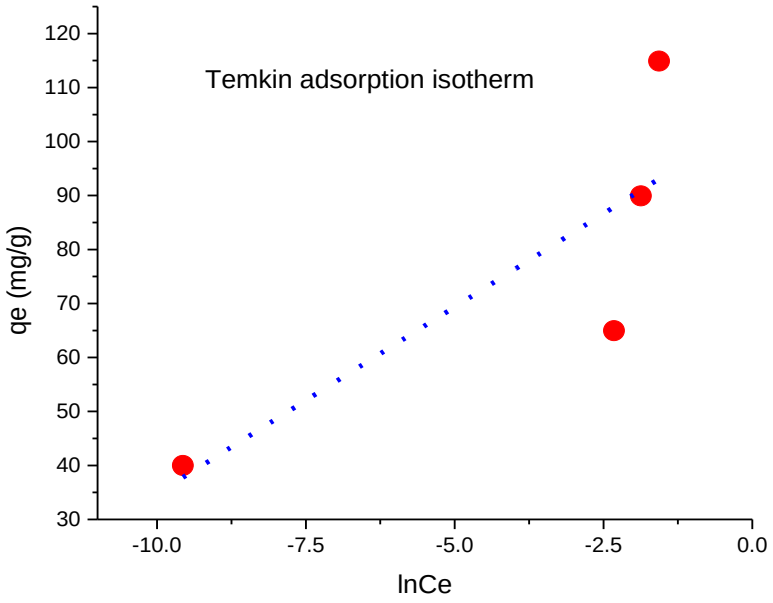

Figure 28: Temkin adsorption isotherm curve

Temkin isotherm model does not fit the experimental data and its parameters were obtained from a graph of qe vs. ln Ce plotted in Figure 29. Its linearity was determined from the correlation coefficient (R^2). As it was observed in Table 21 Temkin adsorption isotherm parameters are KT (320.29), B (6.92), and correlation coefficient $R^2 = 0.713$ which is a weak correlation coefficient. From this point of view adsorption of MB dye on activated bentonite is not packed with a similar structural arrangement.

Table 21: Isotherm models parameters for adsorption of MB from aqueous solution at constant parameters contact time = 30 min, at a temperature of 25˚C, mixing speed at 300rpm, the dosage of adsorbent =0.1 g, and at different initial dye concentration = 80-230 mg/L.

Isotherm models	Parameters	Values
Langmuir model	qmax (mg/g)	76.5
	K_L	0.521
	R_L	0.0234, 0.0145, 0.0105, 0.0083
	R^2	1
Freundlich model	1/n	0.107
	K_F (mg/g)	39.90
	R^2	0.712
Temkin model	B_T (KJ/mol)	6.92
	K_T (L/mg)	320.29
	R^2	0.713

4.7. Adsorption kinetics models

The adsorption kinetics describes the solute uptake rate, which in turn governs the residence time of the sorption reaction. Pseudo-first-order and pseudo-second-order models were applied to analyze the kinetics study of MB dye adsorption. It was one of the important characteristics in defining the efficiency of sorption. In the present study, the kinetics study of MB dye removal was carried out to understand the behavior of the prepared low-cost adsorbent activated bentonite. The corresponding data was given in Tables 22 for pseudo-first-order and pseudo-second-order respectively, which indicates the pseudo-second-order kinetic model fit well for MB adsorption data on activated bentonite than the pseudo-first-order kinetic model.

4.7.1. Pseudo-first-order and pseudo-second-order kinetic models

The pseudo-first-order kinetic model specified that the speed of occupation of adsorption sites is proportional to the number of unoccupied sites. The values of log (qe-qt) were linearly correlated with t. The values of K_1 and qe were calculated from the slopes and intercepts of log (qe-qt) against the t plots and the different parameters of pseudo-first-order kinetics are given in Table 22.

The result for the present study shows the pseudo-first-order model with a correlation coefficient (0.36) was not fit the experimental data as indicated in Figure 30 (a). While the pseudo-second-order model fitted very well with R^2 equal to a unit ($R^2 = 1$) as shown in Figure 30 (b). The MB dye adsorption on activated bentonite can be described as the pseudo-second-order model, which indicated that the adsorption of MB dye on activated bentonite can be described as chemical adsorption. The kinetic model for the present study results reveals that the adsorption of MB dye onto activated bentonite could be well explained by a pseudo-second-order kinetic model. This is good agreement with the work of the present study that was similar result was previously reported by [163] on activated red mud. The results of pseudo-first-order and pseudo-second-order kinetic models are summarized in Table 22.

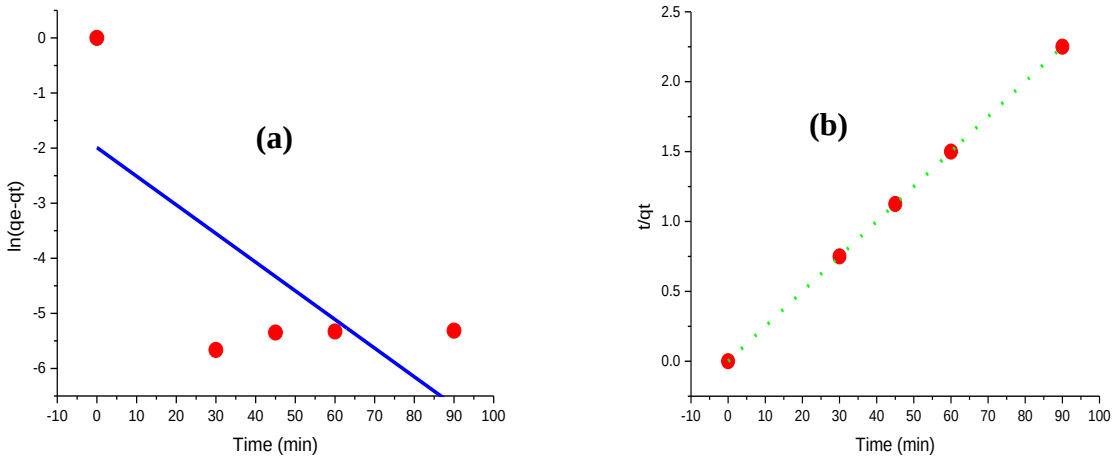

Figure 29: (a) Pseudo first-order kinetic and (b) Pseudo second-order kinetic model curve

Table 22: Parameters of pseudo-first-order and pseudo-second-order kinetics models for MB dye adsorption

Time (min)	The initial concentration of MB 80 mg/L	
	qt	Log(qe-qt)
30	39.994	-5.66
45	39.999	3.23
60	39.999	3.91
90	39.999	4.32
	Adsorption kinetics parameters	

Pseudo-first-order kinetics	Intercept	K_1(1/min)	qe Cal (mg/g)	R^2
	-1.99001	-0.00058	0.1367	0.36

Pseudo-second-order kinetics	Adsorption kinetics parameters					
	Intercept	Slope	qe	qe^2	K_2	R^2
	-1.06362E-5	0.025	40	1600	-0.00031	1

4.8. Thermodynamic study

Adsorption processes are influenced by temperature; thus in the present study, the effect of temperature was carried out in the temperature range of 298 °K to 323 °K. The thermodynamic parameters for the adsorption of MB dye on bentonite adsorbent were calculated to determine the thermodynamic feasibility of the thermal effects of the adsorption; the Gibbs free energy (ΔG°), the entropy ΔS° and the enthalpy (ΔH°) were calculated using Equation (4.2).

$$\ln K_d = \frac{\Delta S°}{R} - \frac{\Delta H°}{RT} = -\frac{\Delta G°}{RT} \quad (4.2)$$

where Kd is the distribution coefficient of adsorption and equal to the ratio between adsorption capacity (qe) to the equilibrium concentration (Ce), ΔH^o (KJ/mol) and ΔS^o (J/mol) are respectively, the changes in Enthalpy and Entropy; T is the absolute temperature in kelvin (^oK) and R is the gas constant (8.314 J/mol/K). The values of ΔH^o and ΔS^o were obtained from the plot of ln (Kd) vs 1/T. The plot of ln (Kd) as a function of 1/T should give a linear relationship with a slope of ΔH°/R and an intercept of ΔS°/R. Then the Gibbs free energy change (ΔG^o), indicating the spontaneity of the adsorption process, was calculated.

The result for the present study indicates the negative values of ΔG° show the adsorption process on the activated bentonite (AB5) was spontaneous. The increase in negative value with increasing temperature indicates that the adsorption process on activated bentonite becomes more favorable at higher temperatures as shown in Table 23. Also, the ΔG° values are in the range between -30 KJ/mol and -20 KJ/mol shows the physisorption was likely the mechanism of the study as reported by [164].

The standard enthalpy of adsorption ΔH° = 56.55 KJ/mol indicates an endothermic process and the positive value of ΔS° reflects the affinity of activated bentonite for MB and suggests an increase in disorder/randomness at the adsorbate-adsorbent interface i.e., some structural changes in dye and activated bentonite which agrees with the observations.

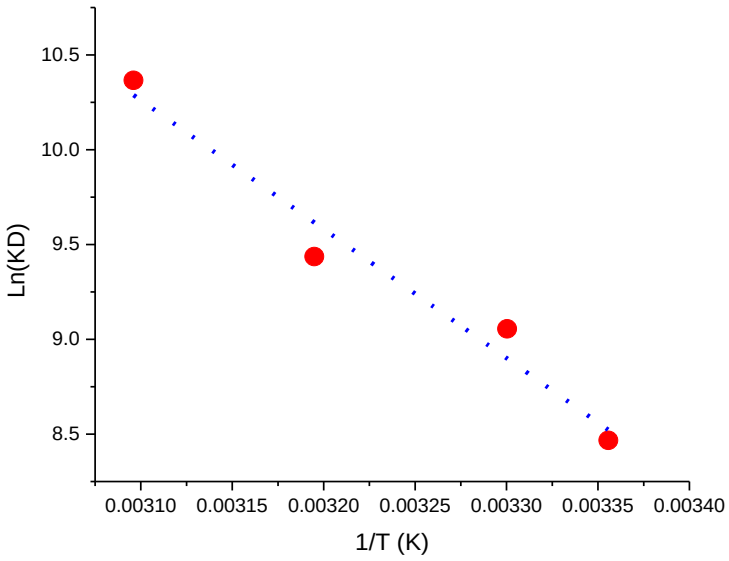

Figure 30: Thermodynamic parameters from adsorption of MB removal as a function of temperature

Table 23: Thermodynamic parameters of adsorption of MB onto activated bentonite

Adsorbent	Temperature (°K)	Kd	ΔG° (KJ/mol)	ΔH° (KJ/mol)	ΔS° (J/mol)	R^2
AB5	298	4755.65	-20.98	56.55	260.61	0.95
	303	8564.67	-22.81			
	313	12534.63	-24.56			
	323	31770.75	-27.84			

4.9. Recyclability of adsorbent & its composites

4.9.1. Desorption of MB dye from the exhausted adsorbent by thermo-chemicals method

The desorption study of MB dye from the exhausted adsorbent is important to investigate the retention stability of AB-MB and validate their reliability for regeneration purposes. This desorption of MB dye from the exhausted adsorbent was carried out by thermochemical method using different solvents. For this study, the dried adsorbent coated by MB dye after adsorption of

MB dye from an aqueous solution was used for the desorption study using distilled water, ethanol, and acetone.

The result for the present study shows desorption of MB dye from the exhausted adsorbent using distilled water (DW) was better when compared with ethanol and acetone as indicated in Figure 32 and Table 24. The desorption of MB from the spent adsorbent by ethanol and acetone was low, but the previous study by [125] shows the ethanol was a good solvent for desorption of MB dye next to inorganic acid HCl by thermochemical methods. However, the low desorption efficiency of MB dye from adsorbent might be due to a strong electrostatic attraction of MB with the adsorbent and requires higher energy to get rid of the dye within the chemical regeneration method. Strong adsorbent-adsorbate (AB-MB) interaction was necessary to ensure no leaching of MB dye adsorbed on activated bentonite occurred during the adsorption process makes the desorption of MB dye from the spent adsorbent low. On the other hand, efficient desorption of MB dye from exhausted adsorbent is the crucial step to allow the adsorbent to be regenerated [158]. After the desorption of MB dye from the exhausted adsorbent, the adsorbent was used for recyclability for the removal of MB dye from an aqueous solution.

Table 24: Desorption of methylene blue dye from the exhausted adsorbent (AB-MB) using thermo-chemicals method

Desorption of MB dye from AB-MB by	Contact time (min)	Concentration of MB in solvent (mg/L)	desorption capacity (mg/g)
Heating at (200 °C)	120	2.25	1.13
Without heating		1.83	0.91
Ethanol (35°C)		0.12	0.06
Acetone (35°C)		0.08	0.04
Distilled water (25°C)		1.27	0.64
Distilled water (35°C)		2.47	1.21
Distilled water (45°C)		2.09	1.04

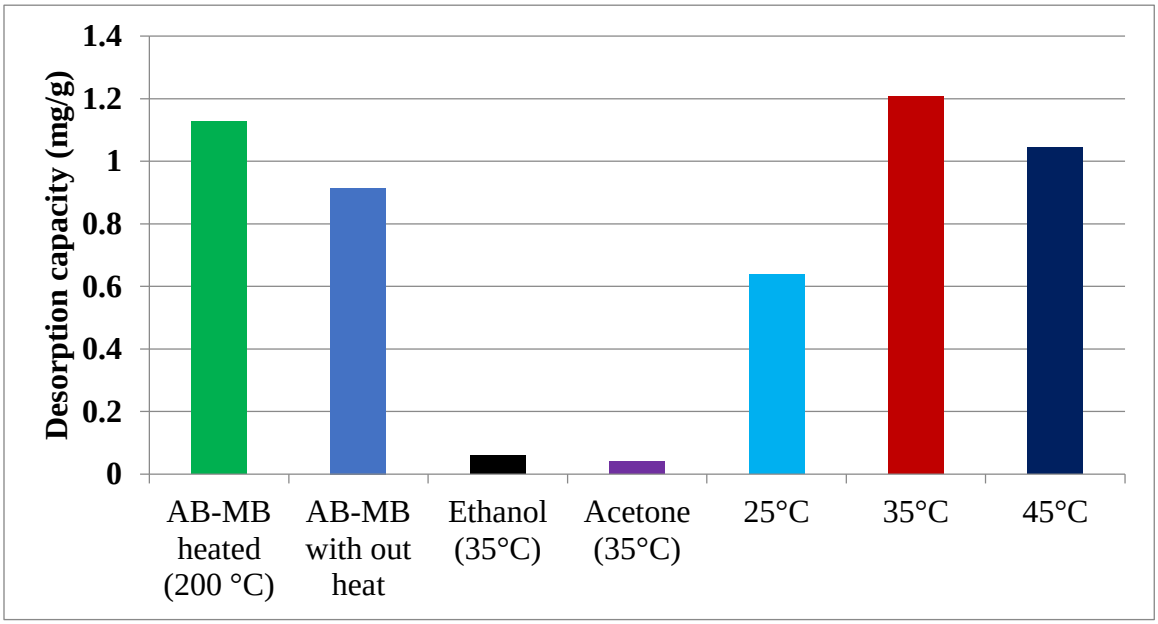

Figure 31: Desorption of MB from the spent adsorbent (AB-MB) by thermo-chemicals method

4.9.2. Recyclability of adsorbent after usage

After the adsorption study, the adsorbent was coated with the MB dye. Discharge of the spent adsorbent with MB dye to the environment is environmentally not good because the MB dye on the adsorbent is toxic and carcinogenic. Due to this reason recycling adsorbents after usage was one of the most important for reducing dyes that are discharged to the environment and water bodies.

In the present study, the recyclability of adsorbent for removal of methylene blue dye from aqueous solution was carried out by spent adsorbent after desorption of MB dye in distilled water at 35°C for 2hrs. The result for this recyclability study indicates the removal efficiency of MB dye from aqueous solution by reused adsorbent for the first, second, and third cycles were (71.89%), (66.71%), and (59.40%) respectively as shown in Table 25. The decreasing removal efficiency of MB dye from an aqueous solution of adsorbent might be due to the low desorption efficiency of MB dye from the active sites on the surfaces of adsorbent (AB5). As shown in Figure 33 the removal efficiency of MB dye after recycling of adsorbent for the first cycle has high removal efficiency than the second and third cycles similar results were reported by [29] on the removal of methylene blue dye from wastewater using periodiated modified nanocellulose.

Table 25: Removal of MB dye by AB5 adsorbent after different cycles (1st, 2nd, and 3rd)

Cycles	Residual concentration (mg/L)	qe (mg/g)	% Removal efficiency of MB
1st	22.49	28.76	71.89
2nd	26.63	26.68	66.71
3rd	32.48	23.76	59.40

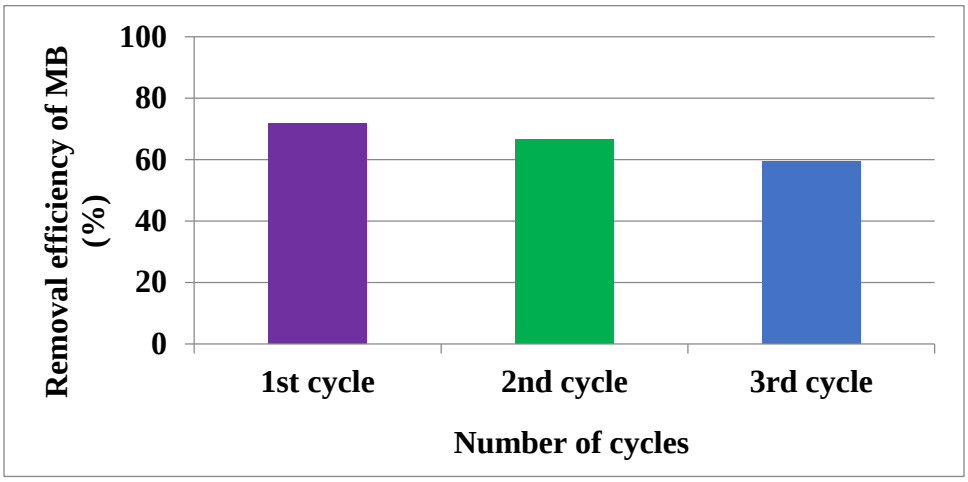

Figure 32: MB dye removal efficiency versus the number of recyclability of AB5 adsorbent

4.9.3. Photodegradation of MB dye by ZnO/bentonite nanocomposites (ZBC)

As shown in section 4.9 the desorption results of the adsorbent and methylene blue are very low, and the disposal of exhausted adsorbent to the environment will create another problem. However, different research reports revealed the high degradation efficiency of organic contaminates with zinc oxide immobilized on bentonite clay surface [115]. Modified bentonite clay increases the adsorptive capacity of organic contaminant (MB dye) and will improve the photocatalytic rate of nano zinc oxide [165], [166]. For this reason, in this work, the photo-degradation test of methylene blue using zinc oxide-bentonites was carried out and the results obtained were discussed below.

Photodegradation of MB dye using ZnO/bentonite nanocomposites for the removal of MB from the aqueous solution was carried out using UV light. The result for this study showed CZBC12 composite has better degradation efficiency (99.53%), as revealed in Table 26 and Figure 34.

Table 26: Absorbance, concentration, and photodegradation efficiency of MB dye after degradation

Sample	Absorbance (a.u)	Concentration of MB dye after photodegradation (mg/L)	Degradation efficiency (%)
CZBC12	0.112	0.376	99.53
CZBC11	0.272	0.91	98.68
CZBC32	1.896	6.38	92.02

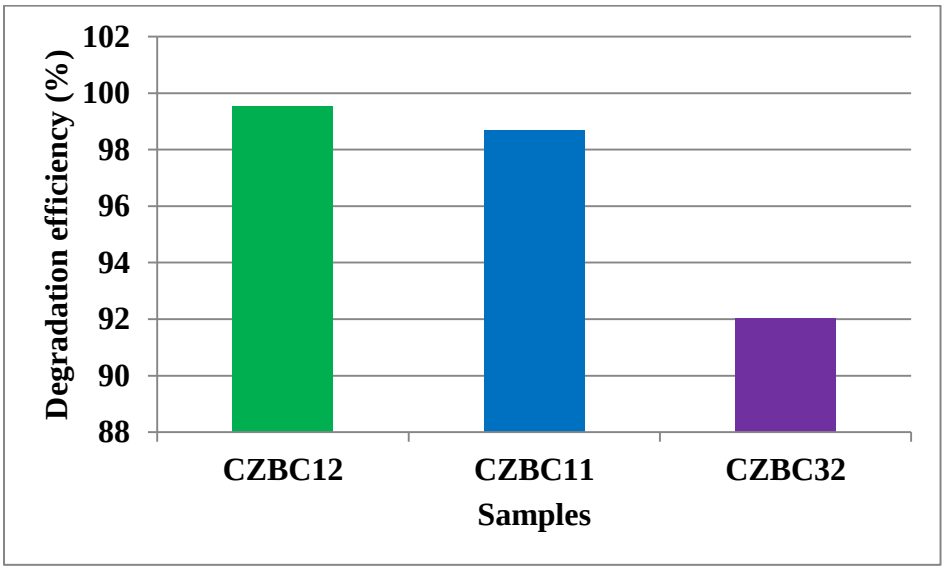

Figure 33: Bar graph revealing photocatalytic degradation of methylene blue dye using ZnO/bentonite nanocomposites with different ratios

Figure 34 shows the photodegradation efficiency of MB dye using ZnO/bentonite nanocomposites (CZBC12, CZBC11, and CZBC32) with the aid of UV-Visible spectroscopy to identify the degradation of methylene blue dye. The summary of the result of this study indicates that the CZBC32 (3:2) ZnO/bentonite nanocomposites showed better removal efficiency (99.94%) of MB, but CZBC32 lower degradation efficiency relative to the other tested composites (92.02%). On the other hand, the CZBC12 has higher photocatalytic activity for degradation of MB from aqueous solution (99.53%) as indicated in Table 26 and Figure 34.

5. CONCLUSIONS AND RECOMMENDATIONS

5.1. Conclusions

For the development of Green or environmentally friendly adsorbent; bentonite was collected from Afar regional state, dried, ball-milled, sieved, purified, and activated with sodium carbonate with different percentages. The bentonite activated with 5% Na_2CO_3 (AB_5) has 100% removal efficiency of the targeted organic dye (i.e., methylene blue) from an aqueous solution. The batch adsorption experiments were conducted using AB5 to optimize the variables like temperature; pH, initial concentration, adsorbent dosage, and contact time. The results of the optimized parameters for this study are pH=7, contact time = 30 min, initial concentration of dye = 80 mg/L, at a temperature of 25 C°, and mixing speed 300 rpm. The adsorption isotherm studies result shows the removal of MB from aqueous solution using activated bentonite by Na_2CO_3 was best fits the Langiumer adsorption isotherm model with the correlation coefficient $R^2 = 1$. The kinetic adsorption study was best fits the pseudo-second-order model with the correlation coefficient $R^2 = 1$. The thermodynamic study conducted in the temperature range of 298 °K to 323 °K results with the negative values of $\Delta G°$, which indicates the adsorption process on the developed adsorbent(AB5) was spontaneous. The standard enthalpy of adsorption $\Delta H° = 56.55$ KJ/mol determined, indicates an endothermic process and the positive value of $\Delta S°$ reflects the affinity of activated bentonite for MB dye. Desorption tests of MB from exhausted adsorbent (AB5-MB) after adsorption using the thermo-chemical method were carried out to reuses both the adsorbent and the dye. The highest result of the desorption study of MB dye in distilled water from exhausted adsorbent obtained is about 50%. Because of this low desorption result, the photocatalytic degradation test conducted using ZnO/bentonite nanocomposites synthesized for the MB dye degradation showed better results (99.53%) efficiency.

5.2. Recommendations

The low desorption efficiency of the exhausted adsorbent is the major limitation to reuse the adsorbent and adsorbate. Hence, more investigation work is needed on the photo-degradation of organic dyes like methylene blue by using metal oxide bentonite nanocomposites as a result of the high adsorption capacity of bentonite (adsorbent) but low desorption efficiency through thermochemical methods.

6. REFERENCES

[1] Sabarish Radoor, Jasila Karayil, Aswathy Jayakumar, Jyotishkumar Parameswaranpillai, and Suchart Siengchin, "Removal of Methylene Blue Dye from Aqueous Solution using PDADMAC Modified ZSM-5 Zeolite as a Novel Adsorbent," *Journal of Polymers and the Environment,* pp. 1-14, 2021.

[2] Yi Lin, et al., "Green Synthesis of ZnO-GO Composites for the Photocatalytic Degradation of Methylene Blue," *Journal of Nanomaterials,* pp. 1-11, 2020.

[3] Sham, and Notley, "Adsorption of organic dyes from aqueous solutions using surfactant exfoliated graphene," *Journal of Environmental Chemical Engineering,* vol. 6, no. 1, pp. 495-504, 2018.

[4] Katheresan, V et al., "Efficiency of various recent wastewater dye removal methods: A review," *Journal of environmental chemical engineering,* 2018.

[5] Chauhan P et al., "Facile synthesis of ZnO/GO nanoflowers over Si substrate for improved photocatalytic decolorization of MB dye and industrial wastewater under solar irradiation," *Materials Science in Semiconductor Processing,* vol. 89, pp. 6-17, 2019.

[6] Yagub, M et al., "Dye and its removal from aqueous solution by adsorption," *Adv. Colloid Interface,* vol. 209, p. 172–184, 2014.

[7] Bhatti, M et al., "Efficient photocatalysts based on silver doped ZnO nanorods for the photodegradation of methyl orange," *Ceram. Int,* vol. 232, no. 45, 2019.

[8] Zhang, W et al., "The decolorization of methyl orange by persulfate activated with natural vanadium-titanium magnetite," *Appl. Surf. Sci,* no. 509, p. 144886, 2020.

[9] Calimli, M et al., "Preparation, characterization and adsorption kinetics of methylene blue dye in reduced-graphene oxide supported nano adsorbents," *J. Mol. Liq,* vol. 309, p.

113171, 2020.

[10] Vakili, M et al., "Application of chitosan and its derivatives as adsorbents for dye removal from water and wastewater.," *Carbohydrate polymers,* vol. 113, pp. 115-130, 2014.

[11] Sarma, SenGupta, and Bhattacharyya, "Methylene blue adsorption on natural and modified clays," *Sci. Technol,* vol. 46, pp. 1602-1614, Sep 2011.

[12] Chih-Huang, and Yi-Fong, "Adsorption of a cationic dye (methylene blue) onto spent activated clay," *Journal of Hazardous Materials,* vol. 144, pp. 355-362, 2007.

[13] Weng, Chih-Huang, Pan, and Yi-Fong, "Adsorption of a cationic dye “methylene blue onto spent activated clay," *Journal of Hazardous Materials,* vol. 144, p. 355–362, 2006.

[14] Singh, Nagpal, and Agrawal, "Water purification by using adsorbents," *Environmental Technology & Innovation,* 2018.

[15] Enslin, Van der Mey, and Waanders, "Acid leaching of heavy metals from bentonite clay, used in the cleaning of acid mine drainage.," *The journal of the South African,* 2010.

[16] Livy Laysandra et al. , "Adsorption and photocatalytic performance of bentonite-titanium dioxide composites for methylene blue and rhodamine B decoloration," *Elsevier Ltd,* pp. 1-22, 2017.

[17] Gunvant H. Sonawane, Sandip P. Patil, and Shirish H. Sonawane, "Nanocomposites and Its Applications," *Elsevier Ltd,* pp. 1-22, 2018.

[18] Mustapha S et al., "Application of TiO2 and ZnO nanoparticles immobilized on clay in wastewater treatment," *Applied Water Science ,* p. 10:49, 2020.

[19] Bruno Lellis, Cíntia Zani Fávaro-Polonio, João Alencar Pamphile and Julio Cesar Polonio, "Effects of textile dyes on health and the environment and bioremediation potential of living organisms," *Biotechnology Research and Innovation,* pp. 1-16, 2019.

[20] Karthik, V et al., "Composite, Comparative and Equilibrium Studies on Anionic and Cationic Dyes Removal by Nano-Alumina-Doped Catechol Formaldehyde," *Journal of*

Chemistry, pp. 1-15, 2020.

[21] Hamid S, Shahadat M, and Ismail S, "Development of cost-effective bentonite adsorbent coating for the removal of organic pollutant.," *Applied Clay Science,* vol. 149, pp. 79-86, 2017.

[22] Michael, I et al., "Urban wastewater treatment plants as hotspots for the release of antibiotics in the environment: a review.," *Water Research,* vol. 47, no. 3, pp. 957-995, 2013.

[23] Ogugbue CJ, and Sawidis T, "Bioremediation and detoxification of synthetic wastewater containing triarylmethane dyes by Aeromonas hydrophila isolated from industrial effluent.," *Biotechnology research international,* 2011.

[24] Welham A, "The theory of dyeing (and the secret of life)," *Journal of the Society of Dyers and Colourists,* vol. 116, pp. 140-143, 2000.

[25] Robinson, T et al., "Remediation of dyes in textile effluent: a critical review on current treatment technologies with a proposed alternative," *Bioresource Technology,* vol. 77, pp. 247-255, 2001.

[26] Livy Laysandra, Meri Winda et. al., "Adsorption and photocatalytic performance of bentonite-titanium dioxide composites for methylene blue and rhodamine B decoloration," *Elsevier Ltd,* pp. 1-22, 2017.

[27] Zaghbani N, Hafiane A, and Dhahbi M, "Separation of methylene blue from aqueous solution by micellar enhanced ultrafiltration," *Purif. Technol,* vol. 55, p. 117–124, 2007.

[28] Ghosh D, and Bhattacharyya K, "Adsorption of Methylene Blue on Kaolinite," *Applied Clay Science,* vol. 20, no. 6, pp. 295-300, 2002.

[29] Hizkeal Tsade Kara, Sisay Tadesse Anshebo, Fedlu Kedir Sabir, and Getachew Adam Workineh, "Removal of Methylene Blue Dye from Wastewater Using Periodiated Modified Nanocellulose," *International Journal of Chemical Engineering,* pp. 1-16, 2021.

[30] Djilani, C et al., "Adsorption of dyes on activated carbon prepared from apricot stones and commercial activated carbon.," *J. Taiwan Inst. Chem. Eng*, vol. 53, p. 112–121, 2015.

[31] Hou, Y et al., "Fabrication of N-doped carbons from waste bamboo shoot shell with a high removal efficiency of organic dyes from water.," *J. Bioresour. Technol*, vol. 303, p. 122939, 2020.

[32] Pearce C, Lloyd J, and Guthrie J, "The removal of color from textile wastewater using whole bacterial cells," *Dyes and pigments*, vol. 58, no. 3, pp. 179-196, 2003.

[33] Rahman F, and Akter M, "Removal of dyes from textile wastewater by adsorption using shrimp shell," *Int. J. Waste Resour*, vol. 6, p. 244, 2016.

[34] Ardejani F et al., "Numerical modeling and laboratory studies on the removal of Direct Red 23 and Direct Red 80 dyes from textile effluents using orange peel, a low-cost adsorbent," *Dyes and pigments*, vol. 73, no. 2, pp. 178-185, 2007.

[35] Sanjay K. Sharma, "Green chemistry for dyes removal from wastewater," *Green Process Synth 2015*, vol. 4, p. 507–508, 2015.

[36] Ahmad, M et al., "Porous Eleocharis@ MnPE Layered Hybrid for Synergistic Adsorption and Catalytic Biodegradation of Toxic Azo Dyes from Industrial Wastewater. E," 2019.

[37] Shaheen, S, M et al., "Wood-based biochar for the removal of potentially toxic elements in water and wastewater: a critical review. International Materials Reviews.," pp. 1-32, 2018.

[38] Deepika Bhatia, Neeta Raj Sharma, Joginder Singh and Rameshwar S. Kanwar, "Biological methods for textile dye removal from wastewater: A review," *Critical Reviews in Environmental Science and Technology*, pp. 1-41, 2017.

[39] Holkar, CR et al., "A critical review on textile wastewater treatments: possible approaches," *Journal of environmental management*, vol. 182, pp. 351-366, 2016.

[40] Thao, N et al., "Advanced oxidation of rhodamine B with hydrogen peroxide over ZnCr layered double hydroxide catalysts.," *Journal of Science: Advanced Materials and*

Devices, vol. 2, no. 3, pp. 317-325, 2017.

[41] Lee C, Robinson J, and Chong M, "A review on application of flocculants in wastewater treatment," *Process Safety and Environmental Protection,* vol. 92, no. 6, pp. 489-508, 2014.

[42] Mollah M Y, Schennach R, Parga J, and Cocke D, "Electrocoagulation (EC)—science and applications," *Journal of hazardous materials,* vol. 84, no. 1, pp. 29-41, 2001.

[43] Emmanuel A, and Unuabonah I, "Clay–polymer nanocomposites (CPNs): adsorbents of the future for water treatment," *Appl. Clay Sci,* 2014.

[44] C. G, "Non-conventional low-cost adsorbents for dye removal," *Bioresour. Technol,* vol. 97 , pp. 1061-1085, 2006 .

[45] Zakaria, R M et al., "Lactic Acid Removal from Wastewater by Using Different Types of Activated Clay," *In Thirteenth International Water Technology Conference,* vol. 13, pp. 403-416, 2009.

[46] Kaykhaii M, Sasani M, and Marghzari S, "Removal of dyes from the environment by adsorption process," *Chemical and Materials Engineering,* vol. 6, no. 2, pp. 31-35, 2018.

[47] Kandisa, R V et al., "Dye removal by adsorption," *J. Bioremed Biodegr,* vol. 7, p. 317, 2016.

[48] Jaafar, and Sharifah Nhatasha Syed, "Adsorption study dye removal using clay," *University College of Engineering & Technology Malaysia,* 2006.

[49] Chowdhury S, and Bhattacharyya K, "Use of Cu (II)-incorporated zeolite Y for decolorization of dyes in water: a case study with aqueous methylene blue and Congo red.," *SN Applied Sciences,* vol. 1, no. 1, p. 87, 2019.

[50] Elmoubarki R, Mahjoubi F, Tounsadi H, Moustadraf J, Abdennouri M, Zouhri A, El Albani A, and Barka N, "Adsorption of textile dyes on raw, and decanted Moroccan clays: kinetics, equilibrium and thermodynamics," *Water Resources and Industry,* vol. 9, p. 16–

29, 2015.

[51] Gürses A, Doğar C, Yalçin M, Açikyildiz M, Bayrak R, et al., "The adsorption kinetics of the cationic dye, methylene blue, onto clay," *J. Hazard Mater,* vol. 131, pp. 217-228, 2006.

[52] Brito D F, da Silva Filho E C, Fonseca M G, and Jaber M, "Organophilic bentonites obtained by microwave heating as adsorbents for anionic dyes," *Journal of environmental chemical engineering,* vol. 6, pp. 7080-7090, 2018.

[53] Bhattacharya G, Chowdhury R, and Metya S, "Residual factor as a variable in slope reliability analysis," *Bulletin of Engineering Geology and the Environment,* vol. 78, no. 1, pp. 147-166, 2019.

[54] Şen, F et al., "The dye removal from aqueous solution using polymer composite films," *Applied Water Science,* vol. 8, no. 7, p. 206, 2018.

[55] Murray H, "Industrial Clays Case Study," *Int Inst Environ Dev (IIED),* vol. 64, pp. 1-9, 2002.

[56] Zhang, L et al., "Removal of Arsenic(V) from Aqueous Solutions using Iron-Oxide-Coated Modified Activated Carbon," *Water Environ. Res,* vol. 79, pp. 931-936, 2007.

[57] F. Tesfamariam, "Characterization and Optimization of Iron (III) Modified Bentonite Adsorbent for Efficient Removal of Fluoride from Aqueous Solution," *Addis Ababa Institute of Technology, Addis Ababa University,* pp. 1-98, 2018.

[58] Ahmad, A. et al., "Recent advances in new generation dye removal technologies: novel search for approaches to reprocess wastewater.," *RSC Advances,* vol. 39, no. 5, pp. 30801-30818, 2015.

[59] Kanika Guptaa, and Om P. Khatri, "Fast and efficient adsorptive removal of organic dyes and active pharmaceutical ingredient by microporous carbon: Effect of molecular size and charge," *Chemical Engineering Journal,* vol. 38, pp. 1-12, 2019.

[60] Shazlina Abd Hamida, Mohammad Shahadat, and Suzylawati Ismail, "Development of

cost-effective bentonite adsorbent coating for the removal of organic pollutant," *Applied Clay Science,* pp. 1-8, 2017.

[61] Chandana Lakshmi V, and Gollapalli Suvarna Laxmi, "Removal of dyes by using low-cost adsorbents agricultural wastes and sand," *International Journal of Engineering Research & Technology (IJERT),* vol. 3, no. 1, pp. 1749-61, 2014.

[62] Sadanand Pandey, and James Ramontja, "Natural bentonite clay and its composites for dye removal: current state and future potential," *American Journal of Chemistry and Applications,* vol. 3, no. 2, pp. 8-19, 2016.

[63] Shaobin Wanga, and Yuelian Peng, "Natural zeolites as effective adsorbents in water and wastewater treatment," *Chemical Engineering Journal,* vol. 156, pp. 11-24, 2010.

[64] Abdullahi, S L and Audu, A A, "Comparative analysis on the chemical composition of bentonite clays," *ChemSearch Journal,* vol. 8, no. 2, p. 35 – 40, 2017.

[65] Fabryanty, R et al., "Removal of crystal violet dye by adsorption using bentonite – alginate composite," *Journal of Environmental Chemical Engineering,* vol. 5, p. 5677–5687, 2017.

[66] Liu Zhirong Md, Azhar Uddin, and Sun Zhanxue, "FT-IR and XRD analysis of natural Na-bentonite and Cu(II)-loaded Na-bentonite," *Spectrochimica Acta Part A,* vol. 79, pp. 1013-1016, 2011.

[67] Yan, L and Shan, R, "Adsorption of acid dyes from aqueous solution by CTMAB modified bentonite: kinetic and isotherm modeling," *J. Mol. Liq,* vol. 21, pp. 1074-1081, 2015.

[68] Yeşilyurt, Z et al, "Simultaneous purification and modification process for organo-bentonite production," *Applied Clay Science,* vol. 95, pp. 176-181, 2014.

[69] Morais, I et al., "Influence of the activation process on cation exchange capacity and viscosity of bentonitic clay dispersions," *Cerâmica,* vol. 66, pp. 81-87, 2020.

[70] Raghavendra, S et al., "Preparation and evaluation of heavy metal rejection properties of Polyetherimide/Porous activated bentonite clay nanocomposite membrane," *RSC*

Advances, 2014.

[71] Ghebre, Wondafrash, "Local Industrial Applications of Bentonite Deposits from Afar-Ethiopia," *Acta Scientific Agriculture,* vol. 3, no. 10, pp. 85-90, 2019.

[72] Yang T, Wen X, and Yang L, "Theoretical and Experimental Investigations on the Structures of Purified Clay and Acid Activated Clay," *Appl. Surface Sci,* vol. 252, pp. 6154-6161, 2006.

[73] Parker, S, "McGraw-Hill Encyclopedia of the geological sciences," *2nd ed McGraw-Hill,* vol. 722, p. 118, 1988.

[74] Adamis Z, and Williams R B, "Environmental Health Criteria 231 Bentonite, kaolin, and selected clay mineral," *World Health Organization,* 2005.

[75] Thomas, G, "Soil pH and soil acidity methods of soil analysis," *Soil Science Society of America,* vol. 5, pp. 321-352, 1996.

[76] Stephan Kaufhold et al., "The pH of aqueous bentonite suspensions," *Clays and Clay Minerals,* vol. 56, no. 3, pp. 338-343, 2008.

[77] Kaufhold, S and Dohrmann, R, "Detachment of colloidal particles from bentonites in water," *Applied Clay Science,* vol. 39, pp. 50-59, 2008.

[78] Rihayat T, Salim S, Arlina A, Fona Z, Jalal R et.al., "Determination of CEC value (Cation Exchange Capacity) of Bentonites from North Aceh and Bener Meriah, Aceh Province, Indonesia using three methods," *IOC: Materials Science and Engineering,* vol. 334, pp. 1-6, 2018.

[79] Salwa D, Abayazeed, and Essam El-Hinnawi, "Characterization of Egyptian smectitic clay deposits by Methylene blue adsorption," *American Journal of Applied Sciences,* vol. 8, no. 12, pp. 1282-1286, 2011.

[80] Meier LP, and Kahr G, "Determination of the cation exchange capacity (CEC) of the clay minerals using the complexes of copper (II) ions with triethylenetetramine and tetra

ethylene pentaamine," *Clay Miner,* vol. 47, pp. 386-388, 1999.

[81] Wang, M , "Rapid estimation of cation exchange capacities of soils and clays with methylene blue exchange," *Soil Sci. Soc. Am. J,* vol. 60, pp. 138-141, 1996.

[82] Yukselen Y, and Kaya A, "Suitability of the methylene blue test for surface area, cation exchange capacity and swell potential determination of clayey soils," *Journal of Engineering Geology,* vol. 102, pp. 38- 45, 2008.

[83] Caglar B, Afsin B, Tabak A, and Eren E, "Characterization of the cation-exchanged bentonites by XRPD, ATR, DTA/TG analyses and BET measurement," *Chemical Engineering Journal,* vol. 149, p. 242–248, 2009.

[84] Berez A et.al., "Adsorption-desorption processes of azo dye on natural bentonite: batch experiments and modeling," *Clay Minerals,* vol. 49, pp. 747-763, 2014.

[85] de Oliveira et.al, "Characterization of bentonite clays from Cubati, Paraíba (Northeast of Brazil)," *Cerâmica,* vol. 62, pp. 272-277, 2016.

[86] Toor, Manjot Kaur, "Enhancing adsorption capacity of bentonite for dye removal: Physiochemical modification and characterization," *Chemical Engineering thesis,* pp. 1-209, 2010.

[87] Jaqueline A et.al., "Determination of the cation exchange capacity of bentonite exposed to hyper alkaline fluid," *International Nuclear Atlantic Conference,* pp. 1-24, 2013.

[88] Erich Wieland , Hans Wanner , Yngve Albinsson , Paul Wersin , and Ola Kärnland, "A surface chemical model of the bentonite-water interface and its implications for modeling the near field chemistry in a repository for spent fuel," *Swedish Nuclear Fuel and Waste Management Co. (SKB),* pp. 1-78, 1994.

[89] Lorenz P. Meier, and Guenter Kahr, "Determination of the cation exchange capacity (CEC) of clay minerals using the complexes of copper(ii) ion with triethylenetetramine and tetraethylenepentamine," *Clays and Clay Minerals,* vol. 47, no. 3, pp. 386-388, 1999.

[90] Sheela Evangeline Y, Vinod S, and Manju A, "Permeability variation of sodium activated bentonites," *Indian Geotechnical society,* 2009.

[91] Solenicki G, Budic I, Kladaric I, and Novoselovic D, "Compressive stresses of mold mixture, Metalurgija," vol. 53, no. 4, pp. 591-593, 2014.

[92] Faur-Brasquet C, Reddad Z, Kadirvelu K, and Le Cloirec P, "Modeling the Adsorption of Metal Ions (Cu2+, Ni2+, Pb2+) Onto Aacs Using Surface Complexation Models," *Appl. Surf. Sci,* vol. 196, pp. 356-365, 2002.

[93] Pushpaletha P, Rugmini S, and Lalithambika M, "Correlation between Surface Properties and Catalytic Activity of Clay Catalysts," *Appl. Clay Sci,* vol. 30, pp. 141-153, 2005.

[94] Toor B, & Jin M, "Adsorption characteristics, isotherm, kinetics, and diffusion of modified natural bentonite for removing diazo dye," *Chemical Engineering Journal,* vol. 187, pp. 79-88, 2012.

[95] Chakraborty T, Chakraborty A, Shukla M, Chattopadhyay, and Tanmay, "ZnO-Bentonite nanocomposite: An efficient catalyst for discharge of dyes, phenol, and Cr (VI) from water.," *Journal of Coordination Chemistry,* pp. 1-30, 2018.

[96] Şahin O, Kaya M, and Saka C, "Plasma-surface modification on bentonite clay to improve the performance of adsorption of methylene blue.," *Appl Clay Sci,* vol. 116, pp. 46-53, 2015.

[97] R. Srinivasan, "Advances in Application of Natural Clay and Its Composites in Removal of Biological, Organic, and Inorganic Contaminants from drinking water," *Advances in Materials Science and Engineering,* pp. 1-17, 2011.

[98] Abdullah NH, Shameli K, Abdullah EC, and Abdullah LC, "Low cost and efficient synthesis of magnetic iron oxide/activated sericite nanocomposites for rapid removal of methylene blue and crystal violet dyes," *Mater Charact,* vol. 163, pp. 110-275, 2020.

[99] Abdullah NH, Shameli K, Abdullah EC, and Abdullah LC, "Solid matrices for fabrication of magnetic iron oxide nanocomposites: synthesis, properties, and application for the

adsorption of heavy metal ions and dyes," *Compos Part B Eng,* vol. 162, pp. 538-568, 2019.

[100] Herney-Ramírez J, and Madeira LM, "Use of pillared clay-based catalysts for wastewater treatment through Fenton-like processes," *Pillared clays and related catalysts,* 2010.

[101] Abuzerr S, Darwish M, and Mahvi AH, "Simultaneous removal of cationic methylene blue and anionic reactive red 198 dyes using magnetic-activated carbon nanoparticles," *equilibrium, and kinetics analysis. Samer Abuzerr Maher Darwish Amir Hossein Mahvi,* p. 534–45, 2017.

[102] Ganjar Fadillah, Septian Perwira Yudha, Suresh Sagadevan, Fatimah, and Oki Muraza, "Magnetic iron oxide/clay nanocomposites for adsorption and catalytic oxidation in water treatment applications," *Open Chemistry,* vol. 18, pp. 1148-1166, 2020.

[103] Hashem S, "Adsorption of Methylene Blue from Aqueous Solutions using Fe3O4/ Bentonite Nanocomposite.," *Hydrology Current Research,* vol. 3, p. 5, 2012.

[104] Jianmin R, Yongmin Z, Siwei W, Sheguang D, and Peipei G, "Thermodynamics and kinetics of adsorption of methylene blue by Na-bentonite," *Ion Exchange and Adsorption,* vol. 02, 2010.

[105] Yang C, Zhu Y, Wang J, Li Z, Su X, and Chunge Niu, "Hydrothermal synthesis of TiO2–WO3–bentonite composites: Conventional versus ultrasonic pretreatments and their adsorption of methylene blue," *Applied Clay Science,* pp. 105–106, 243–251, 2015.

[106] Amina Aichour,and Hassina Zaghouane-Boudiaf, "Synthesis and characterization of hybrid activated bentonite/alginate composite to improve its efective elimination of dyes stuf from wastewater," *Applied Water Science* , vol. 10, no. 146, pp. 1-13, 2020.

[107] Yanru S, Zhenhua X, and Ximing W, "Removal of methylene blue from aqueous solution by sorption on lignocellulose-g-poly (acrylic acid)/montmorillonite three-dimensional cross-linked polymeric network hydrogels," *Polymer Bulletin,* vol. 70, pp. 1163-1179, 2013.

[108] Anirudhan T S, and Ramachandran, M, "Adsorptive removal of basic dyes from aqueous solutions by surfactant modified bentonite clay (organoclay): kinetic and competitive adsorption isotherm, Process," *Saf. Environ. Prot,* vol. 95, p. 215–225, 2015.

[109] Mouzdahir Y El, Elmchaouri A, Mahboub R, Gil A, and Korili S A, "Equilibrium modeling for the adsorption of methylene blue from aqueous solutions on activated clay minerals," *Desalination,* vol. 250, p. 335–338, 2010.

[110] Moniz, S.J.A., et al., "Visible-light driven heterojunction photocatalysts for water splitting – a critical review," *Energy & Environmental Science,* vol. 8, no. 3, pp. 731-759, 2015.

[111] Kavitha MK, Pillai SC, Gopinath P, and John H, "Hydrothermal synthesis of ZnO decorated reduced graphene oxide: understanding the mechanism of photocatalysis," *J Environ Chem Eng,* vol. 3, pp. 1194-1199, 2015.

[112] Haithem Bel Hadjltaief, et al., "Photocatalytic decolorization of cationic and anionic dyes over ZnO nanoparticle immobilized on natural Tunisian clay," pp. 1-24, 2018.

[113] Zhang A, Zhang R, Zhang N, Hong S, and Zhang M, "Synthesis and characterization of TiO2-montmorillonite nanocomposites and their photocatalytic activity," *Kinet. Catal,* vol. 51, no. 4, p. 529–533, 2010.

[114] Akkari M. et al., "Sepiolite nanoplatforms for the simultaneous assembly of magnetite and zinc oxide nanoparticles as photocatalyst for improving the removal of organic pollutants," *J. Hazard Mater,* vol. 340, pp. 281-290, 2017.

[115] Suchithra Padmajan Sasikala, et al., "Competitive photo-degradation performance of ZnO modified bentonite clay in water containing both organic and inorganic contaminant," *Sustainable Environment,* vol. 29, no. 1, pp. 1-12, 2019.

[116] Darvishi Cheshmeh Soltani R, Jorfi S, Safar M, and Rajaei M, "Enhanced Sonocatalysis of textile wastewater using bentonite supported ZnO nanoparticles: response surface methodological approach," *Journal of Environmental Management,* vol. 179, p. 47–57, 2016.

[117] Sandip P Patil, Shrivastava V S, and Sonawane G H, "Photocatalytic degradation of Rhodamine 6G using ZnO-montmorillonite nanocomposite: a kinetic approach," *Desalin. Water Treat,* vol. 54, pp. 374-381, 2017.

[118] Nemade K R, Barde R V, and Waghuley, S A, "Photocatalytic study of alumina-zirconia ceramic nanocomposite synthesized by spray pyrolysis," *Ceram. Int,* vol. 41, pp. 4836-4840, 2015.

[119] Omorogie M O, Babalola J O, and Unuabonah E I, "Regeneration strategies for spent solid matrices used in adsorption of organic pollutants from surface water: A critical review," *Desalin. Water Treat,* vol. 57, pp. 518-544, 2016.

[120] Shahadat M, and Ismail S, "Regeneration performance of clay-based adsorbents for the removal of industrial dyes A review," *RSC Adv,* vol. 8, p. 24571–24587, 2018.

[121] Wu H, Salles F, and Zajac J, "A critical review of solid materials for low-temperature thermochemical storage of solar energy based on solid-vapor adsorption given space heating use, Molecules," vol. 24, p. 945, 2019.

[122] Azha S, Ahmad A, and Ismail S, "Thin coated adsorbent layer: Characteristics and performance study," *Desalin.Water Treat,* vol. 55, p. 956–969, 2015.

[123] Greluk M, and Hubicki Z, "Efficient removal of Acid Orange 7 dye from water using the strongly basic anion exchange resin Amberlite IRA-958," *Desalination,* vol. 278, p. 219–226, 2011.

[124] Daneshvar E, et al., "Desorption of Methylene blue dye from brown macroalgae effects of operating parameters, isotherm study, and kinetic modeling," *J. Clean. Prod,* vol. 152, p. 443–453, 2017.

[125] Momina, Mohd Rafatullah, Suzylawati Ismail, and Anees Ahmad, "Optimization Study for the Desorption of Methylene Blue Dye from Clay Based Adsorbent Coating," *Water,* vol. 11, pp. 1-13, 2019.

[126] Takayuki Hayakawa, Makoto Minase, Ken- Ichi F Ujita, and Makoto Ogawa, "Modified method for bentonite purification and characterization; A case study using bentonite from Tsunagi Mine, Niigata, Japan," *Clays and Clay Minerals,* vol. 64, no. 3, p. 275–282, 2016.

[127] Leena S, "Activation of raw bentonite (afar region) using sulfuric acid for rapeseed and niger seed oil bleaching," 19 June 2017. [Online].

[128] Ertaş, A., et al, " Evaluation of Antioxidant, Cholinesterase Inhibitory and Antimicrobial Properties of Mentha longifolia subsp. noeana and Its Secondary Metabolites," *Records of Natural Products,* vol. 9, no. 1, 2015.

[129] Moones Honarmand, Morteza Golmohammadi, & Atena Naeimi, "Green synthesis of SnO2-bentonite nanocomposites for the efficient photodegradation of methylene blue and eriochromeeriochrome black-T," *Materials Chemistry and Physics,* 2019.

[130] Asha Embrandiri, et al., "Treatment of Dye Wastewater by Functionalization of Bentonite-Methylene Blue with Sodium Persulfate.," *Journal of Environmental Treatment Techniques,* vol. 7, no. 2, pp. 229-233, 2019.

[131] K. Fisseha, "Modification of Bentonite Clay for Adsorption Enhancement for Congo Red Dye Removal from Textile Waste Water," 2017. [Online].

[132] Sruthi B Dharan, and Rani V, "Study on the effect of pH on clay," *International Research Journal of Engineering and Technology*, vol. 4, no. 11, pp. 1751-1755, 2017.

[133] Zdravković S A, "Application of activated bentonite for the removal of direct and reactive dye from aqueous solutions," *Chemical Industry & Chemical Engineering Quarterly,* vol. 4, no. 25, p. 341−351, 2019.

[134] Jae-Myung Lee, Charles D, and Shackelford, "Solution Retention Capacity as an Alternative to the Swell Index Test for Sodium Bentonite," *Geotechnical Testing Journal,* vol. 28, no. 1, pp. 61-70, 2005.

[135] Yukselen Y, and Kaya, A, "Suitability of the methylene blue test for surface area, cation exchange capacity and swell potential determination of clayey soils," *Engineering*

Geology, vol. 102, pp. 38-45, 2008.

[136] Moulton B, et al., "The origin of the unusual DSC peaks of supercooled barium disilicate liquid," *Cryst Eng Comm,* vol. 21, p. 2768–2778, 2019.

[137] Djelloul Bendaho, Tabet Ainad Driss, and Djillali Bassou, "Removal of Cationic Dye Methylene Blue from Aqueous Solution by Adsorption," *International Journal of Waste Resources,* vol. 5, no. 1, pp. 1-6, 2015.

[138] Crini, G and Badot P, "Application of chitosan, a natural amino polysaccharide, for dye removal from aqueous solutions by adsorption processes using batch studies," *Progress in Polymer Science,* vol. 33, no. 4, pp. 399-447, 2008.

[139] Bennani Karim A, et al., "Adsorption/desorption behavior of cationic dyes on Moroccan clay: equilibrium and mechanism," *Journal of Materials and Environmental Sciences,* vol. 8, no. 3, pp. 1082-1096, 2017.

[140] Mohammad Ilyas Khan, "Adsorption of methylene blue onto natural Saudi Red Clay: isotherms kinetics, and thermodynamic studies," *Materials Research Express,* vol. 7, pp. 1-13, 2020.

[141] Piccin, et al., "Adsorption isotherms and thermochemical data of FD & Congo red n° 40 bindings by chitosan," *Brazilian Journal of Chemical Engineering,* vol. 28, no. 2, pp. 295 - 304, 2011.

[142] El Miz, et al., "Adsorption-desorption and kinetics studies of Methylene Blue Dye on Na-bentonite from Aqueous Solution," *IOSR Journal of Applied Chemistry (IOSR-JAC),* vol. 7, no. 7, pp. 60-78, 2014.

[143] Muhammad Munir, et al., "Effective Adsorptive Removal of Methylene Blue from Water by Didodecyldimethylammonium Bromide-Modified Brown Clay," *American Chemical Society (ACS) Omega,* vol. 5, pp. 16711-16721, 2020.

[144] Hailemariam and Sishu, "Characterization and Thermal Modification of Local Bentonite

for Removal of Zinc Ion from Aqueous Solution," *Thesis paper,* pp. 1-88, 19 June 2017.

[145] Silva Da, *Cerâmica,* vol. 64, no. 369, p. 109, 2018.

[146] Reshma R Unnithan, and Soorya S R, "Characterization of Na2CO3 activated Calcium Bentonite and its application as a GCL," *International Journal of Engineering Research & Technology (IJERT),* vol. 5, no. 8, pp. 1-4, 2017.

[147] Hailemariam, Sishu, "Characterization and Thermal Modification of Local Bentonite for Removal of Zinc Ion from Aqueous Solution," 19 June 2017. [Online].

[148] Meshram S, Limaye R, Ghodke S, Nigam S, Sonawane S, Chikate R, *J. Chem. Eng* , vol. 172, pp. 1008-1015, 2011.

[149] Hamideh Pouraboulghasem, Mohammad Ghorbanpour, Razieh Shayegh and Samaneh Lotfiman , "Synthesis, characterization and antimicrobial activity of alkaline ion-exchanged ZnO/bentonite nanocomposites," *J. Cent. South Univ,* vol. 23, pp. 787-792, 2016.

[150] Gawade V et al., " Green synthesis of ZnO nanoparticles by using Calotropis procera leaves for the photodegradation of methyl orange," *Journal of Materials Science: Materials in Electronics,* vol. 28, no. 18, pp. 14033-14039, 2017.

[151] Motlagh, K et al., "Effect of Acid activation on structural and bleaching properties of a bentonite," *Journal of Materials Science & Engineering,* vol. 8, pp. 53-54, 2011.

[152] Mekedes Tenkolu, "Musa acuminata peel extract assisted green Synthesis of ZnO/CuO Nanocomposite for Photocatalytic Degradation of Methylene Blue Dye," pp. 1-74, 2020.

[153] S. Evangeline, "Permeability variation of sodium activated bentonites," *IGC,* pp. 43-46, 2009.

[154] Wei, W et.al., *J. Nanomater. Biostruct,* vol. 19, p. 1343, 2015.

[155] Zhansheng, W C et al., "Characterization, acid activation and bleaching performance of

bentonite from Xinjiang," *J. Chem. Eng*, vol. 14, p. 253–258, 2006.

[156] Mahmoudian. Sh, "Removal of cationic dyes from aqueous solution using Organomodified nano-clay," *Int. J. Bio-Inorg. Hybr. Nanomatererials*, vol. 8, no. 2, pp. 95-99, 2019.

[157] Ullah, Z et al., "Use of HCl-modified bentonite clay for the adsorption of Acid Blue 129 from aqueous solutions," *Desalin. Water Treat*, vol. 19, no. 57, p. 8894–8903, 2016.

[158] Nurul Ain Safiqah Mohd Sandollah, et al., "Adsorption-Desorption Profile of Methylene Blue Dye on Raw and Acid Activated Kaolinite," *J. Chem*, vol. 20, no. 4, pp. 755 - 765, 2020.

[159] Lixia Li, and Xindong Zhai, "Adsorption of Methylene Blue on Modified Bentonite," *Advanced Materials Research*, Vols. 726-731, pp. 2380-2383, 2013.

[160] Kunquan Li, and Xiaohua Wang, *Bioresour. Technol*, vol. 100, pp. 2810-2815, 2009.

[161] Nurul Ain Safiqah Md Sandollah et al., "Adsorption-Desorption Profile of Methylene Blue Dye on Raw and Acid Activated Kaolinite," *J. Chem*, vol. 20, no. 4, pp. 755 - 765, 2020.

[162] Kavitha D, and Namasivayam C, "Experimental and kinetic studies on methylene blue adsorption by coir pith carbon," *Biores. Tech*, vol. 98, p. 14–21, 2007.

[163] Hu, Z-P et al., "High-surface-area activated red mud for efficient removal of methylene blue from wastewater," *Adsorption Science & Technology*, vol. 36, p. 62–79, 2018.

[164] Wei, Yang, and Zhong, "Fast removal of methylene blue from aqueous solution by adsorption onto poorly crystalline hydroxyapatite nanoparticles Digest," *Journal of Nanomaterials and Biostructures*, vol. 10, p. 1343–63, 2015.

[165] Vahid Javanbakht, and Marzieh Mohammadian, "Photo-assisted advanced oxidation processes for efficient removal of anionic and cationic dyes using Bentonite/TiO2 nano-photocatalyst immobilized with silver nanoparticles," *Journal of Molecular Structure*, vol. 1239, pp. 84175-443, 2021.

[166] Sandip Pandurang Patila, et al., "Kinetics of photocatalytic degradation of Methylene Blue by ZnO-bentonite nanocomposite," *Iranian Chemical Communication,* 2017.

APPENDICES

Appendix A: Experimental data

1) Moisture content calculation for raw bentonite and activated bentonite (AB5)

$$\%Mc = \frac{W_1 - W_2}{W_1} * 100$$

Where; %Mc is the percentage of moisture in bentonite, $W_1$is weight of the wet bentonite, W_2 is the weight of the dry bentonite; W_3 is Mass of empty crucible

$$\%Mc = \frac{2 - 1.81}{2} * 100$$

$$\underline{\%\text{Mc} = 9.5\%\ \text{For RB trial 1}}$$

For trials 2 & 3 the moisture content was done in the same manner as the above.

Table A1: Determination of moisture % content of bentonite

Type of Sample	Trail	Mass of dry (g)	Mass of wet (g)	% Moisture content	Average of % moisture content
Raw bentonite	1	1.81	2	9.5	9.67
	2	1.80		10	
	3	1.81		9.5	
Activated bentonite (AB5)	1	1.82	2	9	9.17
	2	1.82		9	
	3	1.81		9.5	

2) Determination of bulk density for bentonite

$$\rho\text{B} = \frac{\text{Msc} - \text{Mec}}{\text{Vc}}$$

Where ρB= Bulk density of bentonite in g/ml, Msc is mass of bentonite plus cylinder in g, Mec is mass of empty cylinder in g, and Vc is the volume of the cylinder in ml.

a) Bulk density for raw bentonite

$$\text{B}\rho_{\text{RB}} = \frac{34.059 - 27.044}{5}$$

$$\text{B}\rho_{\text{RB}} = 1.40\ \text{g/cm3}$$

c) Bulk density of 5% Na_2CO_3 activated bentonite

$$B\rho_{AB5} = \frac{34.41 - 27.044}{5}$$

$$B\rho_{AB5} = 1.45\ g/cm3$$

Table A2: Result of bulk density of bentonite sample

Sample	Mec (g)	Vc (ml)	Trail	Msc (g)	Bulk density (g/cm^3)	Average bulk density
RB	27.044	5	1	34.070	1.405	1.40
			2	33.997	1.391	
			3	34.110	1.413	
AB5			1	34.230	1.437	1.45
			2	34.440	1.479	
			3	34.260	1.443	

Table A3: Determination of pH of raw bentonite and activated bentonite (AB5)

Trial	Mass of Raw bentonite (g)	Volume added water (ml)	pH of RB	pH of AB5
1	2.5	25	10.03	10.49
2	2.5	25	10.01	10.48
3	2.5	25	10.00	10.50
Average of pH			10.013	10.49

3) Determination pHzpc

$$\Delta pH = pHf - pHi$$

Table A4: Determination of zero-point charge of the raw and activated bentonite

Initial pH	pH final of RB	ΔpH of RB	pH final of AB5	ΔpH of AB5
2	4.52	2.52	2.22	0.22
3	8.58	5.58	8.38	5.38
4	9.37	5.37	8.98	4.98
5	8.88	3.88	8.89	3.89
6	9.44	3.44	8.92	2.92
7	9.42	2.42	9.04	2.04
8	9.07	1.07	9.00	1
9	9.47	0.47	9.00	0
10	9.57	-0.43	9.11	-0.89
11	9.93	-1.07	8.85	-2.15

4) Calculation of specific surface area (SSA) and cation exchange capacity (CEC) determined by methylene blue test $SSA = \frac{mMB}{MMB} * AN * AMB * \frac{1}{ms}$

$$CEC = 100 * \frac{VMB}{ms} * NMB$$

Where; m_{MB} is the mass of the adsorbed methylene blue at the point of a complete replacement in gram, m_s is the mass of the bentonite adsorbent used in gram, M_{MB} is the molecular weight of methylene blue dye which is 319.87g/mol, Av is Avogadro's number ($6.02 * 10^{23}$/mol), A_{MB} is an area covered by one methylene blue molecule which is 130Å² (1*A*°= 0.1nm=10^{-10} m), V_{MB} is the volume of methylene blue added to the suspension in the beaker and, N_{MB} - is the normality of the methylene blue (meq/100g).

- A mole of MB is calculated as follows; $nMB = \frac{mMB}{MMB} => nMB = \frac{4g}{319.87g/mol} = 0.0125mol$

$$C = \frac{n}{V} => 0.0125\ mol/L$$

$$NMB = Z * C = 1eq/mol * 0.0125mol/L = 0.0125eq/L$$

Where: - Z- is the valence of methylene blue which is equal to 1eq/mol.

- To calculate mMB adsorbed at the endpoint of a complete replacement, first calculate mole of methylene blue adsorbed from methylene blue solution and added volume to the suspension.

  A) A mole of Raw bentonite; $C = \frac{nMB}{VMB} =>, n = C * VMB = 0.0125 \frac{mol}{L} * 0.09L = 0.001125mol$

- Then the mass of adsorbed MB was calculated as follows; $mMB = n * MMB =>$ $0.001125mol * 319.87 \frac{g}{mol} = 0.36g$

  B) A mole of activated bentonite (AB5); $C = \frac{nMB}{VMB}$, $n = C * VMB = 0.0125 \frac{mol}{L} * 0.11L = 0.001375mol$

- Then the mass of adsorbed MB was calculated as follows; $mMB = n * M. 0.001375mol *$ $319.87 \frac{g}{mol} = 0.44g$

- Determination of specific surface area and CEC of adsorbent from the determined values

  1) The specific surface area of RB and AB5 was calculated as follows:-

SSA_{RB} $SSA = \frac{mMB}{M} * AV * AMB * \frac{1}{ms}$

$$SSA_{RB} = [(0.36g)/319.87g/mol]*(1.3*10^{-18}) *6.02*10^{23}$$

$$= (1.123*1.3*6.02) *10^{-3-18+23}$$

$$= 8.79*10^{2} = 879\ m^2/g$$

SSA_{AB5}, $SSA = \frac{mMB}{M} * AV * AMB * \frac{1}{ms}$

$$SSA_{AB5} = (0.44g)/319.87g/mol * (1.3*10^{-18}) *6.02*10^{23}$$

$$= (1.375*1.3*6.02) *10^{-3-18+23}$$

$$= 10.76 *10^{2} = 1076\ m^2/g$$

  2) Cation Exchange Capacity (CEC)

  a) Cation Exchange Capacity (CEC) for Raw bentonite;

$$CEC = 100 * \frac{VMB}{ms} * NMB$$

$$CEC = 100 * \frac{0.09L}{1g} * \frac{0.0125eq}{L}$$

$$\text{CEC} = 0.1136\ \text{eq} = \text{g}113.63\ \text{meq/g}$$

b) Cation Exchange Capacity (CEC) for 5% Na_2CO_3 Activated Bentonite (AB5)

$$\text{CEC} = 100 * \frac{\text{VMB}}{\text{ms}} * \text{NMB}$$

$$\text{CEC} = 100 * \frac{0.11\text{L}}{1\text{g}} * \frac{0.0125\text{eq}}{\text{L}}$$

$$\text{CEC} = 0.1375\ \text{eq/g} = 137.5\ \text{meq/g}$$

Table A5: Cation exchange capacity and specific surface area of raw and activated bentonite

No.	Sample item	Added volume of MB Vi (ml)	Total added volume of MB (ml)	CEC (meq/g)	SSA (m^2/g)
1	RB	5	90	113.63	879
2	AB5	5	110	137.5	1076

Appendix B: Experimental Pictures

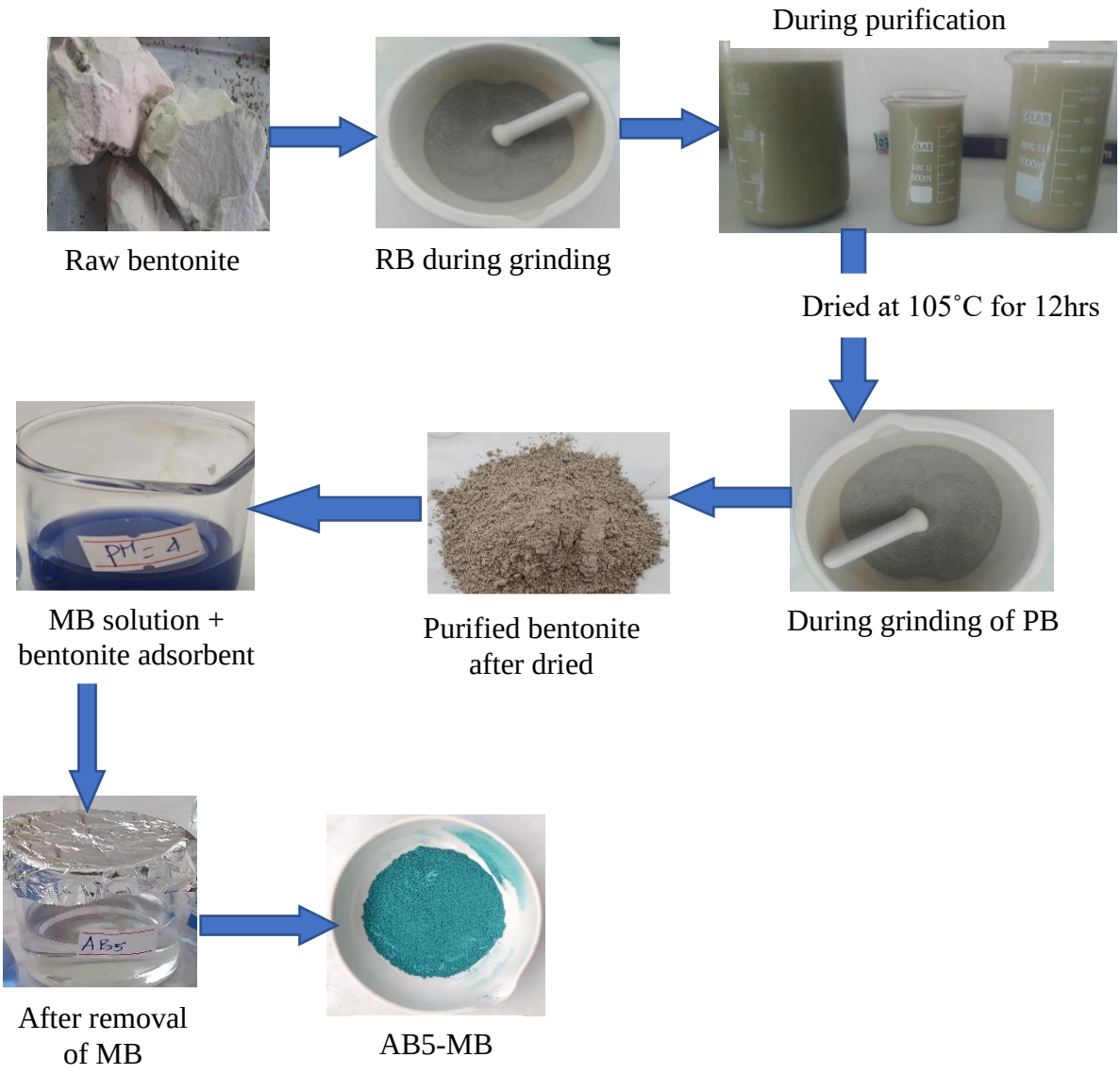

Figure B1: Experimental flow charts from the raw materials to the end product

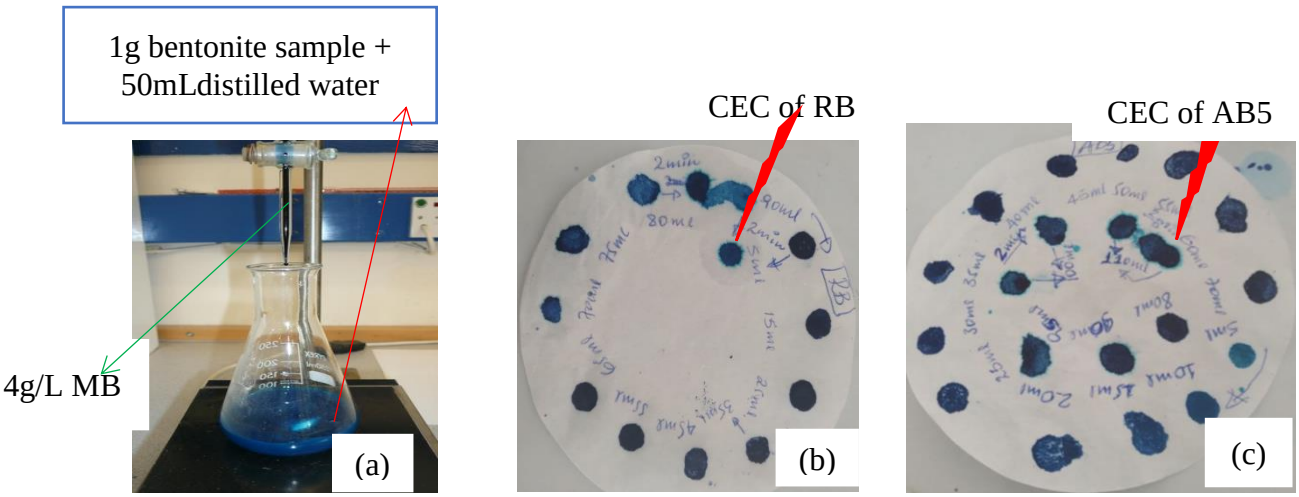

Figure B2: Spot test for the endpoint (a) by MB titration for (b) raw bentonite and (c) activated bentonite

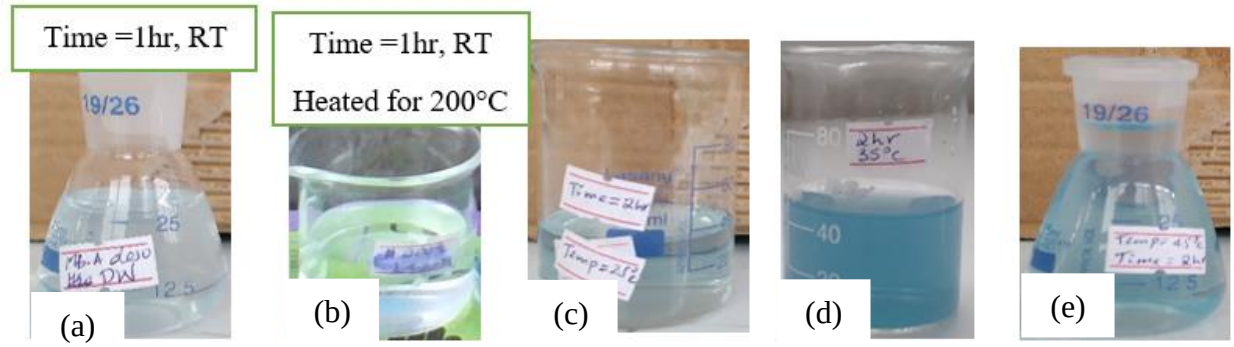

Figure B3: Desorption of MB by distilled water

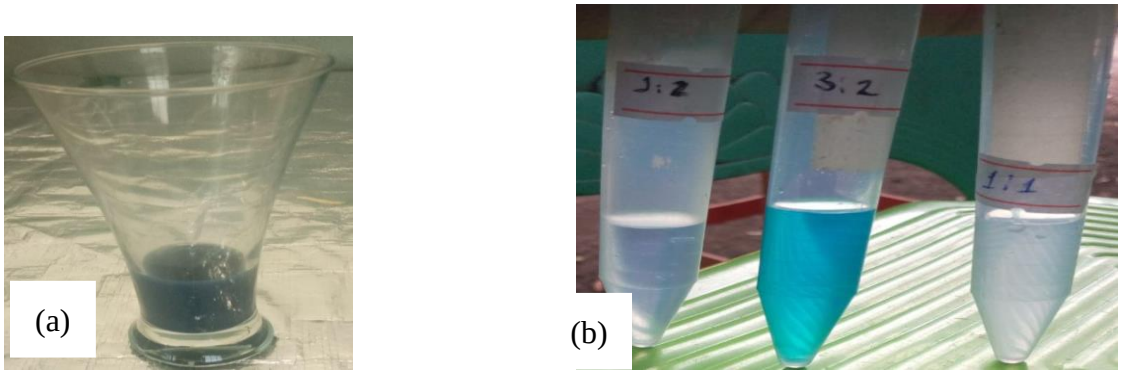

Figure B4: (a) Photodegradation of MB by ZnO/Bent nanocomposites before photodegradation (b) after photodegradation